Prague Medical REPORT

(Sborník lékařský)

Multidisciplinary Biomedical Journal
of the First Faculty of Medicine,
Charles University

Vol. 121 (2020) No. 4

Reviews

Primary Scientific Studies

Case Reports


D
E
C
Fig. 7.
B
C
A
Fig. 6.
B
A
Fig. 8.
C
B
A
B
Fig. 2.
D
A
D
E
Fig. 9.
A
E

Prague Medical Report (Prague Med Rep) is indexed and abstracted by Index-medicus, MEDLINE, PubMed, EuroPub, CNKI, DOAJ, EBSCO, and Scopus.

Abstracts and full-texts of published papers can be retrieved from the World Wide Web (https://pmr.lf1.cuni.cz).

Engraving overleaf: Laurentius Heister, Institutiones chirurgicae, Amsterdam 1750.
Illustration provided by the Institute for History of Medicine and Foreign Languages.

A Review on Role of Arecoline and Its Metabolites in the Molecular Pathogenesis of Oral Lesions with an Insight into Current Status of Its Metabolomics

Aparajita Das, Sarbani Giri
Laboratory of Molecular and Cell Biology, Department of Life Science and Bioinformatics, Assam University, Silchar, India

Received June 5, 2018; Accepted November 9, 2020.

Key words: Arecoline – Molecular pathogenesis – Metabolism of arecoline – Arecoline N-oxide – Oral submucous fibrosis – Oral cancer

Abstract: Areca nut consumption is a popular habit in Southeast Asian countries. One of the important biologically active alkaloids of areca nut is arecoline, which plays a role in mediating the development of several pathologies of the primary exposure site, the oral cavity. Studies on the metabolism of arecoline revealed the formation of several metabolites which themselves might be toxic. Moreover, polymorphisms in genes encoding enzymes involved in the metabolism of arecoline might predispose an organism towards the development of oral cancer. The present review tries to accumulate all the relevant existing literature and then elucidate the molecular mechanism by which arecoline plays a role in the development of oral submucous fibrosis and oral cancer. Existing information regarding arecoline metabolism, enzymes involved in the metabolic process and biological effects of the metabolites of arecoline have also been compiled and compared to study the toxicity of metabolites with its parent compound arecoline and whether they play any role in the pathogenesis of oral cancer mediated by areca nut consumption. A repertoire of molecular targets has come up in the discussion whose expression profile is perturbed by arecoline. Construction of induction cascade from existing literature has given an idea about the process of molecular pathogenesis. The summarized and analysed data can help to determine the molecular mechanism and drug targets,

This study was supported by the University Grants Commission (UGC), India, under UGC Junior Research Fellowship scheme.

Mailing Address: Prof. Sarbani Giri, PhD., Laboratory of Molecular and Cell Biology, Department of Life Science and Bioinformatics, Assam University, Silchar 788011, Assam, India; Phone +91 384 224 04 00; Fax: +91 384 227 08 06; e-mail: girisarbani@gmail.com

https://doi.org/10.14712/23362936.2020.19

which in turn could be helpful in the prevention or treatment of these pathological conditions. It also brings into light areas where further research needs to be directed.

Introduction

Mortality is a severe issue in the case of oral cancer, as indicated by the International Agency for Research in Cancer (IARC) report, GLOBOCAN series, 2012. According to this data, globally, 300,000 cases of oral cancer and 145,000 cases of death were reported in the year 2012 (Ferlay et al., 2015). As this form of cancer majorly develops from the squamous cell region of the oral cavity, it is also called oral squamous cell carcinoma (OSCC) (Rivera, 2015). The metastatic form is preceded by several pre-malignant stages, including leukoplakia, erythroplakia, oral lichen planus, and oral submucous fibrosis (OSF). These lesions show different rates of transformation to the cancerous stage: 3.6 to 17.5% in leukoplakia, 70.3% in proliferative verrucous leukoplakia, 14 to 50% in erythroplakia, 0.04 to 1.74% in oral lichen planus and 7 to 13% in oral submucous fibrosis (Reichart and Philipsen, 2005; Tilakaratne et al., 2006; Kademani, 2007).

Areca nuts have been classified as a Class I carcinogen by IARC (IARC Working Group on the Evaluation of Carcinogenic Risks to Humans, 2004). The chemical composition of areca nut comprises alkaloids, flavonoids, tannins, along with carbohydrates, proteins, fats, crude fibre, and elements (IARC Working Group on the Evaluation of Carcinogenic Risks to Humans, 2004; Peng et al., 2015). Of these, an important constituent is the alkaloid arecoline (IARC Working Group on the Evaluation of Carcinogenic Risks to Humans, 2004). In a study by Cox et al. (2010), most of the habitual areca nut consumers were found to have a baseline concentration of arecoline in saliva reaching up to 2.4 μg/ml (0.01 mM). Apart from saliva, arecoline was detected in blood plasma, hair samples and breast milk samples from areca nut consumers (Marchei et al., 2005; Pellegrini et al., 2007; Wu et al., 2010). It was also detected in the excreta collected from new-borns, whose mothers had consumed areca nut during their gestation period (Pichini et al., 2003). Therefore, the effects induced by arecoline might be due to its stability in the system apart from direct exposure.

The metabolic profile of arecoline has brought into light the existence of several metabolites (Nery, 1971; Giri et al., 2006). Few of these metabolites have been detected in body fluids of areca nut consumers opening up another area of research involved in investigating the role of these metabolites in areca nut mediated oral pathologies.

In this review, we try to (1) create a metabolic map of arecoline from existing literature, (2) discuss the molecular mechanisms and pathways induced by arecoline that are responsible for the development of oral submucous fibrosis (OSF) and oral squamous cell carcinoma (OSCC), (3) describe the biological effects of arecoline metabolites and thereby assess if the metabolites are more toxic than the parent compound itself and play a part in the pathogenesis of OSF and OSCC, and finally

(4) understand the mechanism of metabolism of arecoline and arecoline N-oxide by gathering knowledge about enzymes involved, which in turn may enable to estimate predisposition of an individual towards the development of oral cancer in areca nut consumers.

Metabolism of arecoline

The metabolic profile of arecoline might play a role in areca nut mediated pathogenesis of OSF and OSCC. This brings out the need to delve into the depths

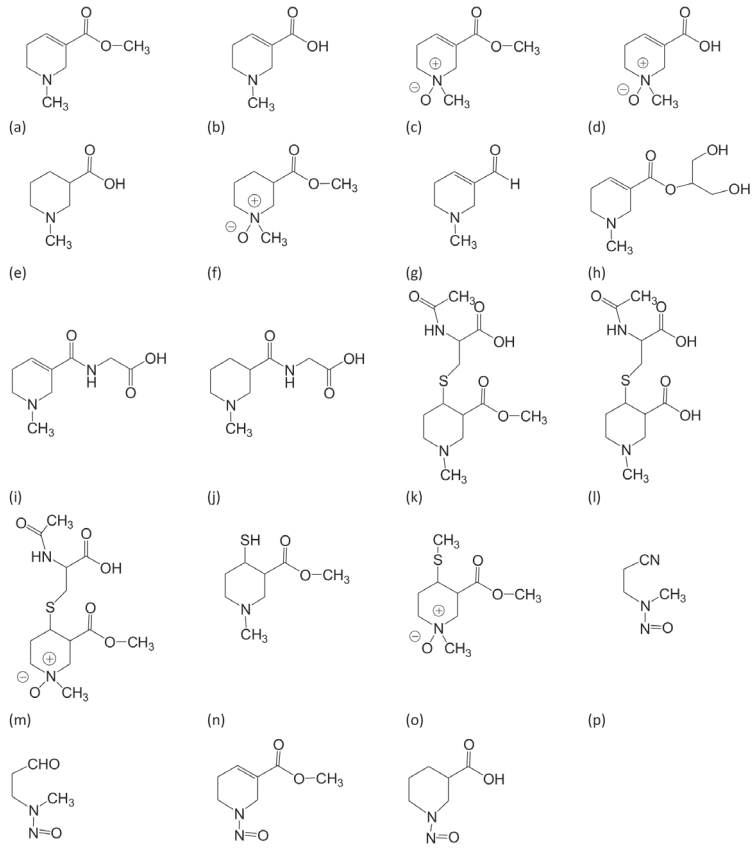

Figure 1 – Chemical structure of arecoline and metabolites.
(a) arecoline; (b) arecaidine; (c) arecoline N-oxide; (d) arecaidine N-oxide; (e) N-methylnipecotic acid; (f) 1-methylnipecotic acid 1-oxide methylester; (g) 1-methyl-3,4-dehydropiperidine-3-carboxaldehyde; (h) arecaidinylglycerol; (i) arecaidinylglycine; (j) N-methylnipecotylglycine; (k) mercapturic acid of arecoline; (l) mercapturic acid of arecaidine; (m) mercapturic acid of arecoline N-oxide; (n) 4-mercapto-1-methylnipecotic acid methylester; (o) 4-methylmercapto-1-methylnipecotic acid 1-oxide methylester; (p) 3-methylnitrosaminopropionitrile; (q) 3-methylnitrosaminopropionaldehyde; (r) N-nitrosoguvacoline; (s) N-nitrosonipecotic acid.
(b, c, d, e, h, i, j, k, l, m, p, q, r – metabolites of arecoline; d, e, h, i, j, l – metabolites of arecaidine; a, b, f, g, k, m, n, o – metabolites of arecoline N-oxide; s – metabolite of N-nitrosoguvacoline)

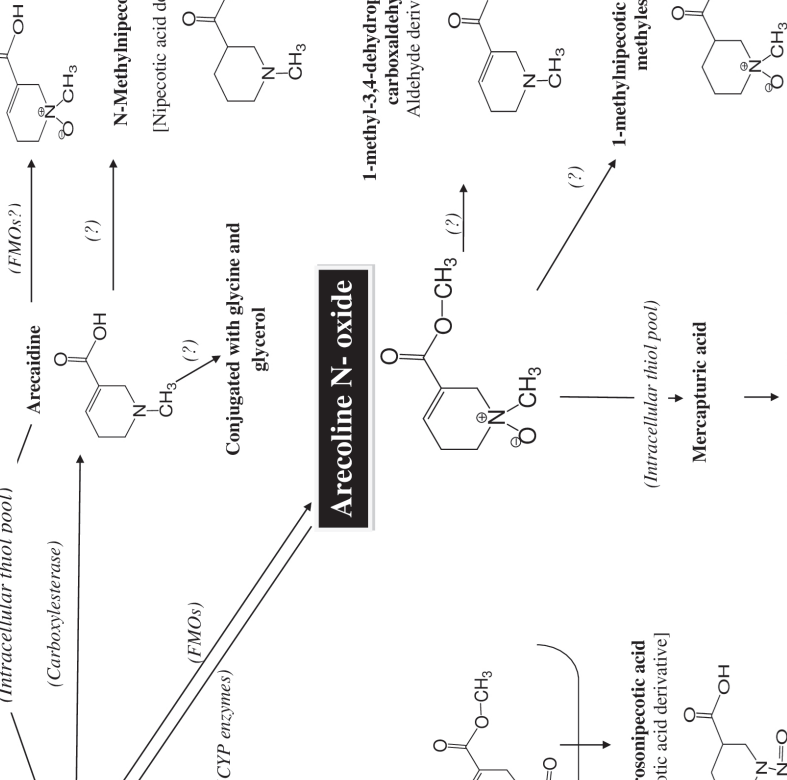

Figure 2 – Metabolic map of arecoline and its metabolites. Pathway adapted from Wenke and Hoffman (1983), Ohshima et al. (1989), Miyazaki et al. (2005), Giri et al. (2006, 2007). The symbol "?" represents the unavailability of knowledge about the enzyme involved. Enzyme involved in each step has been mentioned in italics.

of the metabolomics of arecoline and explore its potential towards the development of oral pathology. Metabolism of arecoline starts in the oral cavity itself. Both nitrite and thiocyanate (catalyst for nitrosation reaction) are present in human saliva (Boyland et al., 1971; Shivapurkar et al., 1980; Wenke et al., 1984a). When arecoline was incubated with sodium nitrite with or without sodium thiocyanate, the formation of three compounds was observed: 3-(methylnitrosamino)propionaldehyde (MNPA), 3-(methylnitrosamino)propionitrile (MNPN) and N-nitrosoguvacoline (NGL) (Wenke and Hoffmann, 1983). Of these, NGL and MNPN were detected in the saliva of betel quid chewers (without tobacco) in the range of 2.2–9.5 μg/l and 0.5–11.4 μg/l, respectively (Wenke et al., 1984a; Prokopczyk et al., 1987). These findings indicate that nitrosation of arecoline does take place in the oral cavity of areca nut consumers, and thereby, buccal cells do get exposed to these nitrosated metabolites on chewing areca nut. In a mammalian test system, N-nitrosonipecotic acid (NNIP) was detected as a product of metabolism of NGL (Ohshima et al., 1989). MNPA has not been detected in saliva samples of areca nut consumers. However, as the formation of MNPA from arecoline takes place under *in vitro* conditions, fast metabolism of MNPA to its metabolites *in vivo* might explain this finding. The metabolome of arecoline, arecaidine and arecoline N-oxide *in vivo* was investigated by Nery (1971) and Giri et al. (2006, 2007). This research revealed several unknown and novel metabolites (Figure 1). Of these, arecaidine and N-methyl nipecotic acid were detected in the urine of areca nut consumers (Hu et al., 2010).

Figure 2 depicts a metabolic map of arecoline.

Role of arecoline in induction of oral pathologies

Genotoxic effects of arecoline were proved in mice using tests evaluating the formation of chromosomal aberrations and micronucleus (Shirname et al., 1984; Deb and Chatterjee, 1998). At the molecular level, arecoline induces a DNA damage response cascade involving phosphorylation of ataxia-telangiectasia (ATM) kinase and its downstream targets checkpoint kinase 1/2 (Chk1/2), p53 and Nbs1, leading to a G2/M cell cycle arrest. However, the overall expression of p53 is down-regulated by arecoline, which is followed by suppression of p53 mediated DNA repair activities and expression of its downstream target $p21^{WAF1}$ (Tsai et al., 2008). Arecoline has also been found to induce decreased expression of p21 and p27 via a p53 independent process that includes reactive oxygen species (ROS) and activation of mammalian target of rapamycin complex-1 (mTORC1) pathway (Ji et al., 2012). According to Ji et al. (2012), down-regulation of these inhibitors of cell cycle might lead to erroneous DNA replication as the cells escape the G1/S checkpoint. Arecoline also disturbs the fluidity of polymerisation-depolymerisation kinetics of α-tubulin by favouring their polymerisation. It leads to a disfigurement of the mitotic spindle and an erroneous arrangement of chromosomes, thereby inducing the pro-metaphase cell cycle arrest (Wang et al., 2010). Apart from these alterations,

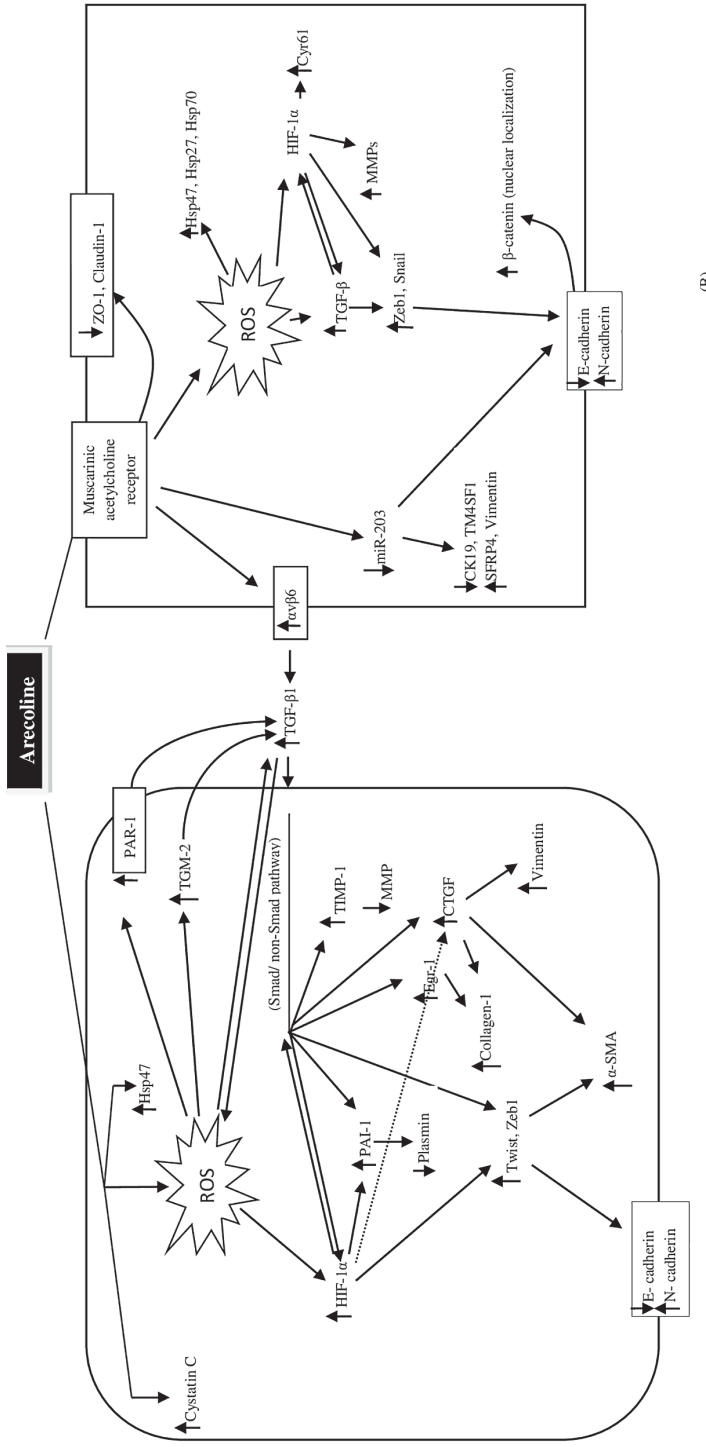

Figure 3 – Induction cascade induced by arecoline in fibroblast (A) and epithelial cell/carcinoma cell of epithelial origin (B) facilitating development of oral pathologies. All abbreviations have been elaborated in text except: N-cadherin – neural-cadherin; CK19 – cytokeratin 19; TM4SF1 – transmembrane 4 L six family member 1; SFRP4 – secreted frizzled related protein 4. Both hard dashed arrows and dotted arrow indicate the same.

protein expression of several other cell cycle regulatory molecules like cdc25c in basal carcinoma cells (Huang et al., 2012), cyclin B1 and Wee-1 in KB epithelial cells (Lee et al., 2006) and cyclin D1, cyclin A, cyclin E, CDK4, and CDK2 in HaCaT keratinocytes (Zhou et al., 2013) have been found to be modulated by arecoline.

Arecoline treatment leads to the down-regulation of the immune system in mice (Dasgupta et al., 2006; Wen et al., 2006). By contrast, Hung et al. (2011) reported the production of ROS in endothelial cells on exposure to arecoline, which resulted in an up-regulated expression of adhesion molecules (intercellular adhesion molecule – ICAM, and vascular cell adhesion molecule – VCAM). This effect increased adhesion between mononuclear cells and endothelial cells, which might play a role in augmenting the inflammation. Additionally, several inflammatory cytokines have also been found to be induced by arecoline, such as interleukin-1α, prostaglandin E-2, and cycloxygenase-2 in fibroblasts (Jeng et al., 2003; Tsai et al., 2003; Thangjam and Kondaiah, 2009).

DNA damage and impaired DNA repair, along with chronic inflammation, can be emphasized as the main causes of arecoline induced oral pathologies. Moreover, expression profiles of several extracellular matrix (ECM) proteins, enzymes, growth factors, and transcription factors are altered under the effect of arecoline (Figure 3). All these factors work in an association as indicated by several studies involving fibroblasts, epithelial cells and cancer cell lines (Tables 1 and 2).

Oral submucous fibrosis (OSF) is a pre-cancerous condition that develops from an abnormal wound healing process under continuous exposure to the components of areca nut (Angadi et al., 2011). Inhibition of elements involved in the degradation of extracellular matrix (ECM) or enhanced stability and synthesis of matrix components disturbs the homeostasis of ECM, which can give rise to disease conditions like fibrosis. Arecoline works positively in both these aspects. It enhances the expression of several inhibitors of proteinases, including tissue inhibitors of metalloproteinases (TIMPs), plasminogen activator inhibitors (PAI-1) and cysteine proteinase inhibitor cystatin C in fibroblasts (Chang et al., 2002a; Yang et al., 2003; Tsai et al., 2007) along with induction of factors that enhance the stability of ECM, such as heat shock protein-47 (Hsp-47) and transglutaminase-2 (TGM-2) (Yang et al., 2008; Lee et al., 2015). Moreover, arecoline has been found to decrease the phagocytosis of collagen by fibroblasts (Shieh et al., 2004).

An analysis of the repertoire of moieties affected by arecoline (data compiled in Tables 1 and 2) has bought into light several mediators of the effects induced by arecoline of which three, ROS, transforming growth factor-β1 (TGF-β1) and hypoxia-inducible factor-1α (HIF-1α), might play key roles in the pathogenesis of OSF and OSCC.

Of the several isoforms of TGF-β (TGF-β1/2/3), TGF-β1 is a critical mediator of oral pathologies. Its overexpression has been observed in OSF tissue samples (Kamath et al., 2015). Up-regulated expression of αvβ6 integrin on keratinocytes under arecoline's affect supports the activation of latent TGF-β1 present in ECM that

Table 1 – A collective representation of various studies conducted *in vitro* to assess the effect of arecoline on the expression of proteins whose expression profile is perturbed in oral submucous fibrosis (OSF) cases

Serial no.	Cell type and dose of arecoline	Effects	ROS/receptor/ pathways involved	Expression in OSF specimen (compared to normal mucosal specimen)	Reference
1.	Buccal mucosal fibroblasts (0–200 μg/ml)	Arecoline induced upregulation of vimentin expression.	–	Moderately advanced/advanced OSF specimen showed higher expression of intermediate filament vimentin in cytoplasm of fibroblasts in the connective tissue.	Chang et al. (2002b)
2.	Buccal mucosal fibroblasts (0–160 μg/ml)	Arecoline induced cylcloxygenase-2 expression, the induction subsided after sometime.	Decreased thiol content involved in induction.	Moderate cases of OSF showed higher expression of cycloxygenase-2 in epithelial cells, fibroblasts and inflammatory cells whereas advanced cases showed weak expression.	Tsai et al. (2003)
3.	Buccal mucosal fibroblasts (0–160 μg/ml)	Arecoline induced upregulation of plasminogen activator inhibitor-1 (PAI-1) expression.	–	Moderately advanced/advanced OSF specimen showed higher expression of plasminogen activator inhibitor-1 in fibroblasts, endothelial cells and inflammatory cells.	Yang et al. (2003)
4.	Buccal mucosal fibroblasts (0–80 μg/ml)	Arecoline induced upregulation of insulin like growth factor-1 expression.	–	Moderately advanced/advanced OSF specimen showed higher expression of insulin like growth factor-1 in fibroblasts, endothelial cells and inflammatory cells of connective tissue.	Tsai et al. (2005a)
5.	Buccal mucosal fibroblasts (0–80 μg/ml)	Arecoline induced upregulation of keratinocyte growth factor-1 expression.	–	Moderately advanced/advanced OSF specimen showed higher expression of keratinocyte growth factor-1 in the epithelial cells and to a lesser degree in fibroblast, endothelial and inflammatory cells.	Tsai et al. (2005b)
6.	Buccal mucosal fibroblasts (0–80 μg/ml)	Arecoline induced upregulation of cystatin C expression.	–	Connective tissue of moderately advanced/advanced OSF specimen showed higher expression of cystatin C in fibroblasts, endothelial cells and inflammatory cells.	Tsai et al. (2007)
7.	Buccal mucosal fibroblasts (0–160 μg/ml)	Arecoline induced upregulation of heat shock protein 47 (Hsp-47) expression.	PI3K, Cox-2, MEK pathways involved. Decreased intracellular thiol content involved in induction.	OSF specimen showed higher expression of heat shock protein 47 mRNA.	Yang et al. (2008)

Serial no.	Cell type and dose of arecoline	Effects	ROS/receptor/ pathways involved	Expression in OSF specimen (compared to normal mucosal specimen)	Reference
8.	Buccal mucosal fibroblasts (0–160 μg/ml)	Arecoline induced upregulation of hemeoxygenase-1 (HO-1) expression.	–	OSF specimen showed higher expression of hemeoxygenase-1 in fibroblasts, epithelial cells and inflammatory cells.	Tsai et al. (2009)
9.	Buccal mucosal fibroblasts (0–0.4 mM)	Arecoline induced upregulation of connective tissue growth factor (CTGF) expression.	NF-κB, JNK, p38 pathways involved. Decreased intracellular thiol content involved in induction.	OSF specimen showed higher expression of connective tissue growth factor in fibroblasts, endothelial cells and epithelial cells (in some cases).	Deng et al. (2009)
10.	HaCaT keratinocyte (0–50 μg/ml)	Arecoline induced expression of transforming growth factor-β2.	Muscarinic acetylcholine receptor – intracellular $[Ca^{2+}]$ rise-PKC activation pathway involved. Decreased intracellular thiol content involved in induction.	OSF specimen showed higher expression of transforming growth factor β2 mRNA.	Thangjam et al. (2009)
11.	Keratinocyte (5–10 μg/ml)	Arecoline induced upregulation of αvβ6 integrin expression.	Muscarinic acetylcholine receptor involved.	OSF specimen showed higher expression of αvβ6 integrin.	Moutasim et al. (2011)
12.	Buccal mucosal fibroblasts (0–20 μg/ml)	Arecoline induced upregulation of S100A4 expression.	NF-κB, ERK, mTOR pathways involved.	OSF specimen showed higher expression of S100A4.	Yu et al. (2013)
13.	Buccal mucosal fibroblasts (0–160 μg/ml)	Arecoline induced upregulation of protease activated receptor-1 (PAR-1) expression.	ERK, PI3K, Cox-2, TK pathways involved. Decreased intracellular thiol content involved in induction.	Moderately advanced/advanced OSF specimen showed higher expression of protease activated receptor-1 in fibroblasts and inflammatory cells.	Tsai et al. (2013)
14.	Buccal mucosal fibroblasts (0–20 μg/ml)	Arecoline induced ZEB1, αsmooth muscle actin (αSMA) and vimentin expression.	–	OSF specimen showed higher expression of ZEB1 localised in nucleus of fibroblast and αSMA in fibroblast and blood vessel.	Chang et al. (2014)

Serial no.	Cell type and dose of arecoline	Effects	ROS/receptor/ pathways involved	Expression in OSF specimen (compared to normal mucosal specimen)	Reference
15.	Buccal mucosal fibroblasts (0–160 μg/ml)	Arecoline induced upregulation of hypoxia inducible factor-1α expression.	–	Moderately advanced/advanced OSF specimen showed higher expression of hypoxia inducible factor-1α in fibroblasts, epithelial cells and inflammatory cells.	Tsai et al. (2015)
16.	Buccal mucosal fibroblasts (0–0.4 mM)	Arecoline induced upregulation of early growth response-1 (Egr-1) expression.	JNK, ERK pathways involved. Decreased intracellular thiol content involved in induction.	OSF specimen showed higher expression of early growth response-1 in epithelial cells, fibroblasts, inflammatory cells.	Hsieh et al. (2015)
17.	HaCaT keratinocytes (0–0.16 mM)	Arecoline induced downregulation of miR-203, downregulation of cytokeratin CK19 and E-cadherin; upregulation of N-cadherin and vimentin, increased expression of SFRP4 and decreased expression of TM4SF1.	–	OSF specimen showed lower expression of miR-203 and transmembrane 4 L six family member 1 (TM4SF1) and higher expression of secreted frizzled related protein 4 (SPRP4).	Zheng et al. (2015)
18.	Buccal mucosal fibroblasts (0–20 μg/ml)	Arecoline induced upregulation of Twist.	–	OSF specimen showed higher expression of Twist mRNA and protein.	Lee et al. (2016)
19.	Buccal mucosal fibroblasts (0–160 μg/ml)	Arecoline induced upregulation of transglutaminase-2 (TGM-2) expression.	Reactive oxygen species involved in induction.	Moderate/advanced OSF specimen showed higher expression of transglutaminase-2 in fibroblasts.	Lee et al. (2016)

ROS – reactive oxygen species; PI3K – phosphatidylinositol 3-kinase; Cox-2 – cycloxygenase-2; MEK – mitogen activated protein kinase; JNK – c-Jun NH_2-terminal kinase; ERK – extracellular signal-regulated protein kinase; PKC – protein kinase C; TK – tyrosine kinase; NF-κB – nuclear factor-kappa B; mTOR – mechanistic target of rapamycin

in turn triggers the myofibroblastic transformation of fibroblasts (Moutasim et al., 2011). After being activated via integrin, plasminogen activated receptor-1 (PAR-1) or TGM-2, TGF-β1 binds to its receptor and sets on a cascade of signalling events that induce the expression of growth factors, cytokines and transcription factors in resident fibroblasts thereby transforming them into myofibroblasts (Figure 3) (Eickelberg et al., 1999; Griffin et al., 2002; Samarakoon et al., 2008; Lin et al., 2013; Yang et al., 2013, 2016; Chang et al., 2014; Lamouille et al., 2014; Chen et al., 2016; Hsieh et al., 2017). Myofibroblasts are cells specialized for wound healing with capacity for the secretion of ECM materials and cellular contraction (Micallef et al., 2012). TGF-β1 stimulates myofibroblasts to produce modulators of ECM proteins (PAI-1, TIMP-1, CTGF, etc.) and transcription factors involved in epithelial-to-mesenchymal transition (EMT) (Twist, Zeb, etc.) (Figure 3). Up-regulated expression of TGF-β1 has also been observed in cancer tissue samples (Lu et al., 2004).

Another important mediator of arecoline induced effects is HIF-1α. Apart from being induced by arecoline itself in fibroblasts and epithelial cells (Lee et al., 2010; Tsai et al., 2015), it plays a part in the induction of several downstream factors that overlaps the repertoire induced by TGF-β1 (Figure 3) (Higgins et al., 2004; Tsai and Wu, 2012). Hypoxia prevails in fibrotic as well as tumour conditions, which prevents degradation of HIF-1α. Under the hypoxic condition, stabilized HIF-1α dimerizes with HIF-1β and, in association with co-activators, it participates in the transcription of genes with hypoxia-responsive element (HRE) (Tsai and Wu, 2012; Eckert et al., 2016; Rankin and Giaccia, 2016). As reviewed by Tsai and Wu (2012) and Rankin and Giaccia (2016), several genes involved in metastasiring are regulated by HIF-1α, including transcription factors involved in EMT (Twist, Snail, Aeb1/2, etc.), enzymes like matrix metalloproteinases (MMP 1/3), matricellular proteins (cysteine rich protein 61 [Cyr61]), and angiogenic factors (vascular endothelial growth factor).

Several of the pro-fibrotic or carcinogenic factors induced by arecoline are coupled with a decrease in intracellular thiol content and show reversible expression after treatment with antioxidants (Tables 1 and 2). This emphasizes ROS generation by arecoline to be a "cause" of the various arecoline driven "effects" that trigger OSF or OSCC. Interplay can be observed between ROS and TGF-β1 as well as HIF-1α. For instance, ROS plays a part in the activation of latent TGF-β1 complex tethered to the ECM (Jobling et al., 2006). In turn, TGF-β1 acts to increase ROS production via the activity of its downstream target NADPH oxidase-4 (NOX-4) along with suppression of the antioxidant defence system of exposed cells (Richter and Kietzmann, 2016). Apart from sharing a common array of downstream targets, TGF-β1 and HIF-1α augment each other's expression too. HIF-1α supports transcription of TGF-β1 under hypoxic conditions, whereas, under normoxic conditions, TGF-β1 enhances the stability of HIF-1α by decreasing expression of HIF-1α inhibitor prolyl hydroxylase 2 (PHD2) (McMohan et al., 2006; Hung et al., 2013). ROS induces HIF-1α stability and thereby its transcriptional activity via an adenosine monophosphate-activated protein kinase (AMPK) pathway (Jung et al., 2008).

Table 2 – A collective representation of various studies conducted *in vitro* to assess the effect of arecoline on the expression of proteins whose expression profile is modulated in oral squamous cell carcinoma (OSCC) cases

Serial no.	Cell line and dose of arecoline (μg/ml)	Effects	ROS/receptor/ pathways involved	Association of expression with oral squamous cell carcinoma (OSCC)	Reference
1.	OECM-1, CE81T/VGH cells (200 μg/ml) (LT)	Arecoline exposure induced expression of matrix metallo proteinase-1 (MMP-1).	–	Higher expression of matrix metallo proteinase-1 mRNA in OSCC samples.	Lee et al. (2008)
2.	GNM epithelial cells (0–160 μg/ml)	Arecoline induced higher expression of heat sock protein 70 (Hsp-70).	AP-1, ERK, PKC pathway. Decreased intracellular thiol content involved in induction.	Higher expression was seen in OSCC cases of poor differentiation. In between OSCC specimen, association found between low grade expression and lymph node metastasis.	Lee et al. (2008a)
3.	GNM epithelial cells (0–160 μg/ml)	Arecoline induced higher expression of metallothionene-1 transcriptionally.	Decreased intracellular thiol content involved in induction.	Higher expression was seen in OSCC cases. Association found with lymph node metastasis.	Lee et al. (2008b)
4.	GNM epithelial cells (0–160 μg/ml)	Arecoline induced higher expression of hemeoxygenase-1 (HO-1) transcriptionally.	Decreased intracellular thiol content involved in induction.	Higher expression was seen in OSCC cases. Association found with lymph node metastasis.	Lee et al. (2008c)
5.	OC2 epithelial cells (0–160 μg/ml)	Arecoline induced higher expression of heat sock protein 47 (Hsp-47).	ERK, Cox-2, PI3K, tyrosine kinase pathways. Decreased intracellular thiol content involved in induction.	Higher expression was seen in OSCC cases. In between OSCC specimen, association found between low grade expression and lymph node metastasis.	Lee et al. (2011)
6.	Human oral keratinocytes (0–160 μg/ml)	Arecoline induced higher expression of heat sock protein 27 (Hsp-27).	Cox-2, ERK, p38 pathways. Decreased intracellular thiol content involved in induction.	Higher expression was seen in OSCC cases. In between OSCC specimen, association found between low grade expression and lymph node metastasis.	Lee et al. (2012a)

Serial no.	Cell line and dose of arecoline (μg/ml)	Effects	ROS/receptor/ pathways involved	Association of expression with oral squamous cell carcinoma (OSCC)	Reference
7.	Human oral keratinocytes, OECM-1 cancer cells (0–160 μg/ml)	Arecoline induced higher expression of Snail.	ROS involved in induction.	Higher expression is seen in cases of OSCC samples. Association found with lymph node metastasis and poor differentiation of OSCC samples.	Lee et al. (2013)
8.	S-G epithelial cells, FaDu carcinoma cells (0–20 μg/ml)	Arecoline induced higher expression of zinc finger E-box binding homeobox-1 (ZEB1).	–	Higher expression of ZEB1 mRNA was seen in recurrent cases of OSCC than in initial stages.	Ho et al. (2015)
9.	S-G epithelial cells, FaDu carcinoma cells (0–20 μg/ml)	Arecoline induced higher expression of cell lineage abnormal 28 B (Lin28B) protein.	–	Higher expression of Lin28B mRNA is seen in cases of OSCC samples. Association found with lymph node metastasis.	Lin et al. (2015)
10.	S-G epithelial cells OECM-1 cancer cells (0–20 μg/ml)	Arecoline induced higher expression of S100A4.	PI3K, JNK pathway. Hypoxia inducible factor 1α involved.	Higher expression seen in cases of OSCC samples, especially those that were moderately or poorly differentiated. Association found with lymph node metastasis.	Hu et al. (2015)

LT – long-term; ROS – reactive oxygen species; PI3K – phosphatidylinositol 3-kinase; Cox-2 – cycloxygenase-2; JNK – c-Jun NH_2-terminal kinase; ERK – extracellular signal-regulated protein kinase; PKC – protein kinase C; AP-1 – activator protein-1

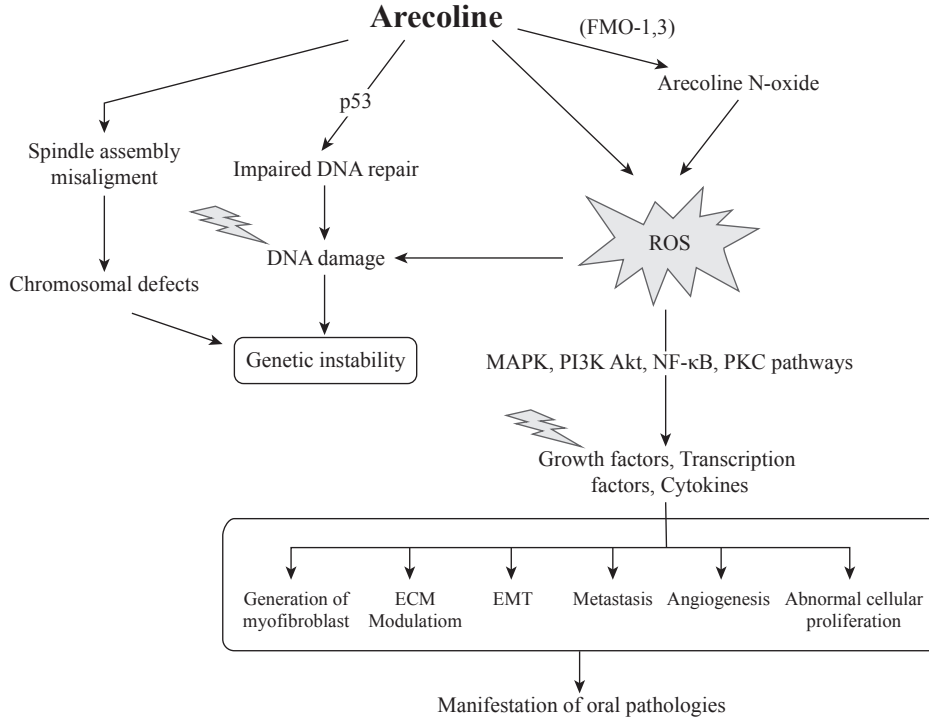

Figure 4 – A hypothetical mechanistic pathway of arecoline mediated oral pathologies. Induction indicated by the symbol:

ROS involvement in cancer includes induction of pathways like mitogen-activated protein kinase (MAPK), phosphatidylinositol-3-kinase (PI3K)/Akt and nuclear factor kappa-light chain enhancer of activated B-cells (NF-κB) (Liou and Storz, 2010). Analysis of the data compiled in Tables 1 and 2 also indicates these pathways to be involved in the up-regulation of pro-fibrotic or carcinogenic factors in cell systems affected by arecoline. Targeting these pathways might be a promising tool in the therapy of ROS induced OSF and OSCC.

Figure 4 depicts hypothetical mechanistic pathways where ROS induced DNA damage along with perturbation of expression profile of growth factors, transcription factors and ECM proteins drive the development of areca nut mediated oral pathologies.

As mentioned earlier, OSF can develop into a malignant phenotype. Therefore, it is important to understand how arecoline triggers the expression of effectors that mediate this transition. Under continuous exposure to hypoxic conditions and HIF-1α activity, the transformation from fibrotic to cancer condition might take place, thereby highlighting arecoline's role as a tumour promoter. Arecoline induced stabilisation of HIF-1α and activation of TGF-β1 play roles in the regulation of

several transcription factors, such as ZEB-1, Snail, Twist, that induce both type 1 and type 2 EMT leading to fibrosis and cancer, respectively (Lee et al., 2013; Chang et al., 2014; Ho et al., 2015; Lee et al., 2016).

Another interesting aspect of arecoline, which was discovered during the study, is its differential activity to induce ECM modulators in fibroblasts and cancer cells. Exposed fibroblasts up-regulate TIMP-1, whereas MMP-2 is inhibited (Chang et al., 2002a). In cancer cells, MMP-9 is induced, but TIMP-1 is inhibited (Chang et al., 2013a). TGF-β1 has been found to regulate the expression of MMP-9 via Snail transcription factor in cancer cells (Sun et al., 2008). After exposure of cells from cancer cell line to arecoline for an extended period of time, increased expression of metalloproteinases MMP-8 and MMP-1 was observed (Liu et al., 2007; Lee et al., 2008). This might indicate that under already initiated and promoted tumour conditions, arecoline might play a role in the progression of areca nut induced carcinogenesis.

Junctional protein disruption is an essential phenomenon by which cells can acquire a metastatic phenotype (Parker et al., 2001). Giri et al. (2010) found arecoline to down-regulate tight junctional protein zona occludens-1 (ZO-1) and claudin-1 along with delocalisation of both ZO-1 and E-cadherin. Down-regulation of E-cadherin during junctional protein disruption leads to the dislocation of β-catenin from the plasma membrane. Under the influence of Wnt signalling in cancer conditions, degradation of cytoplasmic β-catenin is also inhibited. Both junctional and cytoplasmic β-catenin then moves to the nucleus and acquires transcriptional control over genes, leading to abnormal cell proliferative activity (Kam and Quaranta, 2009; Camilli and Weeraratna, 2010; Liu and Millar, 2010). Arecoline exposure induces elevated expression of β-catenin in epithelial cells (Lee et al., 2012b). Signalling cascades have been constructed using the accumulated data in Figure 3.

Role of arecoline metabolites in areca nut induced oral pathologies

Formation of these metabolites *in vitro* or in *in vivo* systems indicates the probability of exposure of humans to these metabolites. An assessment of the biological effects of these metabolites is, therefore, necessary to understand the areca nut mediated pathogenesis of OSF or OSCC.

The N-nitrosated metabolites, NMPA, NMPN and NGL, induce DNA single-stranded breaks in epithelial cells where NMPA was the strongest while NMPN and NGL were weak inducers (Sundqvist et al., 1989). Of the *in vivo* metabolites, genotoxic effects were displayed by arecaidine in mice via induction of sister chromatid exchanges (SCE) in bone marrow cells (Panigrahi and Rao, 1984). Arecoline N-oxide was also found to be genotoxic in both mice model and fibroblasts (Kuo et al., 2015). The genotoxic potential of the other metabolites of arecoline is unknown.

Both MNPA and MNPN were found to be carcinogenic in rats (Wenke et al., 1984b; Nishikawa et al., 1992). NGL was neither found to be a strong mutagen in

the bacterial test system nor a strong carcinogen in the murine test system (Rivenson et al., 1988; Miyazaki et al., 2005). Activated N-nitrosamines can cause alkylation of DNA base pairs (Miyazaki et al., 2005). Hence, activated areca nut derived nitrosamines can initiate carcinogenicity via alkylation of DNA, as indicated by the study where MNPN was observed to induce methylation and cyanoethylation of guanine residues in rats, especially in the genetic material obtained from nasal mucosa, esophagus and liver (Prokopczyk et al., 1987, 1988). The role of arecaidine as a pro-fibrotic agent remains unclear as indicated by contradictory reports in *in vitro* models (Harvey et al., 1986; Tsai et al., 1999; Chang et al., 2013b).

The most important metabolite of arecoline might be arecoline N-oxide. It was found to be mutagenic in bacteria without any metabolic activation (Lin et al., 2011). In mice, the compound induced increased collagen deposition in the tongue along with hyperplasia. Several pro-fibrotic genes (TGF-β1, IL-6, S100A4, and fibronectin) were induced by the compound in fibroblasts along with suppression of E-cadherin (Kuo et al., 2015). Therefore, fibrosis induced by areca nut chewing can be mediated partially by arecoline N-oxide. In another study, N-oxide induced sub-lingual hyperplastic lesions in mice along with the up-regulated expression of caspase-8, which, instead of producing a pro-apoptotic effect, enhanced cell survival and proliferation (Ko et al., 2018). 8-hydroxydeoxy guanosine level in fibroblasts cultured in the presence of arecoline N-oxide indicates oxidative stress induced DNA damage (Kuo et al., 2015). Similarly to arecoline, supplementation of thiol-containing agents can reverse the mutagenic property of the compound (Lin et al., 2011). These facts indicate oxidative stress to be an important factor for both arecoline and arecoline N-oxide induced pathologies. Hence, the consumption of antioxidants can be a preventive factor against the development of fibrosis and areca nut driven oral cancer.

Table 3 summarizes the various effects of arecoline metabolites. It also provides an assessment of the potential harmfulness of the metabolites based on the possibility of involvement in areca nut induced pathologies. Although arecoline N-oxide has been discovered as a possible candidate mediating areca nut effects, in the *in vivo* studies mentioned above, arecoline N-oxide was administered via oral brushing. On the other hand, Lin et al. (2011) observed that the compound lost its mutagenicity after metabolic activation by S9 fraction of rat liver. Hence, the specific role of the compound *in vivo* remains uncertain because the knowledge about direct exposure through areca nut is still unknown.

Involvement of enzymes in the metabolism of arecoline and arecoline N-oxide

A study of arecoline metabolism along with metabolism of its metabolites arecaidine and arecoline N-oxide has revealed basic routes that these compounds undergo. It involves de-esterification, N-oxidation and reduction of the double bond leading to the formation of metabolites, including mercapturic acids, mercapturic acid derivatives and nipecotic acid derivatives (Nery, 1971; Giri et al., 2006, 2007).

According to Patterson and Kosh (1993), cytochrome P450 (CYP450) family of enzymes do not play a significant role in arecoline metabolism because most of arecoline was metabolized by mice liver homogenate even in the presence of nonspecific CYP450 inhibitor. However, these enzymes might be involved in the metabolic activation of N-nitrosamine compounds formed from arecoline. This is supported by a study conducted in a bacterial test system where metabolic activation of MNPN, MNPA and NGL was observed to be carried out by human CYP450 enzymes, especially by members of family CYP2A and CYP1A1 (Miyazaki et al., 2005). CYP enzymes activate N-nitrosamines and the products formed, thereby lead to alkylation of nucleic acid base pairs (Miyazaki et al., 2005). Genetic polymorphisms of CYP enzyme encoding genes (CYP2A6 and CYP1A1) have been found to be associated with oral cancer (Kao et al., 2002; Topcu et al., 2002).

In contrast to CYP450, flavin-containing monooxygenases participate in the metabolism of arecoline to its N-oxide (Giri et al., 2007). No association study has been found so far between the FMO polymorphism and oral cancer. As arecoline N-oxide is biologically active and might have a prominent role in areca nut mediated fibrotic disorders, the existence of polymorphic variants of the gene encoding this enzyme in the general population might develop predisposition towards development of areca nut mediated fibrosis. FMO-1 carries out the process most efficiently of all the other isozymes (Giri et al., 2007). It is abundantly expressed in the kidney (Zhang and Cashman, 2006). An association has been found between betel quid chewing and chronic kidney disorder in a population-based study. However, the association was influenced by several other factors (Hsu et al., 2011). In addition, a portion of the formed N-oxide undergoes reduction and forms the parent compound arecoline. CYP450 family of enzymes plays a role in this type of deoxygenation (Krueger and Williams, 2005; Montellano, 2013).

Carboxylesterases are involved in the metabolism of arecoline to arecaidine (Patterson and Kosh, 1993). *In vitro*, mercapturic acid formation from arecoline does not require any enzymatic assistance (Boyland and Nery, 1969). Therefore, under *in vivo* condition, mercapturic acid formation from the parent compound and metabolites might involve reaction with glutathione without the involvement of any enzymes. Although glutathione S-transferases (GSTs) participate in the phase 2 metabolism of xenobiotics, producing mercapturic acids (Hayakawa, 1977), the involvement of GSTs in arecoline metabolism is not known.

Apart from the study conducted by Patterson and Kosh (1993) and Giri et al. (2007), direct involvement of enzymes in the metabolism of arecoline in mammals has not been studied. In a study carried out by Chiang et al. (2007), arecoline has been found to suppress the expression of several phase I and phase II xenobiotic-metabolizing enzymes, which might indirectly affect the metabolism of arecoline itself. Moreover, mechanism of formation of other metabolites like nipecotic acid derivatives and the aldehyde derivative of arecoline (1-methyl-3,4-dehydropiperidine-3-carboxaldehyde) has not been studied yet.

Table 3 – Summarizes the biological effects of the metabolites of arecoline

Serial no.	Metabolites	Biological activity	Risk assessment
1.	Arecaidine	Mutagenic in bacterial tester strains (TA100, TA 1535, TA 98, TA 1538) (Shirname et al., 1983). Induced sister chromatid exchange in mice bone marrow cells (Panigrahi and Rao, 1984). Weakly induced DNA single strand break in cultured human epithelial cells (Sundqvist et al., 1989). Induced both collagen formation by fibroblasts and collagen phagocytic ability reduction of fibroblasts (Harvey et al., 1986; Tsai et al., 1999). Had no effect on the myofibroblastic transdifferentiation of fibroblasts (Chang et al., 2013b). Induced senescence, DNA double stranded breaks along with transforming growth factor-β and matrix metalloproteinase-2 expressions in fibroblasts (Rehman et al., 2016).	Possibly harmful
2.	Arecoline N-oxide	Mutagenic in bacterial tester strains (TA100, TA 98) (Lin et al., 2011). Induced DNA damage in both mammalian test system and cultured fibroblasts (Kuo et al., 2015). Induced pro-fibrotic genes in cultured fibroblasts (Kuo et al., 2015). Induced caspase-8 activation which rather had a cell proliferative effect (Ko et al., 2018).	Possibly harmful
3.	3-methylnitrosamino-propionitrile	Induced tumour in several organ of exposed rats (Wenke et al., 1984b). Induced modification of DNA base pair in exposed rats (Prokopczyk et al., 1988; Rivenson et al., 1988). Weak inducer of DNA single strand breaks in cultured human epithelial cells (Sundqvist et al., 1989).	Possibly harmful
4.	3-methylnitrosamino-propionaldehyde	Induced DNA single strand break in cultured human epithelial cells (Sundqvist et al., 1989). Induced tumour in several organ of exposed rats (Nishikawa et al., 1992).	Possibly harmful

Serial no.	Metabolites	Biological activity	Risk assessment
5.	N-nitrosoguvacoline	Weakly carcinogenic in rats (Rivenson et al., 1988). Weak inducer of DNA single strand breaks in cultured human epithelial cells (Sundqvist et al., 1989). Weakly mutagenic in bacterial tester strains (TA100, TA 98) (Wang and Peng, 1996).	Possibly harmless
6.	Arecaidine N-oxide	Unknown	–
7.	N-methylnipecotic acid	Unknown	–
8.	1-methylnipecotic acid 1-oxide methylester	Unknown	–
9.	1-methyl-3,4-dehydropiperidine-3-carboxaldehyde	Unknown	–
10.	Arecaidinylglycerol	Unknown	–
11.	Arecaidinylglycine	Unknown	–
12.	N-methylnipecotylglycine	Unknown	–
13.	Mercapturic acid of arecoline	Unknown	–
14.	Mercapturic acid of arecaidine	Unknown	–
15.	Mercapturic acid of arecoline N-oxide	Unknown	–
16.	4-mercapto-1-methylnipecotic acid methylester	Unknown	–
17.	4-methylmercapto-1-methylnipecotic acid 1-oxide methylester	Unknown	–
18.	N-nitrosonipecotic acid	Unknown	–

CYP450 and FMO mediated metabolism of arecoline N-oxide has been found to take place in the mitochondria of liver cells in a study conducted by Wang et al. (2018). Mitochondrial metabolism of arecoline N-oxide by the above-mentioned enzymes might be responsible for the generation of ROS, which mediates the toxic effects of the compound.

Conclusion

Apart from arecaidine and arecoline N-oxide, the biological effects of other metabolites also need to be elucidated. Some of them might be promptly modified by enzymes in a manner similar to mercapturic acids so that their excretion is facilitated, and subsequently, they pose a lesser threat for carcinogenic activity. Other compounds as well as metabolites that possess a high toxic potential might

also be present in areca nut and oral cells might be directly exposed to them on the consumption of the nut. For example, both arecaidine and N-methylnipecotic acid are also present in areca nut (IARC Working Group on the Evaluation of Carcinogenic Risks to Humans, 2004; Hu et al., 2010). But as the toxicity of N-methylnipecotic acid is not known, its effect on the site of exposure cannot be determined.

Knowledge about the enzymes and genes that encodes them can provide an important insight into the metabolism of these xenobiotics. This will open another field of research correlating the differential expression and polymorphisms of these genes to an individual predisposition to oral cancer in betel nut consumers. Even the metabolites might be more potent in causing hazardous effects than the parent compound, as seen in the case of arecoline N-oxide.

References

Angadi, P. V., Kale, A. D., Hallikerimath, S. (2011) Evaluation of myofibroblasts in oral submucous fibrosis: correlation with disease severity. *J. Oral Pathol. Med*. **40**, 208–213.

Boyland, E., Nery, R. (1969) Mercapturic acid formation during the metabolism of arecoline and arecaidine in rat. *Biochem. J.* **113**, 123–130.

Boyland, E., Nice, E., Williams, K. (1971) The catalysis of nitrosation by thiocyanate from saliva. *Food Cosmet. Toxicol.* **9(5)**, 639–643.

Camilli, T. C., Weeraratna, A. T. (2010) Striking the target in Wnt-y conditions: Intervening in Wnt signalling during cancer progression. *Biochem. Pharmacol*. **80**, 702–711.

Chang, M. C., Chan, C. P., Wang, W. T., Chang, B. E., Lee, J. J., Tseng, S. K., Yeung, S. Y., Hahn, L. J., Jeng, J. H. (2013a) Toxicity of areca nut ingredients: Activation of CHK1/CHK2, induction of cell cycle arrest, and regulation of MMP-9 and TIMPs production in SAS epithelial cells. *Head Neck* **35**, 1295–1302.

Chang, M. C., Lin, L. D., Wu, H. L., Ho, Y. S., Hsien, H. C., Wang, T. M., Jeng, P. Y., Cheng, R. H., Hahn, L. J., Jeng, J. H. (2013b) Areca nut-induced buccal mucosa fibroblast contraction and its signalling: A potential role in oral submucous fibrosis – a precancer condition. *Carcinogenesis* **34**, 1096–1104.

Chang, Y. C., Yang, S. F., Tai, K. W., Chou, M. Y., Hsieh, Y. S. (2002a) Increased tissue inhibitor of metalloproteinase-1 expression and inhibition of gelatinase A activity in buccal mucosal fibroblasts by arecoline as possible mechanisms for oral submucous fibrosis. *Oral Oncol*. **38**, 195–200.

Chang, Y. C., Tsai, C. H., Tai, K. W., Yang, S. H., Chou, M. Y., Lii, C. K. (2002b) Elevated vimentin expression in buccal mucosal fibroblasts by arecoline *in vitro* as a possible pathogenesis for oral submucous fibrosis. *Oral Oncol*. **38**, 425–430.

Chang, Y. C., Tsai, C. H., Lai, Y. L., Yu, C. C., Chi, W. Y., Li, J. J., Chang, W. W. (2014) Arecoline-induced myofibroblast transdifferentiation from human buccal mucosal fibroblasts is mediated by ZEB1. *J. Cell. Mol. Med.* **18**, 698–708.

Chen, Y. C., Chen, B. C., Yu, C. C., Lin, S. H., Lin, C. H. (2016) miR-19a, -19b, and -26b mediate CTGF expression and pulmonary fibroblast differentiation. *J. Cell. Physiol.* **231**, 2236–2248.

Chiang, S. L., Jiang, S. S., Wang, Y. J., Chiang, H. C., Chen, P. H., Tu, H. P., Ho, K. Y., Tsai, Y. S., Chang, I. S., Ko, Y. C. (2007) Characterization of arecoline-induced effects on cytotoxicity in normal human gingivial fibroblasts by global gene expression profiling. *Toxicol. Sci.* **100(1)**, 66–74.

Cox, S., Vickers, E. R., Ghu, S., Zoellner, H. (2010) Salivary arecoline levels during areca nut chewing in human volunteers. *J. Oral Pathol. Med.* **39**, 465–469.

Dasgupta, R., Saha, I., Pal, S., Bhattacharyya, A., Sa, G., Nag, T. C., Das, T., Maiti, B. R. (2006) Immunosuppression, hepatotoxicity and depression of antioxidant status by arecoline in albino mice. *Toxicology* **227**, 94–104.

Deb, S., Chatterjee, A. (1998) Influence of buthionine sulfoximine and reduced glutathione on arecoline-induced chromosomal damage and sister chromatid exchange in mouse bone marrow cells *in vivo*. *Mutagenesis* **13**, 243–248.

Deng, Y. T., Chen, H. M., Cheng, S. J., Chiang, C. P., Kuo, M. Y. P. (2009) Arecoline-stimulated connective tissue growth factor production in human buccal mucosal fibroblasts: Modulation by curcumin. *Oral Oncol.* **45**, e99–e105.

Eckert, A. W., Wickenhauser, C., Salins, P. C., Kappler, M., Bukur, J., Seliger, B. (2016) Clinical relevance of the tumor microenvironment and immune escape of oral squamous cell carcinoma. *J. Transl. Med.* **14**, 85.

Eickelberg, O., Köhler, E., Reichenberger, F., Bertschin, S., Woodtli, T., Eme, P., Perruchoud, A. P., Roth, M. (1999) Extracellular matrix deposition by primary human lung fibroblasts in response to TGF-beta1 and TGF-beta3. *Am. J. Physiol.* **276(5)**, 814–824.

Ferlay, J., Soerjomataram, I., Dikshit, R., Eser, S., Mathers, C., Rebelo, M., Parkin, D. M., Forman, D., Bray, F. (2015) Cancer incidence and mortality worldwide: Sources, methods and major patterns in GLOBOCAN 2012. *Int. J. Cancer* **136**, E359–E386.

Giri, S., Idle, J. R., Chen, C., Zabriskie, T. M., Krausz, K. W., Gonzalez, F. J. (2006) A metabolomic approach to the metabolism of the areca nut alkaloids arecoline and arecaidine in the mouse. *Chem. Res. Toxicol.* **19(6)**, 818–827.

Giri, S., Krausz, K. W., Idle, J. R., Gonzalez, F. J. (2007) The metabolomics of (±)-arecoline 1-oxide in the mouse and its formation by human flavin-containing monooxygenases. *Biochem. Pharmacol.* **73(4)**, 561–573.

Giri, S., Poindexter, K. M., Sundar, S. N., Firestone, G. L. (2010) Arecoline induced disruption of expression and localization of the tight junctional protein ZO-1 is dependent on the HER 2 expression in human endometrial Ishikawa cells. *BMC Cell Biol.* **11**, 53.

Griffin, M., Casadio, R., Bergamini, C. M. (2002) Transglutaminases: Nature's biological glues. *Biochem. J.* **368**, 377–396.

Harvey, W., Scutt, A., Meghji, S., Canniff, J. P. (1986) Stimulation of human buccal mucosa fibroblasts *in vitro* by betel-nut alkaloids. *Arch. Oral Biol.* **31(1)**, 45–49.

Hayakawa, T. (1977) Glutathione S-transferases in the metabolism of foreign compounds. *Ecotoxicol. Environ. Saf.* **1(3)**, 305–309.

Higgins, D. F., Biju, M. P., Akai, Y., Wutz, A., Johnson, R. S., Haase, V. H. (2004) Hypoxic induction of *Ctgf* is directly mediated by Hif-1. *Am. J. Physiol. Renal Physiol.* **287**, 1223–1232.

Ho, C. M., Hu, F. W., Lee, S. S., Shieh, T. M., Yu, C. H., Lin, S. S., Yu, C. C. (2015) ZEB1 as an indicator of tumor recurrence for areca quid chewing-associated oral squamous cell carcinomas. *J. Oral Pathol. Med.* **44**, 693–698.

Hsieh, Y. P., Chen, H. M., Chang, J. Z. C., Chiang, C. P., Deng, Y. T., Kuo, M. Y. P. (2015) Arecoline stimulated early growth response-1 production in human buccal fibroblasts: Suppression by epigallocatechin-3-gallate. *Head Neck* **37**, 493–497.

Hsieh, Y. P., Chen, H. M., Lin, H. Y., Yang, H., Chang, J. Z. C. (2017) Epigallocatechin-3-gallate inhibits transforming-growth-factor-β1-induced collagen synthesis by suppressing early growth response-1 in human buccal mucosal fibroblasts. *J. Formos. Med. Assoc.* **116**, 107–113.

Hsu, Y. H., Liu, W. H., Chen, W., Kuo, Y. C., Hsiao, C. Y., Hung, P. H., Jong, I. C., Chiang, P. C., Hsu, C. C. (2011) Association of betel nut chewing with chronic kidney disease: A retrospective 7-year study in Taiwan. *Nephrology (Carlton)* **16**, 751–757.

Hu, F. W., Lee, S. S., Yang, L. C., Tsai, C. H., Wang, T. H., Chou, M. Y., Yu, C. C. (2015) Knockdown of S100A4 impairs arecoline-induced invasiveness of oral squamous cell carcinomas. *Oral Oncol.* **51**, 690–697.

Hu, W. C., Chang, Y. Z., Wang, H. W., Chao, M. R. (2010) High-throughput simultaneous analysis of five urinary metabolites of areca nut and tobacco alkaloids by isotope-dilution liquid chromatography-tandem mass spectrometry with on line solid phase extraction. *Cancer Epidemiol. Biomarkers Prev.* **19(10)**, 2570–2581.

Huang, L. W., Hsieh, B. S., Cheng, H. L., Hu, Y. C., Chang, W. T., Chang, K. L. (2012) Arecoline decreases interleukin-6 production and induces apoptosis and cell cycle arrest in human basal cell carcinoma cells. *Toxicol. Appl. Pharmacol.* **258**, 199–207.

Hung, S. P., Yang, M. H., Tseng, K. F., Lee, O. K. (2013) Hypoxia-induced secretion of TGF-β1 in mesenchymal stem cell promotes breast cancer cell progression. *Cell Transplant.* **22**, 1869–1882.

Hung, T. C., Huang, L. W., Su, S. J., Hsieh, B. S., Cheng, H. L., Hu, Y. C., Chen, Y. H., Hwang, C. C., Chang, K. L. (2011) Hemeoxygenase-1 expression in response to arecoline-induced oxidative stress in human umbilical vein endothelial cells. *Int. J. Cardiol.* **151**, 187–194.

IARC Working Group on the Evaluation of Carcinogenic Risks to Humans (2004) Betel-quid and areca-nut chewing and some areca-nut-derived nitrosamines. *IARC Monogr. Eval. Carcinog. Risks Hum.* **85**, 1–334.

Jeng, J. H., Wang, Y. J., Chiang, B. L., Lee, P. H., Chan, C. P., Ho, Y. S., Wang, T. M., Lee, J. J., Hahn, L. J., Chang, M. C. (2003) Roles of keratinocyte inflammation in oral cancer: Regulating the prostaglandin E2, interleukin-6 and TNF-α production of oral epithelial cells by areca nut extract and arecoline. *Carcinogenesis* **24**, 1301–1315.

Ji, W. T., Yang, S. R., Chen, J. Y. F., Cheng, Y. P., Lee, Y. R., Chiang, M. K., Chen, H. R. (2012) Arecoline downregulates levels of p21 and p27 through the reactive oxygen species/mTOR complex 1 pathway and may contribute to oral squamous cell carcinoma. *Cancer Sci.* **103**, 1221–1229.

Jobling, M. F., Mott, J. D., Finnegan, M. T., Jurukovski, V., Erickson, A. C., Walian, P. J., Taylor, S. E., Ledbetter, S., Lawrence, C. M., Rifkin, D. B., Barcellos-Hof, M. H. (2006) Isoform-specific activation of latent transforming growth factor beta (LTGF-beta) by reactive oxygen species. *Radat. Res.* **166**, 839–848.

Jung, S. N., Yang, W. K., Kim, J., Kim, H. S., Kim, E. J., Yun, H., Park, H., Kim, S. S., Choe, W., Kang, I., Ha, J. (2008) Reactive oxygen species stabilize hypoxia-inducible factor-1 alpha protein and stimulate transcriptional activity via AMP-activated protein kinase in DU145 human prostate cancer cells. *Carcinogenesis* **29(4)**, 713–721.

Kademani, D. (2007) Oral cancer. *Mayo Clin. Proc.* **82(7)**, 878–887.

Kao, S. Y., Wu, C. H., Lin, S. C., Yap, S. K., Chang, C. S., Wong, Y. K., Chi, L. Y., Liu, T. Y. (2002) Genetic polymorphism of cytochrome P4501A1 and susceptibility to oral squamous cell carcinoma and oral precancer lesions associated with smoking/betel use. *J. Oral Pathol. Med.* **31(9)**, 505–511.

Kam, Y., Quaranta, V. (2009) Cadherin-bound β-catenin feeds into the Wnt pathway upon adherens junction dissociation: Evidence for an intersection between β-catenin pools. *PLoS One* **4(2)**, e4580.

Kamath, V. V., Krishnamurthy, S., Satelur, K. P., Rajkumar, K. (2015) Transforming growth factor-β1 and TGF-β2 act synergistically in the fibrotic pathway in oral submucous fibrosis: An immunohistochemical observation. *Indian J. Med. Paediatr. Oncol.* **36(2)**, 111–116.

Ko, Y. C., Chang, P. Y., Kuo, T. M., Chen, P. K., Lin, Y. Z., Hua, C. H., Chen, Y. C. (2018) Arecoline N-oxide up-regulates caspase-8 expression in oral hyperplastic lesions of mice. *J. Agric. Food Chem.* **65(47)**, 10197–10205.

Krueger, S. K., Williams, D. E. (2005) Mammalian flavin containing monooxygenases: Structure/function, genetic polymorphisms and role in drug metabolism. *Pharmacol. Ther.* **106(3)**, 357–387.

Kuo, T. M., Luo, S. Y., Chiang, S. L., Yeh, K. T., Hsu, H. T., Wu, C. T., Lu, C. Y., Tsai, M. H., Chang, J. G.,

Ko, Y. C. (2015) Fibrotic effects of arecoline N-oxide in oral potentially malignant disorders. *J. Agric. Food Chem.* **63(24)**, 5787–5794.

Lamouille, S., Xu, J., Derynck, R. (2014) Molecular mechanisms of epithelial-mesenchymal transition. *Nat. Rev. Mol. Cell Biol.* **15**, 178–196.

Lee, C. H., Liu, S. Y., Lin, M. H., Chiang, W. F., Chen, T. C., Huang, W. T., Chou, D. S., Chiu, C. T., Liu, Y. C. (2008) Upregulation of matrix metalloproteinase-1 (MMP-1) expression in oral carcinomas of betel quid (BQ) users: Roles of BQ ingredients in the acceleration of tumour cell motility through MMP-1. *Arch. Oral Biol.* **53**, 810–818.

Lee, P. H., Chang, M. C., Chang, W. H., Wang, T. M., Wang, Y. J., Hahn, L. J., Ho, Y. S., Lin, C. Y., Jeng, J. H. (2006) Prolonged exposure to arecoline arrested human KB epithelial cell growth: Regulatory mechanisms of cell cycle and apoptosis. *Toxicology* **220**, 81–89.

Lee, S. S., Tsai, C. H., Ho, Y. C., Chang, Y. C. (2008a) The upregulation of heat shock protein 70 expression in areca quid chewing-associated oral squamous cell carcinomas. *Oral Oncol.* **44**, 884–890.

Lee, S. S., Yang, S. F., Ho, Y. C., Tsai, C. H., Chang, Y. C. (2008b) The upregulation of metallothionein-1 expression in areca quid chewing-associated oral squamous cell carcinomas. *Oral Oncol.* **44**, 180–186.

Lee, S. S., Yang, S. F., Tsai, C. H., Chou, M. C., Chou, M. Y., Chang, Y. C. (2008c) Upregulation of heme oxygenase-1 expression in areca-quid-chewing-associated oral squamous cell carcinoma. *J. Formos. Med. Assoc.* **107**, 355–363.

Lee, S. S., Tsai, C. H., Yang, S. F., Ho, Y. C., Chang, Y. C. (2010) Hypoxia inducible factor-1α expression in areca quid chewing-associated oral squamous cell carcinomas. *Oral Dis.* **16**, 696–701.

Lee, S. S., Tseng, L. H., Li, Y. C., Tsai, C. H., Chang, Y. C. (2011) Heat shock protein 47 expression in oral squamous cell carcinomas and up-regulated by arecoline in human oral epithelial cells. *J. Oral Pathol. Med.* **40**, 390–396.

Lee, S. S., Tsai, C. H., Ho, Y. C., Yu, C. C., Chang, Y. C. (2012a) Heat shock protein 27 expression in areca quid chewing-associated oral squamous cell carcinomas. *Oral Dis.* **18**, 713–719.

Lee, S. S., Tsai, C. H., Tsai, L. L., Chou, M. C., Chou, M. Y., Chang, Y. C. (2012b) β-catenin expression in areca quid chewing associated oral squamous cell carcinomas and up-regulated by arecoline in human oral epithelial cells. *J. Formos. Med. Assoc.* **111**, 194–200.

Lee, S. S., Tsai, C. H., Yu, C. C., Chang, Y. C. (2013) Elevated snail expression mediates tumor progression in areca quid chewing-associated oral squamous cell carcinoma via reactive oxygen species. *PLoS One* **8**, e67985.

Lee, S. S., Chen, Y. J., Tsai, C. H., Huang, F. M., Chang, Y. C. (2015) Elevated transglutaminase-2 expression mediates fibrosis in areca quid chewing-associated oral submucocal fibrosis via reactive oxygen species generation. *Clin. Oral Investig.* **20**, 1029–1034.

Lee, Y. H., Yang, L. C., Hu, F. W., Peng, C. Y., Yu, C. H., Yu, C. C. (2016) Elevation of Twist expression by arecoline contributes to the pathogenesis of oral submucous fibrosis. *J. Formos. Med. Assoc.* **115**, 311–317.

Lin, C. H., Yu, M. C., Tung, W. H., Chen, T. T., Yu, C. C., Weng, C. M., Tsai, Y. J., Bai, K. J., Hong, C. Y., Chien, M. H., Chen, B. C. (2013) Connective tissue growth factor induces collagen I expression in human lung fibroblasts through the Rac1/MLK3/JNK/AP-1 pathway. *Biochim. Biophys. Acta* **1833**, 2823–2833.

Lin, K. H., Lin, C. Y., Liu, C. C., Chou, M. Y., Lin, J. K. (2011) Arecoline N-oxide: Its mutagenicity and possible role as ultimate carcinogen in areca oral carcinogenesis. *J. Agric. Food Chem.* **59(7)**, 3420–3428.

Lin, W. T., Shieh, T. M., Yang, L. C., Wang, T. Y., Chou, M. Y., Yu, C. C. (2015) Elevated Lin28B expression is correlated with lymph node metastasis in oral squamous cell carcinomas. *J. Oral Pathol. Med.* **44**, 823–830.

Liou, G. Y., Storz, P. (2010) Reactive oxygen species in cancer. *Free Radic. Res.* **44(5)**, 479–496.

Liu, F., Millar, S. E. (2010) Wnt/β-catenin signaling in oral tissue development and disease. *J. Dent. Res.* **89**, 318–330.

Liu, S. Y., Liu, Y. C., Huang, W. T., Huang, G. C., Chen, T. C., Lin, M. H. (2007) Up-regulation of matrix metalloproteinase-8 by betel quid extract and arecoline and its role in 2D motility. *Oral Oncol.* **43**, 1026–1033.

Lu, S. L., Reh, D., Li, A. G., Woods, J., Corless, C. L., Martin, M. K., Wang, X. J. (2004) Overexpression of transforming growth factor-1 in head and neck epithelia results in inflammation, angiogenesis, and epithelial hyperproliferation. *Cancer Res.* **64**, 4405–4410.

Marchei, E., Durgbanshi, A., Rossi, S., Garcia-Algar, O., Zuccaro, P., Pichini, S. (2005) Determination of arecoline (areca nut alkaloid) and nicotine in hair by high-performance liquid chromatography/electrospray quadrupole mass spectrometry. *Rapid Commun. Mass Spectrom.* **19**, 3416–3418.

McMohan, S., Charbonneau, M., Grandmont, S., Richard, D. E., Dubois, C. M. (2006) Transforming growth factor β1 induces hypoxia-inducible factor-1 stabilization through selective inhibition of PHD2 expression. *J. Biol. Chem.* **281(34)**, 24171–24181.

Micallef, L., Vedrenne, N., Billet, F., Coulomb, B., Darby, I. A., Desmoulière, A. (2012) The myofibroblast, multiple origins for major roles in normal and pathological tissue repair. *Fibrogenesis Tissue Repair* **5**, S5.

Miyazaki, M., Sugawara, E., Yoshimura, T., Yamazaki, H., Kamataki, T. (2005) Mutagenic activation of betel quid-specific N-nitrosamines catalyzed by human cytochrome P450 coexpressed with NADPH-cytochrome P450 reductase in *Salmonella typhimurium* YG7108. *Mutat. Res.* **581(1–2)**, 165–171.

Montellano, P. R. O. (2013) Cytochrome P-450-activated prodrugs. *Future Med. Chem.* **5(2)**, 213–228.

Moutasim, K. A., Jenei, V., Sapienza, K., Marsh, D., Weinreb, P. H., Violette, S. M., Lewis, M. P., Marshall, J. F., Fortune, F., Tilakratne, W. M., Hart, I. R., Thomas, G. J. (2011) Betel-derived alkaloid up-regulates keratinocyte alphavbeta6 integrin expression and promotes oral submucous fibrosis. *J. Pathol.* **223**, 366–377.

Nery, R. (1971) The metabolic interconversion of arecoline and arecoline 1-oxide in the rat. *Biochem. J.* **122(4)**, 503–508.

Nishikawa, A., Prokopczyk, B., Rivenson, A., Zang, E., Hoffmann, D. (1992) A study of betel quid carcinogenesis. VIII. Carcinogenicity of 3-(methylnitrosamino)propionaldehyde in F344 rats. *Carcinogenesis* **13(3)**, 369–372.

Ohshima, H., Friesen, M., Bartsch, H. (1989) Identification in rats of N-nitrosonipecotic acid as a major urinary metabolite of the areca-nut alkaloid-derived nitrosamines, N-nitrosoguvacoline and N-nitrosoguvacine. *Cancer Lett.* **44(3)**, 211–216.

Panigrahi, G. B., Rao, A. R. (1984) Induction of *in vivo* sister chromatid exchanges byarecaidine, a betel nut alkaloid, in mouse bone marrow cells. *Cancer Lett.* **23(2)**, 189–192.

Parker, C., Rampaul, R. S., Pinder, S. E., Bell, J. A., Wencyk, P. M., Blamey, R. W., Nicholson, R. I., Robertson, J. F. R., Ellis, I. O. (2001) E-cadherin as a prognostic indicator in primary breast cancer. *Br. J. Cancer* **85**, 1958–1963.

Patterson, T. A., Kosh, J. W. (1993) Elucidation of the rapid *in vivo* metabolism of arecoline. *Gen. Pharmacol.* **24(3)**, 641–647.

Pellegrini, M., Marchei, E., Rossi, S., Vagnarelli, F., Durgbanshi, A., Garcia-Algar, O., Vall, O., Pichini, S. (2007) Liquid chromatography/electrospray ionization tandem mass spectrometry assay for determination of nicotine and metabolites, caffeine and arecoline in breast milk. *Rapid Commun. Mass Spectrom.* **21**, 2693–2703.

Peng, W., Liu, Y. J., Wu, N., Sun, T., He, X. Y., Gao, Y. X., Wu, C. J. (2015) *Areca catechu* L. (*Arecaceae*): A review of its traditional uses, botany, phytochemistry, pharmacology and toxicology. *J. Ethnopharmacol.* **164**, 340–356.

Pichini, S., Pellegrini, M., Pacifici, R., Marchei, E., Murillo, J., Puig, C., Vall, O., Garcia-Algar, O. (2003) Quantification of arecoline (areca nut alkaloid) in neonatal biological matrices by high-performance liquid chromatography/electrospray quadrupole mass spectrometry. *Rapid Commun. Mass Spectrom.* **17**, 1958–1964.

Prokopczyk, B., Rivenson, A., Bertinato, P., Brunnemann, K. D., Hoffmann, D. (1987) 3-(Methylnitrosamino) proprionitrile: Occurrence in saliva of betel quid chewers, carcinogenicity, and DNA methylation in F344 rats. *Cancer Res.* **47(2)**, 467–471.

Prokopczyk, B., Bertinato, P., Hoffmann, D. (1988) Cyanoethylation of DNA *in vivo* by 3-(methylnitrosamino) propionitrile, an *Areca*-derived carcinogen. *Cancer Res.* **48(23)**, 6780–6784.

Rankin, E. B., Giaccia, A. J. (2016) Hypoxic control of metastasis. *Science* **352**, 175–180.

Rehman, A., Ali, S., Lone, M. A., Atif, M., Hassona, Y., Prime, S. S., Pitiyage, G. N., James, E. L. N., Parkinson, E. K. (2016) Areca nut alkaloids induce irreparable DNA damage and senescence in fibroblasts and may create a favourable environment for tumour progression. *J. Oral Pathol. Med*. **45(5)**, 365–372.

Reichart, P. A., Philipsen, H. P. (2005) Oral erythroplakia – a review. *Oral Oncol.* **41**, 551–561.

Richter, K., Kietzmann, T. (2016) Reactive oxygen species and fibrosis: further evidence of a significant liason. *Cell Tissue Res.* **365**, 591–605.

Rivenson, A., Hoffmann, D., Prokopczyk, B., Amin, S., Hecht, S. S. (1988) Induction of lung and exocrine pancreas tumours in F344 rats by tobacco-specific and *Areca*-derived N-nitrosamines. *Cancer Res.* **48(23)**, 6912–6917.

Rivera, C. (2015) Essentials of oral cancer. *Int. J. Clin. Exp. Pathol*. **8**, 11884–11894.

Samarakoon, R., Higgins, S. P., Higgins, C. E., Higgins, P. J. (2008) TGF-β1-induced plasminogen activator inhibitor-1 expression in vascular smooth muscle cells requires pp60(c-src)/EGFR(Y845) and Rho/ROCK signalling. *J. Mol. Cell. Cardiol.* **44**, 527–538.

Shieh, D. H., Chiang, L. C., Lee, C. H., Yang, Y. H., Shieh, T. Y. (2004) Effects of arecoline, safrole, and nicotine on collagen phagocytosis by human buccal mucosal fibroblasts as a possible mechanism for oral submucous fibrosis in Taiwan. *J. Oral Pathol. Med.* **33**, 581–587.

Shirname, L. P., Menon, M. M., Nair, J., Bhide, S. V. (1983) Correlation of mutagenicity and tumorigenicity of betel quid and its ingredients. *Nutr. Cancer* **5(2)**, 87–91.

Shirname, L. P., Menon, M. M., Bhide, S. V. (1984) Mutagenicity of betel quid and its ingredients using mammalian test systems. *Carcinogenesis* **5**, 501–503.

Shivapurkar, N. M., D'Souza, A. V., Bhide, S. V. (1980) Effect of betel-quid chewing on nitrite levels in saliva. *Food Cosmet. Toxicol.* **18(3)**, 277–281.

Sun, L., Diamond, M. E., Ottaviano, A. J., Joseph, M. J., Ananthanarayan, V., Hidayatullah G., Munshi, H. G. (2008) Transforming growth factor-β1 promotes matrix metalloproteinase-9 mediated oral cancer invasion through snail expression. *Mol. Cancer Res.* **6(1)**, 10–20.

Sundqvist, K., Liu, Y., Nair, J., Bartsch, H., Arvidson, K., Grafström, R. C. (1989) Cytotoxic and genotoxic effects of areca nut-related compound in cultured human buccal epithelial cells. *Cancer Res.* **49**, 5294–5298.

Thangjam, G. S., Kondaiah, P. (2009) Regulation of oxidative-stress responsive genes by arecoline in human keratinocytes. *J. Periodontal Res*. **44**, 673–682.

Thangjam, G. S., Agarwal, P., Balapure, A. K., Rao, S. G., Kondaiah, P. (2009) Regulation of extracellular matrix genes by arecoline in primary gingival fibroblasts requires epithelial factors. *J. Periodontal Res*. **44**, 736–743.

Tilakaratne, W. M., Klinikowski, M. F., Saku, T., Peters, T. J., Warnakuasuriya, S. (2006) Oral submucous fibrosis: review on aetiology and pathogenesis. *Oral Oncol.* **42**, 561–568.

Topcu, Z., Chiba, I., Fujieda, M., Shibata, T., Ariyoshi, N., Yamazaki, H., Sevqican, F., Muthumala, M.,

Kobayashi, H., Kamataki, T. (2002) CYP2A6 gene deletion reduces oral cancer risk in betel quid chewers in Sri Lanka. *Carcinogenesis* **23(4)**, 595–598.

Tsai, C. C., Ma, R. H., Shieh, T. Y. (1999) Deficiency in collagen and fibronectin phagocytosis by human buccal mucosa fibroblasts *in vitro* as a possible mechanism for oral submucous fibrosis. *J. Oral Pathol. Med.* **28(2)**, 59–63.

Tsai, C. H., Chou, M. Y., Chang, Y. C. (2003) The up-regulation of cyclooxygenase-2 expression in human buccal mucosal fibroblasts by arecoline: A possible role in the pathogenesis of oral submucous fibrosis. *J. Oral Pathol. Med*. **32**, 146–153.

Tsai, C. H., Yang, S. F., Chen, Y. J., Chou, M. Y., Chang, Y. C. (2005a) The upregulation of insulin-like growth factor-1 in oral submucous fibrosis. *Oral Oncol*. **41**, 940–946.

Tsai, C. H., Yang, S. F., Chen, Y. J., Chou, M. Y., Chang, Y. C. (2005b) Raised keratinocyte growth factor-1 expression in oral submucous fibrosis *in vivo* and up-regulated by arecoline in human buccal mucosal fibroblasts *in vitro*. *J. Oral Pathol. Med.* **34**, 100–105.

Tsai, C. H., Yang, S. F., Chang, Y. C. (2007) The upregulation of cystatin C in oral submucous fibrosis. *Oral Oncol.* **43**, 680–685.

Tsai, C. H., Yang, S. F., Lee, S. S., Chang, Y. C. (2009) Augmented heme oxygenase-1 expression in areca quid chewing-associated oral submucous fibrosis. *Oral Dis.* **15**, 281–286.

Tsai, C. H., Lee, S. S., Huang, F. M., Chang, Y. C. (2013) Regulation of protease-activated receptor-1 expression in human buccal fibroblasts stimulated with arecoline. *Head Neck* **35**, 1314–1318.

Tsai, C. H., Lee, S. S., Chang, Y. C. (2015) Hypoxic regulation of plasminogen activator inhibitor-1 expression in human buccal mucosa fibroblasts stimulated with arecoline. *J. Oral Pathol. Med*. **44**, 669–673.

Tsai, Y. P., Wu, K. J. (2012) Hypoxia-regulated target genes implicated in tumor metastasis. *J. Biomed. Sci.* **19**, 102.

Tsai, Y. S., Lee, K. W., Huang, J. L., Liu, Y. S., Juo, S. H. H., Kuo, W. R., Chang, J. G., Lin, C. S., Jong, Y. J. (2008) Arecoline, a major alkaloid of areca nut, inhibits p53, represses DNA repair, and triggers DNA damage response in human epithelial cells. *Toxicology* **249**, 230–237.

Wang, C. K., Peng, C. H. (1996) The mutagenicities of alkaloids and N-nitrosoguvacoline from betel quid. *Mutat. Res.* **360**, 165–171.

Wang, T. S., Lin, C. P., Chen, Y. P., Chao, M. R., Li, C. C., Liu, K. L. (2018) CYP450-mediated mitochondrial ROS production involved in arecoline N-oxide-induced oxidative damage in liver cell lines. *Environ. Toxicol.* **33**, 1029–1038.

Wang, Y. C., Tsai, Y. S., Huang, J. L., Lee, K. W., Kuo, C. C., Wang, C. S., Huang, A. M., Chang, J. Y., Jong, Y. J., Lin, C. S. (2010) Arecoline arrests cells at prometaphase by deregulating mitotic spindle assembly and spindle assembly checkpoint: Implication for carcinogenesis. *Oral Oncol.* **46**, 255–262.

Wen, X. M., Zhang, Y. L., Liu, X. M., Guo, S. X., Wang, H. (2006) Immune responses in mice to arecoline mediated by lymphocyte muscarinic acetylcholine receptor. *Cell Biol. Int.* **30**, 1048–1053.

Wenke, G., Hoffmann, D. (1983) A study of betel quid carcinogenesis. I. On the *in vitro* N-nitrosation of arecoline. *Carcinogenesis* **4(2)**, 169–172.

Wenke, G., Brunnemann, K. D., Hoffmann, D., Bhide, S. V. (1984a) A study of betel quid carcinogenesis. IV. Analysis of the saliva of betel chewers: a preliminary report. *J. Cancer Res. Clin. Oncol.* **108(1)**, 110–113.

Wenke, G., Rivenson, A., Hoffmann, D. (1984b) A study of betel quid carcinogenesis. 3. 3-(Methylnitrosamino)-propionitrile, a powerful carcinogen in F344 rats. *Carcinogenesis* **5(9)**, 1137–1140.

Wu, I. C., Chen, P. H., Wang, C. J., Wu, D. C., Tsai, S. M., Chao, M. R., Chen, B. H., Lee, H. H., Lee, C. H., Ko, Y. C. (2010) Quantification of blood betel quid alkaloids and urinary 8-hydroxydeoxyguanosine in humans and their association with betel chewing habits. *J. Anal. Toxicol.* **34**, 325–331.

Yang, S. F., Hsieh, Y. S., Tsai, C. H., Chou, M. Y., Chang, Y. C. (2003) The upregulation of type I plasminogen activator inhibitor in oral submucous fibrosis. *Oral Oncol.* **39**, 367–372.

Yang, S. F., Tsai, C. H., Chang, Y. C. (2008) The upregulation of heat shock protein 47 expression in human buccal fibroblasts stimulated with arecoline. *J. Oral Pathol. Med*. **37**, 206–210.

Yang, W. H., Kuo, M. Y., Liu, C. M., Deng, Y. T., Chang, H. H., Chang, J. Z. (2013) Curcumin inhibits TGFβ1-induced CCN2 via Src, JNK, and Smad3 in gingiva. *J. Dent. Res.* **92**, 629–634.

Yang, W. H., Deng, Y. T., Hsieh, Y. P., Wu, K. J., Kuo, M. Y. (2016) Thrombin activates latent TGFβ1 via integrin αvβ1 in gingival fibroblasts. *J. Dent. Res.* **95**, 939–945.

Yu, C. C., Tsai, C. H., Hsu, H. I., Chang, Y. C. (2013) Elevation of S100A4 expression in buccal mucosal fibroblasts by arecoline: Involvement in the pathogenesis of oral submucous fibrosis. *PLoS One* **8**, e55122.

Zhang, J., Cashman, J. R. (2006) Quantitative analysis of FMO gene mRNA levels in human tissues. *Drug Metab. Dispos*. **34**, 19–26.

Zheng, L., Jian, X., Guo, F., Li, N., Jiang, C., Yin, P., Min, A. J., Huang, L. (2015) miR-203 inhibits arecoline-induced epithelial-mesenchymal transition by regulating secreted frizzled-related protein 4 and transmembrane-4 L six family member 1 in oral submucous fibrosis. *Oncol. Rep.* **33**, 2753–2760.

Zhou, Z. S., Li, M., Gao, F., Peng, J. Y., Xiao, H. B., Dai, L. X., Lin, S. R., Zhang, R., Jin, L. Y. (2013) Arecoline suppresses HaCaT cell proliferation through cell cycle regulatory molecules. *Oncol. Rep.* **29**, 2438–2444.

 Prague Medical Report / Vol. 121 (2020) No. 4, p. 236–243

Association Study of MBL2 Gene Polymorphisms and Risk of Tuberculosis in Southeast of Iran

Mohsen Taheri[1,2], Rezvan Karimloo[3], Hosna Sarani[4], Behrouz Molashahi[1], Mohammad Naderi[3], Gholamreza Bahari[4], Mohammad Hashemi[1†]

[1]Genetics of Non-Communicable Disease Research Center, Zahedan University of Medical Sciences, Zahedan, Iran;
[2]Department of Genetic, School of Medicine, Zahedan University of Medical Sciences, Zahedan, Iran;
[3]Infectious Diseases and Tropical Medicine Research Center, Resistant Tuberculosis Institute, Zahedan University of Medical Sciences, Zahedan, Iran;
[4]Children and Adolescent Health Research Center, Resistant Tuberculosis Institute, Zahedan University of Medical Sciences, Zahedan, Iran
[†]Deceased

Received January 10, 2020; Accepted November 5, 2020.

Key words: Tuberculosis – MBL2 – Polymorphism – Genotype

Abstract: Mannose-binding lectin (MBL) is an acute phase protein which recognizes the pathogens through its carbohydrate recognition domain. It is an important part of human innate immunity. The aim of the current study was to evaluate the impact of MBL2 polymorphism on pulmonary tuberculosis in a number of patients from the southeast of Iran. In this case-control study, 2 MBL gene polymorphisms (rs1800450, rs7095891) were genotyped using PCR-RFLP method and polymerase chain reaction for detection of 34bp ins/del of MBL2 gene (rs777980157) polymorphism. The study included 170 patients with PTB (pulmonary tuberculosis) and 175 control subjects. The findings indicated that the GA (GA vs. GG: OR=0.172, 95% CI=0.107–0.275, P<0.001) (OR – odds ratio; CI – confidence interval) genotype as well as GA+AA (GA+AA vs. GG: OR=0.191, 95% CI=0.120–0.302, P<0.001)

This study was supported by a dissertation grant (#8513) from Zahedan University of Medical Sciences.

Mailing Address: Prof. Mohsen Taheri, PhD., Department of Genetic, School of Medicine, Zahedan University of Medical Sciences, Zahedan 9816743463, Iran; Phone: +98 541 333 721 16; e-mails: mohsen.taheri.gene@gmail.com, taheri@zaums.ac.ir

https://doi.org/10.14712/23362936.2020.20

genotype of rs1800450 reduced the risk of PTB compared to GG genotype. The rs7095891 variant significantly decreased the risk of PTB in codominant (GA vs. GG: OR=0.118, 95% CI=0.054–0.258, P<0.001; and AA vs. GG: OR=0.029, 95% CI=0.01–0.082, P<0.001), dominant (GA+AA vs. GG: OR=0.095, 95% CI=0.044–0.207, P<0.001) and recessive (AA vs. GA+GG: OR=0.172, CI=0.081–0.365, P<0.001) inheritance models. No significant relationship was identified between the rs777980157 variant and PTB risk/protection. In conclusion, we found that the MBL2 rs1800450 and rs7095891 polymorphisms provide relative protection against PTB. Additional studies on larger populations with different ethnicities are required to verify our findings.

Introduction

Tuberculosis (TB) is an infectious disease caused by *Mycobacterium tuberculosis* (Mtb) infection, which is a major public health trouble in many countries. Base on World Health Organization (WHO) Global Tuberculosis Report, tuberculosis with 7 million new cases and 1.2 million deaths annually is the second-leading cause of death around the world (Huang et al., 2016; World Health Organization, 2019). However, one third of the world's population is infected with Mtb, where most of them do not develop active tuberculosis and while 5–15% of infected individuals develop the clinical disease (Zhou et al., 2018). In Zahedan (the capital of Sistan and Baluchistan province), the incidence rate of TB is higher than in other regions of Iran and tuberculosis infection is one of the major public problems. Environment and host genetics factors may contribute to the high prevalence of *Mycobacterium tuberculosis* in this region (Metanat et al., 2012; Hashemi et al., 2015; Kouhpayeh et al., 2016). Innate immunity is the first line of defense against infection with Mtb. Mannose-binding lectin 2 (MBL2) belongs to a family of proteins termed collectins in the C-type lectin superfamily and produced in the liver (Liu et al., 2016). MBL2 is an acute-phase protein, an important part of the innate immunity and has a key role in host defense against pathogens (Zheng et al., 2018). After entrance of microorganism to body, MBL2 recognizes the bacterial mannose residues by its carbohydrate recognition domain (Guo et al., 2017) and activate the complement cascade through the lectin pathway while also promoting opsonization and phagocytosis of pathogens (Li et al., 2018). The MBL2 gene is located on chromosome 10 (10q11.2-q21) and contains many polymorphisms in the promoter or structural region of the gene affecting the expression level of MBL2 at transcription level. Low serum level of MBL2 is associated with increased susceptibility to infectious disease such as Mtb (Amiri et al., 2017). Several studies have shown that MBL2 polymorphisms are related to tuberculosis susceptibility though the results were inconsistent (Cao et al., 2018; Mandal et al., 2019; Tong et al., 2019). Thus, we conducted the present study to investigate the possible association between MBL2 gene polymorphisms and pulmonary tuberculosis in a sample of Iranian population.

Material and Methods

A total of 170 patients diagnosed with PTB (pulmonary tuberculosis) were enrolled in the present study from May 2017 to December 2018 who referred to university-affiliated hospital center for TB (Bou-Ali Hospital, Zahedan, Iran). Additionally, during the same time period as the TB patients were collected, 175 healthy subjects with no history of TB or pulmonary disease were recruited as control subjects. Controls were selected from the equal region as the patients with PTB (Southeast Iran); they were not related to each other (family members) and they had the same conditions including socioeconomic status and availability of health accommodations. All participants received BCG vaccination.

Pulmonary tuberculosis was confirmed by clinical appearances, chest X-ray sign, and positive sputum smear for acid-fast bacilli as described in our previous study (Kouhpayeh et al., 2012). Informed consent was taken from all subjects and the project was approved by the local Ethics Committee of Zahedan University of Medical Sciences (IR.ZAUMS.REC.1396.216). About 2 ml peripheral blood was taken from each patient and control, DNA extracted using salting out methods. In this study, we used polymerase chain reaction for detection of 34bp ins/del of MBL2 gene (rs777980157) polymorphism. Genotyping of rs1800450 A/G and rs7095891 A/G MBL2 gene polymorphisms was done by PCR-RFLP method. Primer sequences, restriction enzymes, and length of the fragments are summarized in Table 1. In each 0.20-ml PCR reaction tube, 1 µl of genomic DNA (~100 ng/ml), 1 µl of each primer (10 µM), and 10 µl of 2X Prime Taq Premix (Genet Bio, Korea), and 7 µl ddH_2O were added. The thermal cycling parameters consisted of an initial denaturation at 95 °C for 5 min, 30 cycles of 95 °C for 30 s, 56 °C for rs777980157, 64 °C for rs1800450 and 61 °C for rs7095891 and 72 °C for 30 s and a final

Table 1 – Primer sequences of PCR-RFLP for detection of MBL2 polymorphisms

	Primer sequence (5'→3')	Restriction enzyme	Fragment (bp)
rs1800450 A>G	F: ATGGTGGCAGCGTCTTACTC R: TGGGCTGGCAAGACAACTAT	BanI	A allele: 346 G allele: 222+124
rs7095891	F: GTTAATCTCAGTTAATGAACACATATTTATC R: CCGAAAGCATGTTTATAGTCTTCCA	TaqI	A allele: 257 G allele: 226+31
rs777980157 (34bp ins/del)	F: CCTCCACGTGGCAACTTTATT R: TACCCGGACTTTTTCCAGGG		ins 313bp del 279bp

MBL2 – mannose-binding lectin 2

extension step of 72 °C for 5 min. Then, 10 µl of PCR product was digested with an appropriate restriction enzyme (Table 1). The PCR products were resolved on 2.5% agarose gel electrophoresis.

Statistical analysis

Data were analysed by the statistical package SPSS 20 software (SPSS for Windows, SPSS Inc., Illinois, USA) and the level of significance was set to a P-value of < 0.05. The differences between the variables were evaluated by chi-square test or independent sample *t*-test according to the data. The association between genotypes and PTB was assessed by computing the odds ratio (OR) and 95% confidence intervals (95% CI) from logistic regression analyses.

Results

The study participants included 170 PTB patients (84 males and 86 females, mean age 51.31 ± 19.58) and 175 healthy controls (81 males and 94 females, mean age 49.86 ± 14.08). There was no difference in age and sex between the patient and healthy control groups (P=0.428 and 0.591, respectively). Table 2 reports the genotype and allele distribution of MBL2 rs1800450 and rs7095891 polymorphisms in cases and controls. Our data showed that GA genotype as well as GA+AA genotype of rs1800450 reduced the risk of PTB in comparison with GG genotype (OR=0.17, 95% CI=0.11–0.27, P<0.001; and OR=0.19, 95% CI=0.12–0.30, P<0.001, respectively). Further, A allele significantly decreased the risk of PTB (OR=0.36, 95% CI 0.25–0.52, P<0.001) in comparison with G allele. As listed in Table 2, the findings suggested that rs7095891 was associated with decreased risk of PTB in codominant (GA vs. GG: OR=0.118, 95% CI=0.054–0.258, P<0.001; and AA vs. GG: OR=0.029, 95% CI=0.01–0.082, P<0.001), dominant (GA+AA vs. GG: OR=0.095, 95% CI=0.044–0.207, P<0.001), and recessive (AA vs. GA+GG: OR=0.172, CI=0.081–0.365, P<0.001) inheritance models. The A allele can be considered as protective against PTB (OR=0.373, 95% CI=0.274–0.507, P<0.001) in comparison to G allele. The genotype frequency of rs777980157 polymorphism showed that all PTB patients and healthy controls had Ins/Ins genotype demonstrating that this variant is not polymorphic in our population.

Discussion

Tuberculosis is the second-leading cause of infectious diseases after HIV. Both genetic and environmental factors play an important role in influencing TB susceptibility. Innate immunity is the first line of defense against infection with Mtb. MBL2, is a calcium dependent plasma Collectin which binds to different microorganisms. It profoundly contributes to natural immune protection against infectious agents by activating the lactin complement pathway. It also regulates the inflammatory reactions. Many studies have demonstrated that MBL is involved in control of various microorganisms such as bacteria, fungi, parasites, and viruses

Table 2 – The genotypes and allele distribution of MBL2 polymorphisms in pulmonary tuberculosis (PTB) patients and control groups

	Patients n (%)	Normal n (%)	OR (95% CI)	P
rs1800450				
Codominant				
GG	121 (71)	56 (32)	1.00	
GA	43 (25)	116 (66)	0.172 (0.107–0.275)	<0.001
AA	6 (4)	3 (2)	2.2 (0.90–5.37)	0.080
Dominant				
GG	121 (71)	56 (32)	1.00	
GA+AA	49 (29)	119 (68)	0.191 (0.120–0.302)	<0.001
Recessive				
GG+GA	164 (96)	172 (98)	1.00	
AA	6 (4)	3 (2)	2.098 (0.516–8.526)	0.301
Alleles				
G	285 (84)	228 (65)	1.00	
A	55 (16)	122 (35)	0.360 (0.250–0.518)	<0.001
rs7095891				
Codominant				
GG	57 (34)	8 (4)	1.00	
GA	104 (61)	124 (71)	0.118 (0.054–0.258)	<0.001
AA	9 (5)	43 (25)	0.029 (0.01–0.082)	<0.001
Dominant				
GG	57 (34)	8 (4)	1.00	
GA+AA	113 (66)	167 (96)	0.095 (0.044–0.207)	<0.001
Recessive				
GG+GA	161 (95)	132 (75)	1.00	
AA	9 (5)	43 (25)	0.172 (0.081–0.365)	<0.001
Alleles				
G	218 (64)	140 (40)	1.00	
A	122 (36)	210 (60)	0.373 (0.274–0.507)	<0.001

MBL2 – mannose-binding lectin 2; OR – odds ratio; CI – confidence interval

(Eisen, 2010; Jha et al., 2014). In the current study, we aimed to find out the impact of MBL2 variants and risk of PTB in a sample of a southeast Iranian population. The results showed that GA as well as GA+AA genotype of rs1800450 reduced the risk of PTB. It was also found that rs7095891 variant significantly decreased the risk of PTB. Accordance to our results, Singla et al. (2012) found that mutant allele of rs1800450 has a protective role against TB, but they did not observe this result in extrapulmonary TB. Capparelli et al. (2009) in a study on Italian population illustrated that this polymorphism was protective against PTB in the heterozygote form and was more significantly protective in the homozygote form. When they did haplotype analysis, they found LYB/LYD haplotype increased the risk of tuberculosis

and concluded that MBL may be protective or risk factor of tuberculosis depending on host's haplotype pair (Capparelli et al., 2009). Cosar et al. (2008) discovered that mutant allele frequency of rs1800450 is significantly lower in the patient group. In contrast to this finding, Liu et al. (2016) revealed that subjects with variant allele of rs1800450 (homozygote and heterozygote) had an increased susceptibility to TB in comparison to wild type allele. Li et al. (2018) in a study on Chinese Uygur population found that MBL2 rs7095891 polymorphism was associated with an increased risk of TB; however, they did not find any association between rs1800450 as well as rs7096206 polymorphism and tuberculosis. Meanwhile, many studies have not found any association between MBL2 rs1800450 polymorphism and susceptibility or protection to tuberculosis (Soborg et al., 2007; Araújo et al., 2013; da Cruz et al., 2013; Wu et al., 2015; Amiri et al., 2017). The effect of MBL level on TB susceptibility has been controversial. Cosar et al. (2008) showed MBL plasma level was significantly lower in control groups in comparison with patients, while Capparelli et al. (2009) found that protection against TB was correlated with a high concentration of MBL in plasma. It has been shown that individuals with mutant genotype (0/0) have very low or undetectable levels of MBL (Frederiksen et al., 2006). Tong et al. (2019) in a meta-analysis found that MBL level in PTB patients was significantly lower than in the control group, implying that low expression of MBL2 is associated with an increased risk of PTB. These polymorphisms changed the structure of MBL proteins causing a functional deficiency and reduction of stability; as such they were more rapidly degraded and thus reduced the serum level of MBL (Heitzeneder et al., 2012; Mandal et al., 2019). Also, it seems that these MBL proteins have less binding capacity to mannose and cannot activate complement via the lectin pathway (Amiri et al., 2017). However, Thye et al. (2011) showed higher levels of MBL can promote infection by increasing the uptake of intracellular pathogens by phagocytes.

In conclusion, the present study revealed that rs1800450 and rs7095891 MBL2 polymorphisms reduced the risk of PTB in a sample of Iranian population. Replication in different ethnicities with more samples is required for better understanding of the association between these polymorphisms and risk of tuberculosis.

References

Amiri, A., Sabooteh, T., Shahsavar, F., Anbari, K., Pouremadi, F. (2017) Mannose-binding lectin (MBL) gene polymorphisms in susceptibility to pulmonary tuberculosis among the Lur population of Lorestan Province of Iran. *Genom. Data* **12**, 146–150.

Araújo, M. S., Graça, E. S., Azevedo, V. N., Cayres-Vallinoto, I., Machado, L. F. A., Ishak, M. O. G., Ishak, R., Vallinoto, A. C. R. (2013) No evidence of association between MBL2A/O polymorphisms and *Mycobacterium tuberculosis* infection in populations from the Brazilian Amazon region. *Hum. Immunol.* **74(1)**, 82–84.

Cao, Y., Wang, X., Cao, Z., Wu, C., Wu, D., Cheng, X. (2018) Genetic polymorphisms of MBL2 and tuberculosis susceptibility: a meta-analysis of 22 case-control studies. *Arch. Med. Sci.* **14(6)**, 1212–1232.

Capparelli, R., Iannaccone, M., Palumbo, D., Medaglia, C., Moscariello, E., Russo, A., Iannelli, D. (2009) Role played by human mannose-binding lectin polymorphisms in pulmonary tuberculosis. *J. Infect. Dis*. **199(5)**, 666–672.

Cosar, H., Ozkinay, F., Onay, H., Bayram, N., Bakiler, A. R., Anil, M., Can, D., Ozkinay, C. (2008) Low levels of mannose-binding lectin confers protection against tuberculosis in Turkish children. *Eur. J. Clin. Microbiol. Infect. Dis*. **27(12)**, 1165–1169.

da Cruz, H. L., da Silva, R. C., Segat, L., de Carvalho, M. S., Brandao, L. A., Guimaraes, R. L., Santos, F. C., de Lira, L. A., Montenegro, L. M., Schindler, H. C., Crovella, S. (2013) MBL2 gene polymorphisms and susceptibility to tuberculosis in a northeastern Brazilian population. *Infect. Genet. Evol*. **19**, 323–329.

Eisen, D. P. (2010) Mannose-binding lectin deficiency and respiratory tract infection. *J. Innate Immun*. **2(2)**, 114–122.

Frederiksen, P. D., Thiel, S., Jensen, L., Hansen, A. G., Matthiesen, F., Jensenius, J. C. (2006) Quantification of mannan-binding lectin. *J. Immunol. Methods* **315(1–2)**, 49–60.

Guo, Y. L., Liu, Y., Ban, W. J., Sun, Q., Shi, G. L. (2017) Association of mannose-binding lectin gene polymorphism with the development of pulmonary tuberculosis in China. *BMC Infect. Dis*. **17(1)**, 210.

Hashemi, M., Sharifi-Mood, B., Rasouli, A., Amininia, S., Naderi, M., Taheri, M. (2015) Macrophage migration inhibitory factor –173 G/C polymorphism is associated with an increased risk of pulmonary tuberculosis in Zahedan, Southeast Iran. *EXCLI J*. **14(21)**, 117–122.

Heitzeneder, S., Seidel, M., Forster-Waldl, E., Heitger, A. (2012) Mannan-binding lectin deficiency – Good news, bad news, doesn't matter? *Clin. Immunol*. **143(1)**, 22–38.

Huang, X., Yang, Y., Cui, Z. W., Wang, J., Gao, L. B. (2016) A functional insertion/deletion polymorphism in the IL1A gene is associated with decreased risk of breast cancer. *Genet. Mol. Res*. **15(1)**, 26909967.

Jha, A. N., Sundaravadivel, P., Singh, V. K., Pati, S. S., Patra, P. K., Kremsner, P. G., Velavan, T. P., Singh, L., Thangaraj, K. (2014) MBL2 variations and malaria susceptibility in Indian populations. *Infect. Immun*. **82(1)**, 52–61.

Kouhpayeh, H. R., Hashemi, M., Hashemi, S. A., Moazeni-Roodi, A., Naderi, M., Sharifi-Mood, B., Taheri, M., Mohammadi, M., Ghavami, S. (2012) R620W functional polymorphism of protein tyrosine phosphatase non-receptor type 22 is not associated with pulmonary tuberculosis in Zahedan, southeast Iran. *Genet. Mol. Res*. **11(2)**, 1075–1081.

Kouhpayeh, H. R., Taheri, M., Baziboroon, M., Naderi, M., Bahari, G., Hashemi, M. (2016) CCL5 rs2107538 polymorphism increased the risk of tuberculosis in a sample of Iranian population. *Prague Med. Rep*. **117(2–3)**, 90–97.

Li, X., Cao, X., El-Ashram, S., Zhang, W., Lu, L., Wang, X., Chen, C., Wu, J. (2018) MBL2 rs7095891 G > A polymorphism was associated with an increased risk of tuberculosis in the Chinese Uygur population. *Int. J. Mol. Epidemiol. Genet*. **9(5)**, 64–70.

Liu, C., He, T., Rong, Y., Du, F., Ma, D., Wei, Y., Mei, Z., Wang, Y., Wang, H., Zhu, Y., Zhang, Z., Zheng, L., Wu, X., Liu, H., Ding, W. (2016) Association of mannose-binding lectin polymorphisms with tuberculosis susceptibility among Chinese. *Sci. Rep*. **6**, 36488.

Mandal, R. K., Khan, M. A., Hussain, A., Dar, S. A., Aloufi, S., Jawed, A., Wahid, M., Panda, A. K., Lohani, M., Akhter, N., Khan, S., Mishra, B. N., Haque, S. (2019) Association of MBL2 gene polymorphisms with pulmonary tuberculosis susceptibility: trial sequence meta-analysis as evidence. *Infect. Drug Resist*. **12**, 185–210.

Metanat, M., Sharifi-Mood, B., Shahreki, S., Dawoudi, S. H. (2012) Prevalence of multidrug-resistant and extensively drug-resistant tuberculosis in patients with pulmonary tuberculosis in Zahedan, southeastern Iran. *Iran. Red Crescent Med. J*. **14(1)**, 53–55.

Singla, N., Gupta, D., Joshi, A., Batra, N., Singh, J., Birbian, N. (2012) Association of mannose-binding lectin gene polymorphism with tuberculosis susceptibility and sputum conversion time. *Int. J. Immunogenet*. **39(1)**, 10–14.

Soborg, C., Andersen, A. B., Range, N., Malenganisho, W., Friis, H., Magnussen, P., Temu, M. M., Changalucha, J., Madsen, H. O., Garred, P. (2007) Influence of candidate susceptibility genes on tuberculosis in a high endemic region. *Mol. Immunol*. **44(9)**, 2213–2220.

Thye, T., Niemann, S., Walter, K., Homolka, S., Intemann, C. D., Chinbuah, M. A., Enimil, A., Gyapong, J., Osei, I., Owusu-Dabo, E., Rusch-Gerdes, S., Horstmann, R. D., Ehlers, S., Meyer, C. G. (2011) Variant G57E of mannose binding lectin associated with protection against tuberculosis caused by *Mycobacterium africanum* but not by *M. tuberculosis*. *PLoS One* **6(6)**, e20908.

Tong, X., Wan, Q., Li, Z., Liu, S., Huang, J., Wu, M., Fan, H. (2019) Association between the mannose-binding lectin (MBL)-2 gene variants and serum MBL with pulmonary tuberculosis: An update meta-analysis and systematic review. *Microb. Pathog*. **132**, 374–380.

World Health Organization (2019) *Global Tuberculosis Report*. Available at: https://apps.who.int/iris/bitstream/handle/10665/329368/9789241565714-eng.pdf?ua=1

Wu, L., Deng, H., Zheng, Y., Mansjo, M., Zheng, X., Hu, Y., Xu, B. (2015) An association study of NRAMP1, VDR, MBL and their interaction with the susceptibility to tuberculosis in a Chinese population. *Int. J. Infect. Dis*. **38**, 129–135.

Zheng, M., Shi, S., Wei, W., Zheng, Q., Wang, Y., Ying, X., Lu, D. (2018) Correlation between MBL2/CD14/TNF-alpha gene polymorphisms and susceptibility to spinal tuberculosis in Chinese population. *Biosci. Rep*. **38(1)**, BSR20171140.

Zhou, X., Zhou, Q., Yang, Z. F., Li, W. X. (2018) Genetic polymorphism of human leucocyte antigen and susceptibility to multidrug-resistant and rifampicin-resistant tuberculosis in Han Chinese from Hubei Province. *Int. J. Immunogenet*. **45(1)**, 8–21.

 Prague Medical Report / Vol. 121 (2020) No. 4, p. 244–253

Post-mortem Redistribution of Alprazolam in Rats

Jana Hořínková[1], Petr Kozlík[2], Tomáš Křížek[2], Danica Michaličková[1], Martin Šíma[1], Ondřej Slanař[1]

[1]Institute of Pharmacology, First Faculty of Medicine, Charles University and General University Hospital in Prague, Prague, Czech Republic; [2]Department of Analytical Chemistry, Faculty of Science, Charles University, Prague, Czech Republic

Received March 7, 2020; Accepted November 2, 2020.

Key words: Alprazolam – Benzodiazepines – Overdose – Post-mortem redistribution – Animal model – Forensic toxicology

Abstract: The post-mortem toxicological findings may be misinterpreted, if the drug undergoes substantial post-mortem redistribution. As alprazolam is one of the most frequently evaluated drug for legal/forensic reasons in drug-related fatalities, we studied possible changes in alprazolam distribution after death in a rat model. Rats were sacrificed 30 minutes after alprazolam administration. Blood and tissue samples from 8 animals per sampling time were collected at 0, 2, 6, and 24 h after death. The experimental samples were assayed for alprazolam using validated UHPLC-PDA method. Median blood alprazolam concentrations increased approximately 2 times compared with ante-mortem levels due to the redistribution during early post-mortem phase and then slowly decreased with a half-life of 60.7 h. The highest alprazolam tissue concentrations were found in fat and liver and the lowest levels were observed in lungs and brain. The median amount of alprazolam deposited in the lungs was relatively stable over the 24-h post-mortem period, while in heart, liver and kidney the deposited proportion of administered dose increased by 43–48% in comparison with ante-mortem values indicating continuous accumulation of alprazolam into these tissues. These results provide evidence needed for the interpretation of toxicological results in alprazolam-related fatalities and demonstrate modest alprazolam post-mortem redistribution.

This study was supported by the Charles University Project Progres Q25, Research Centre program No. UNCE/SCI/014, and a grant No. SVV 260523.

Mailing Address: Martin Šíma, PharmDr., PhD., Institute of Pharmacology, First Faculty of Medicine, Charles University and General University Hospital in Prague, Albertov 4, 128 00 Prague 2, Czech Republic; Phone: +420 224 968 161; e-mail: martin.sima@lf1.cuni.cz

https://doi.org/10.14712/23362936.2020.21

Introduction

Drug overdose belongs among common causes of death worldwide with mortality rate of approximately 22.6 and 217 cases per million inhabitants in the EU and USA, respectively (European Monitoring Centre for Drugs and Drug Addiction, 2019). Although the majority of drug-related deaths in Europe occur in men, suicidal drug overdoses are more frequent in women. Most fatal drug overdoses are linked to the use of opioids, central nervous system depressants including benzodiazepines or polydrug use. Alprazolam itself was the fifth most common drug detected in 6,209 drug-related deaths in the USA in 2016 (Hilberg et al., 1999). Alprazolam is therefore frequently evaluated for legal/forensic reasons in drug-related fatalities.

The post-mortem toxicological findings may be misinterpreted if the drug undergoes substantial post-mortem redistribution, which is mainly expected for basic, lipophilic compounds widely distributed into peripheral compartments (Kugelberg et al., 2004; Castaing et al., 2006). The mechanisms of post-mortem redistribution have not been fully characterized, but leakage of intracellular content after cellular death (Musther et al., 2014), disruption of physiological barriers (Banks et al., 1992), degradation of the compounds by gut microorganisms and their diffusion from gastrointestinal content into the body tissues belong among known causes contributing to this phenomenon (European Monitoring Centre for Drugs and Drug Addiction, 2019). Moreover, metabolism may also continue during the first few hours after death (Jonsson et al., 2004).

Post-mortem redistribution has been described for number of drugs involved in fatal drug-related overdoses including haloperidol, morphine, citalopram, triazolam or diazepam (Koren and MacLeod, 1985; Shiota et al., 2004; Kposowa and McElvain, 2006).

Alprazolam with log P of 2.12 belongs among lipophilic compounds; it has apparent volume of distribution of approximately 1 l/kg in man (Greenblatt and Wright, 1993). These characteristics suggest possible role of post-mortem redistribution for this drug. Reports that evaluated central to peripheral blood concentrations ratios in human have suggested that alprazolam may exhibit a modest post-mortem redistribution (Hargrove and McCutcheon, 2008; Han et al., 2012). However, there are no data on post-mortem redistribution from direct measurement of alprazolam concentrations in particular tissues available. Therefore, the aim of our study was to describe possible changes in alprazolam distribution after death in rats.

Methods

Chemicals

Alprazolam was purchased from Sigma-Aldrich (Saint Louis, USA). The drug was then dissolved in a mixture of 70% ethanol and saline (1:1; v/v) for the purpose of intraperitoneal application. Isoflurane was used as IsoFlo 250 ml (Zoetis, Parsippany, USA).

Animals

Female Wistar rats (Velaz, Prague, Czech Republic) were used throughout the study. They were maintained under standard conditions (12-h light-dark cycle, 22 ± 2 °C temperature and 50 ± 10% relative humidity) and fed on water and standard granulated diet *ad libitum*. All experiments were performed in accordance with the Guiding Principles in the Use of Animals in Charles University, First Faculty of Medicine, and every effort was made to minimize animal suffering. The experimental animal project was approved by the Ministry of Education, Youth and Sports of the Czech Republic under the number MSMT-9445/2018-8.

Experimental procedure

Rats were randomly divided into four groups: (1) immediate autopsy, (2) autopsy 2 hours after death, (3) autopsy 6 hours after death, and (4) autopsy 24 hours after death. All animals were anesthetized by inhalation of 2–5% isoflurane and anaesthesia was maintained throughout the procedure. Following anesthetization, rats were injected alprazolam intraperitoneally at a dose of 4 mg or 6 mg for animals weighting ≤ 250 g or more, respectively. Thirty minutes after alprazolam administration, an ante-mortem blood sample was taken via cardiac puncture from each rat. Immediately following the sampling, rats were sacrificed by cervical dislocation and death was confirmed by the lack of a heartbeat. Following death, rats in groups 2–4 were left lying on their backs at room temperature (22 ± 2 °C) for the defined time to autopsy. Post-mortem aortic blood samples were drawn and the following tissue samples were also collected at the time of autopsy: liver (left lateral lobe), left kidney, heart, left lung, brain and abdominal fat. The tissue samples were cleaned with tissue paper, weighted and immediately homogenized with Tissue-Tearor homogenizer model 985-370 (BioSpec Products, Inc., Bartlesville, USA) in two volumes of 80% acetonitrile and then vortexed for 30 s. Both blood samples and tissue homogenates were centrifuged for 10 minutes at 2,500× *g* (4 °C). Blood samples and tissue supernatants were then stored at –80 °C before further processing. Before the chromatography analysis, the blood samples and tissue supernatants were deproteinized by acetonitrile, adding 60 µl of 100% acetonitrile to 20 µl of sample and performing deproteinization in an Eppendorf tube by vortexing for 15 s. Then, both blood and tissue samples were centrifuged at 16,500× *g* for 6 min, and 50 µl of supernatant was transferred into LC vials.

Analysis of alprazolam

Determination of alprazolam in different tissues and blood samples was carried out using Acquity UPLC H-class equipment (Waters Corporation, Milford, MA). LC column Poroshell HPH C18 (3.00 mm i.d. × 100 mm, 2.7 µm) from Agilent Technologies (Waldbronn, Germany), thermostatted at 30 °C, was used for the analysis. The mobile phase consisted of 10 mM ammonium phosphate, pH 2.80 (Solvent A) and acetonitrile (Solvent B). The flow rate of the mobile phase

was maintained at 0.5 ml/min. The optimized gradient program (min/% B) was 0/30, 1/30, 3.5/60, 4/80, 7/80, 7.5/30, and 10/30. The injection volume was 1 µl, and samples were kept at 10 °C. Detection was performed by diode array detector, and the wavelength was set to 245 nm.

The method was validated according to the FDA guidance on analytical procedures and method validation to demonstrate that it is suitable for its intended purpose (U. S. Food and Drug Administration, 2015). The selectivity of the method was verified by mass spectrometry operated in the scan mode (Triple Quad 6460 mass spectrometer; Agilent Technologies, Waldbronn, Germany).

Selectivity was monitored by injecting all studied tissue extracts. These chromatograms showed no interfering compound (no *m/z* was observed except *m/z* corresponding to alprazolam) within the retention time window of alprazolam. Moreover, the DAD peak purity test of all analysed samples was successfully met for the alprazolam peak, which ensures high selectivity. Selectivity was thus confirmed independently by DAD and mass spectrometry. The calibration curve was constructed in the 80% acetonitrile with nine concentration levels (0.1; 0.2; 0.5; 1; 2; 5; 10; 50; 100 µg/ml) by plotting the peak area of alprazolam against its concentration. Calibration was performed before each batch of samples. Standard plots were constructed and linearity was evaluated statistically by linear regression analysis using the least-squares regression method. To confirm the reliability of our results derived from the calibration curve, we performed determination using the standard addition method with selected samples of different tissue extracts and blood. The standard was added into blood and tissue extract samples before deproteinization to include the potential effect of deproteinization. No significant difference in concentration means was observed between results obtained using both methods. This result proved that tissue and blood matrices have no effect on the reliable quantification of alprazolam. The linearity was evaluated through the calibrations providing coefficients of determination (R^2) higher than 0.9997 which indicate excellent linearity. Limit of detection value was 0.02 µg/ml, determined as 3.3×σ/S ratio, where σ is the highest baseline noise obtained from the blank blood/tissue extracts, and S is the slope of the regression line (based on peak heights). Limit of quantification was the lowest point of the calibration (0.1 µg/ml).

Method accuracy and precision were evaluated by measuring 5 replicates at four different concentrations (0.1; 1; 5, and 50 µg/ml) prepared by spiking alprazolam into blank tissue extracts and blood. The accuracy (relative error, %) was within ± 3.0%, and the inter- and intra-day precisions (RSD, %) were within ± 2.5%. These samples were also used as quality control (QC) samples. QC samples were injected after each 7th sample to assess the validity of the analytical method. Recovery was evaluated by comparing the area of the alprazolam standard peak of the pre-protein-precipitation spiked blood sample with that of the corresponding post-protein-precipitation spiked sample at three concentrations (0.1; 10, and 50 µg/ml). Since there is no reference material of different tissues containing alprazolam, the recovery

was simulated by fortifying of different tissue homogenates with the standard of alprazolam at three concentrations (0.1; 10, and 50 μg/ml). Extraction and protein precipitation was performed with 80% acetonitrile and vortexed for 30 s. The recovery ranged from 96.8 to 100.9%.

Data analysis and statistics

Tissue concentrations (μg/g) were calculated from measured supernatant concentrations (μg/ml), used amounts of solvent (ml) and weights of homogenized tissues (g). Subsequently, both tissue and blood concentrations were normalized per dose of 20 mg/kg.

Distribution half-life was calculated as $(t \times \ln 2)/\ln(C_2/C_{24})$, where C_2 and C_{24} are median alprazolam blood concentration 2 and 24 h after death, respectively, and t is 22 h as the time between C_2 and C_{24}.

Median and interquartile range (IQR) values were calculated using MS Excel 2010 (Microsoft Corporation, Redmond, USA). Significance of differences in alprazolam concentrations/tissue distribution between group 1 and the other groups was determined by the Mann-Whitney test, while potential differences in weights and weight-normalized doses between study groups were examined by the Kruscal-Wallis test using GraphPad Prism 8.2.1 (GraphPad Software, Inc., La Jolla, USA). Statistical significance was considered at $p \leq 0.05$.

Results

Thirty-two female rats weighing 162–365 g were enrolled in this study; eight rats per group. Administered alprazolam doses ranged from 16.4 to 24.7 mg/kg. There were no significant differences in animal weight ($p=0.97$) or administered alprazolam doses ($p=0.96$) between study groups.

Post-mortem changes in dose-normalized blood and tissue concentrations of alprazolam are presented in Figure 1. All post-mortem groups showed significantly increased blood drug concentrations compared with ante-mortem alprazolam blood levels. The ratio between median post-mortem and ante-mortem alprazolam blood concentrations were 1.78, 1.54 and 1.39 at 2, 6 and 24 hours after death, respectively. Thus, steep rise in alprazolam blood levels during early post-mortem phase was followed by slow decrease with a half-life of 60.7 h.

Distribution of alprazolam into the tissues expressed as percentages of the total administered alprazolam dose are showed in Table 1.

Discussion

This study was designed to describe possible post-mortem alprazolam redistribution in rat in order to improve our understanding and interpretation of the toxicological findings in alprazolam related fatalities that belong among frequent intentional drug overdoses world-wide. We conducted the study in female rats, since women are 4 times more likely to die from drug poisoning than men (Kposowa and McElvain,

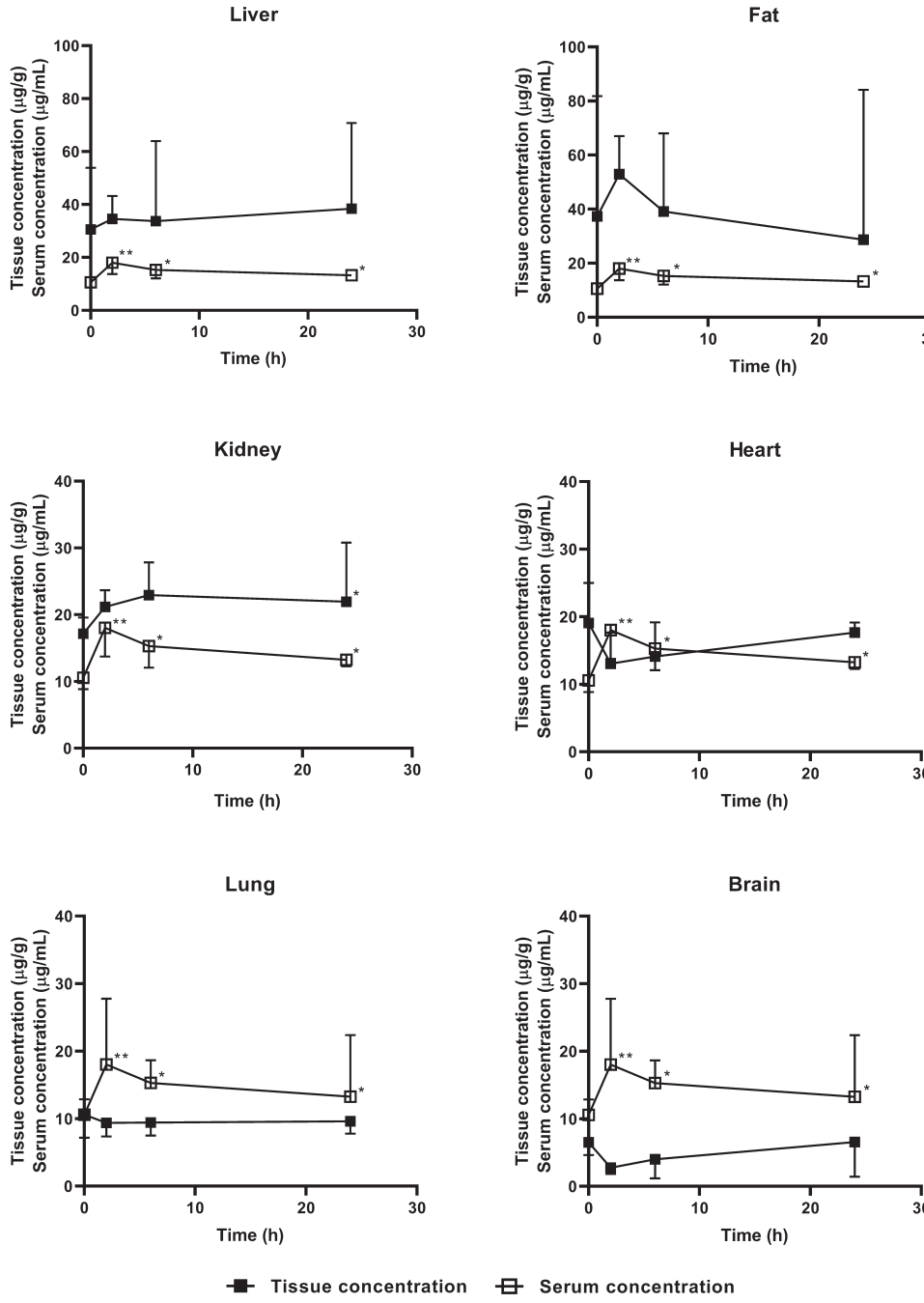

*Figure 1 – Post-mortem changes of alprazolam concentrations normalized per dose of 20 mg/kg in the rat blood and tissues. Values are represented as median (interquartile range); n=8; *p<0.05; **p<0.005 vs. 0 h after death.*

Table 1 – Alprazolam tissue distribution expressed as median percentages of total administered alprazolam dose (%) at time after death

	Group 1 0 h	Group 2 2 h	Group 3 6 h	Group 4 24 h
Liver	5.17	7.11	8.17*	7.38
Kidney (left)	0.29	0.34	0.42	0.43*
Heart	0.21	0.22	0.23	0.32
Lung (left)	0.08	0.08	0.09	0.10
Brain	0.32	0.10	0.14	0.24

*p<0.05 vs. 0 h after death

2006). A fix dose of 4 or 6 mg was administered to each animal with respect to its actual body weight in order to reach approximate dose of 20 mg/kg for each animal, which corresponds to human equivalent dose of 3.3 mg/kg (rat/human dose conversion factor of 6 has been reported) (Nair and Jacob, 2016). The actual doses ingested are usually unknown in human alprazolam-related fatalities, however, the drug has been reported among compounds with the most frequent toxic levels detected in forensic analyses in drug related fatalities (Jonsson et al., 2004). A study in 131 deliberate alprazolam self-poisoning cases reported that the median (IQR) alprazolam dose was 23 defined daily doses (10–40) (Isbister et al., 2004), which is less in comparison with the dose we used. However, other individual case reports have shown high plasma and tissue levels indicating that the dose ingested must have been considerably higher (Jenkins et al., 1997). Since the doses ingested in an intentional overdose are in reality highly uncertain, we have chosen the human equivalent dose for our study corresponding to the possible worst case scenario for acute intoxication after ingestion of whole alprazolam high strength package (100 tablets, 2 mg).

Alprazolam blood levels reported for human fatal intoxications are extremely variable. While some repots mention plasma levels within the toxic range of 0.1–0.4 μg/ml (Jones et al., 2016; McIntyre et al., 2017), Jenkins et al. (1997) detected plasma levels in a human alprazolam fatality of 2.1–2.3 μg/ml that is approximately 20% of the ante-mortal levels seen in our study.

We observed significantly increased blood drug concentrations at all sampling times post-mortem. This phenomenon has been previously described for some other lipophilic drugs, e.g. thioridazine, morphine or citalopram (Koren and Klein, 1992; Kugelberg et al., 2004; Castaing et al., 2006). However, the interindividual variability of the drug concentration increase after death is high, in a few animals the post-mortem increase of alprazolam blood levels was as large as 6-fold. This is again comparable to the previous observations for morphine with up to 5-fold drug level increase (Koren and Klein, 1992).

The highest alprazolam tissue concentrations were found in fat and liver in group 1 (autopsy 30 min after intraperitoneal administration), whereas the lowest levels were observed in lungs and brain. These findings follow a similar distribution pattern described for ^{14}C-alprazolam 30 min after intravenous administration (Banks et al., 1992) and correspond also to distribution of diazepam and triazolam that both belong among benzodiazepines (Shiota et al., 2004). Although alprazolam concentration in the brain was low, the percentual distribution of the administered dose was similar to that found in left kidney at the time of death (Table 1). The highest percentage of alprazolam dose were accumulated in the liver. It can be expected that largest proportion of alprazolam dose accumulates in adipose tissue, however, as the total body fat is unknown the distribution could not be estimated.

The amount of alprazolam deposited in the lung tissue was relatively stable over the 24-h post-mortem period, while in heart, liver and kidney the deposited proportion of administered dose increased by 43–48% at 24 h after death in comparison with pre-mortem values indicating continuous accumulation of alprazolam into these tissues. The tissue concentrations tended to increase correspondingly to the percentage of the dose deposited in liver and kidney, while the drug tissue concentration dropped in the heart early after death contrary to the increasing drug accumulation in the tissue. This was likely caused by an increased intramyocardial water content that may be seen after death especially in females (Boyd and Knight, 1963). On the other hand, both brain alprazolam content and brain tissue concentrations decreased early after death with subsequent tendency to reach equilibrium with blood concentrations. Due to the high variability of tissue concentrations obtained, the differences of tissue concentrations from the post-mortem sample only reached statistical significance for kidney at 24 h.

The clinical data on alprazolam distribution post-mortem are extremely limited. In a single fatal overdose, the ratios between tissue and plasma drug levels in kidney and liver were approximately 1.7 and 4.2, respectively (Jenkins et al., 1997), which well corresponds to the individual tissue to plasma ratios seen in our study ranging from 0.2 to 4.1 for kidney and from 0.9 to 9.2 for liver samples. The anatomical proximity between the different organs in rats in our model thus did not result in unrealistically overestimated post-mortem redistribution values for the human toxicological findings. In case there is an unabsorbed drug in the stomach or gastrointestinal tract at the time of death, this may be redistributed to surrounding tissues (Pounder et al., 1996). In order to eliminate this phenomenon, we administered alprazolam intraperitoneally in this study. Although the most alprazolam overdoses are expected to follow oral ingestion of the drug in humans, the absorption is fast and complete with T_{max} of 1 h and absolute bioavailability 80–100% (Greenblatt and Wright, 1993). Therefore, substantial alprazolam redistribution from the gastrointestinal tract is not expected in clinical settings.

Conclusion

Median central blood alprazolam concentrations increased approximately 1.5–2 times due to the redistribution over the 24-h post-mortem period and there was a substantial variability of the extent of alprazolam redistribution (0.9–6.1 fold).

The median amount of alprazolam deposited in the lung tissue was relatively stable over the 24-h post-mortem period, while in heart, liver and kidney the deposited proportion of administered dose increased by 43–48% at 24 h after death in comparison with pre-mortem values indicating continuous accumulation of alprazolam into these tissues.

These results demonstrate modest alprazolam redistribution post-mortem. However, due to the high variability of alprazolam blood and tissue concentrations seen, the estimation of drug exposure or time from death can't be reliably done based on these pharmacokinetic data.

References

Banks, W. R., Yamakita, H., Digenis, G. A. (1992) Metabolism and distribution of 1-[14C]alprazolam in rats. *J. Pharm. Sci*. **81**, 797–801.

Boyd, E. M., Knight, L. M. (1963) Postmortem shifts in the weight and water levels of body organs. *Toxicol. Appl. Pharmacol*. **5**, 119–128.

Castaing, N., Titier, K., Canal-Raffin, M., Moore, N., Molimard, M. (2006) Postmortem redistribution of two antipsychotic drugs, haloperidol and thioridazine, in the rat. *J. Anal. Toxicol*. **30**, 419–425.

European Monitoring Centre for Drugs and Drug Addiction (EMCDDA) (2019) *European Drug Report: Trends and Developments*. Available at: http://www.emcdda.europa.eu/system/files/publications/11364/20191724_TDAT19001ENN_PDF.pdf

Greenblatt, D. J., Wright, C. E. (1993) Clinical pharmacokinetics of alprazolam. Therapeutic implications. *Clin. Pharmacokinet*. **24**, 453–471.

Han, E., Kim, E., Hong, H., Jeong, S., Kim, J., In, S., Chung, H., Lee, S. (2012) Evaluation of postmortem redistribution phenomena for commonly encountered drugs. *Forensic Sci. Int*. **219**, 265–271.

Hargrove, V. M., McCutcheon, J. R. (2008) Comparison of drug concentrations taken from clamped and unclamped femoral vessels. *J. Anal. Toxicol*. **32**, 621–625.

Hilberg, T., Ripel, A., Slordal, L., Bjorneboe, A., Morland, J. (1999) The extent of postmortem drug redistribution in a rat model. *J. Forensic Sci*. **44**, 956–962.

Isbister, G. K., O'Regan, L., Sibbritt, D., Whyte, I. M. (2004) Alprazolam is relatively more toxic than other benzodiazepines in overdose. *Br. J. Clin. Pharmacol*. **58**, 88–95.

Jenkins, A. J., Levine, B., Locke, J. L., Smialek, J. E. (1997) A fatality due to alprazolam intoxication. *J. Anal. Toxicol*. **21**, 218–220.

Jones, A. W., Holmgren, A., Ahlner, J. (2016) Post-mortem concentrations of drugs determined in femoral blood in single-drug fatalities compared with multi-drug poisoning deaths. *Forensic Sci. Int*. **267**, 96–103.

Jonsson, A., Holmgren, P., Ahlner, J. (2004) Fatal intoxications in a Swedish forensic autopsy material during 1992–2002. *Forensic Sci. Int*. **143**, 53–59.

Koren, G., MacLeod, S. M. (1985) Postmortem redistribution of digoxin in rats. *J. Forensic Sci*. **30**, 92–96.

Koren, G., Klein, J. (1992) Postmortem redistribution of morphine in rats. *Ther. Drug Monit*. **14**, 461–463.

Kposowa, A. J., McElvain, J. P. (2006) Gender, place, and method of suicide. *Soc. Psychiatry Psychiatr. Epidemiol*. **41**, 435–443.

Kugelberg, F. C., Druid, H., Carlsson, B., Ahlner, J., Bengtsson, F. (2004) Postmortem redistribution of the enantiomers of citalopram and its metabolites: an experimental study in rats. *J. Anal. Toxicol*. **28**, 631–637.

McIntyre, I. M., Gary, R. D., Joseph, S., Stabley, R. (2017) A fatality related to the synthetic opioid U-47700: Postmortem concentration distribution. *J. Anal. Toxicol*. **41**, 158–160.

Musther, H., Olivares-Morales, A., Hatley, O. J., Liu, B., Rostami Hodjegan, A. (2014) Animal versus human oral drug bioavailability: do they correlate? *Eur. J. Pharm. Sci*. **57**, 280–291.

Nair, A. B., Jacob, S. (2016) A simple practice guide for dose conversion between animals and human. *J. Basic Clin. Pharm*. **7**, 27–31.

Pounder, D. J., Fuke, C., Cox, D. E., Smith, D., Kuroda, N. (1996) Postmortem diffusion of drugs from gastric residue: an experimental study. *Am. J. Forensic Med. Pathol*. **17**, 1–7.

Shiota, H., Nakashima, M., Terazono, H., Sasaki, H., Nishida, K., Nakamura, J., Taniyama, K. (2004) Postmortem changes in tissue concentrations of triazolam and diazepam in rats. *Leg. Med. (Tokyo)* **6**, 224–232.

U. S. Food and Drug Administration; Department of Health and Human Services (2015) *Analytical Procedures and Methods Validation for Drugs and Biologics: Guidance for Industry*. Available at: https://www.fda.gov/files/drugs/published/Analytical-Procedures-and-Methods-Validation-for-Drugs-and-Biologics.pdf

A Successful Treatment of Encapsulating Peritoneal Sclerosis in an Adolescent Boy on Long-term Peritoneal Dialysis: A Case Report

Zlatan Zvizdic[1], Angela Summers[2], Zia Moinuddin[2], David Van Dellen[2], Irmina Pasic-Sefic[3], Faruk Skenderi[4], Semir Vranic[5], Titus Augustine[2]

[1]Department of Pediatric Surgery, University Clinical Center Sarajevo, Sarajevo, Bosnia and Herzegovina;
[2]Department of Transplant and Endocrine Surgery, Manchester Royal Infirmary, Manchester University Foundation Trust; An United Kingdom National Specialized Centre for Surgery for Encapsulating Peritoneal Sclerosis, Manchester, United Kingdom;
[3]Department of Radiology, University Clinical Center Sarajevo, Sarajevo, Bosnia and Herzegovina;
[4]Department of Pathology, University Clinical Center Sarajevo, Sarajevo, Bosnia and Herzegovina;
[5]College of Medicine, QU Health, Qatar University, Qatar

Received April 10, 2020; Accepted November 2, 2020.

Key words: Encapsulating sclerosing peritonitis – Peritoneal dialysis – Management

Abstract: Encapsulating peritoneal sclerosis (EPS) is a rare life-threatening complication associated with peritoneal dialysis (PD). EPS is characterized by progressive fibrosis and sclerosis of the peritoneum, with the formation of a membrane and tethering of loops of the small intestine resulting in intestinal obstruction. It is very rare in children. We present a case of a 16-year-old adolescent boy who developed EPS seven years after being placed on continuous ambulatory peritoneal dialysis (CAPD) complicated by several episodes of bacterial peritonitis. The diagnosis was based on clinical, radiological, intraoperative and histopathological findings. The patient was successfully treated with surgical enterolysis. During a 7-year follow-up, there have been no further episodes of small bowel obstruction documented. He still continues to be on regular hemodialysis and is awaiting a deceased donor kidney transplant. EPS is a long-term complication of peritoneal dialysis and is typically seen in adults. Rare cases may be seen in the pediatric population and require an appropriate surgical approach that is effective and lifesaving for these patients.

Mailing Address: Semir Vranic, MD., PhD., College of Medicine, QU Health, Qatar University, Qatar; e-mail: semir.vranic@gmail.com

https://doi.org/10.14712/23362936.2020.22

Introduction

First described in 1980 (Gandhi et al., 1980), encapsulating peritoneal sclerosis (EPS) is a rare chronic inflammatory condition characterized by the presence of fibrosis and adhesions of the peritoneum to loops of the small intestine resulting in intermittent, acute or sub-acute gastrointestinal obstruction (Augustine et al., 2009). EPS has been primarily described secondary to treatment with peritoneal dialysis (PD) but it may also occur as a manifestation of several other conditions, such as systemic autoimmune diseases, diseases of the gastrointestinal tract, peritoneal and intra-abdominal malignancies, exposure to talc or particulate matter or the use of intraperitoneal disinfectant for peritoneal lavage and β-blocker administration (Plum et al., 2001; Kawanishi and Moriishi, 2005). EPS has also been reported after organ transplantation suggesting that transplantation may be an additional trigger for its onset (Fieren et al., 2007). Etiological factors that cause EPS in cases of long-term PD are insufficiently clear but there is evidence that high glucose concentration and acidic pH in dialysis fluid, as well as the heat sterilization of PD fluids, cause peritoneal damage and formation of deposits comprising glucose degradation products (GDP) and advanced glycation end products (AGEs) (Jorres et al., 1992; Fieren et al., 2007; Schmitt et al., 2007; Jagirdar et al., 2019). This may be aggravated by recurrent attacks of peritonitis. The reported prevalence of EPS in patients undergoing PD varies from 0.7% and 3.3% and increases with length of time on PD (Schmitt et al., 2007; Brown et al., 2009). Clinical presentation of EPS includes weight loss, nausea, anorexia, intractable anemia, hypoalbuminemia, raised inflammatory markers and recurrent episodes of acute or sub-acute small-bowel obstruction. Occasionally, an abdominal mass, formed of the cocooned gut is palpable (Kawaguchi et al., 2000; Brown et al., 2009). The current management of EPS is based on prevention and treatment of inflammatory and fibrotic changes on the peritoneal membrane by immunosuppressive and antifibrotic agents, respectively (Kawaguchi et al., 2000). However, the optimal treatment for EPS remains controversial. Surgery forms an important aspect in the management of EPS and includes excision of the thickened and restricting membrane with enterolysis. Occasionally small bowel resection with the formation of stomas may be required. Postoperative medical treatment, in the form of steroids, tamoxifen or immunosuppression is also used (Celicout et al., 1998; Samarasam et al., 2005; Liu et al., 2009; Cornelis and Oreopoulos, 2011). Regardless of the treatment modality, the mortality rate for patients with EPS is still high and ranges between 25 and 55% (Kawanishi and Moriishi, 2005; Brown et al., 2009).

Herein, we report a case of a 16-year-old adolescent boy who developed EPS seven years after being placed on PD complicated by several episodes of bacterial peritonitis and who was successfully treated with surgical enterolysis.

Case report

We report a case of a 16-year-old adolescent boy with a history of chronic renal failure due to bilateral high-grade vesicoureteral reflux and neuropathic bladder who

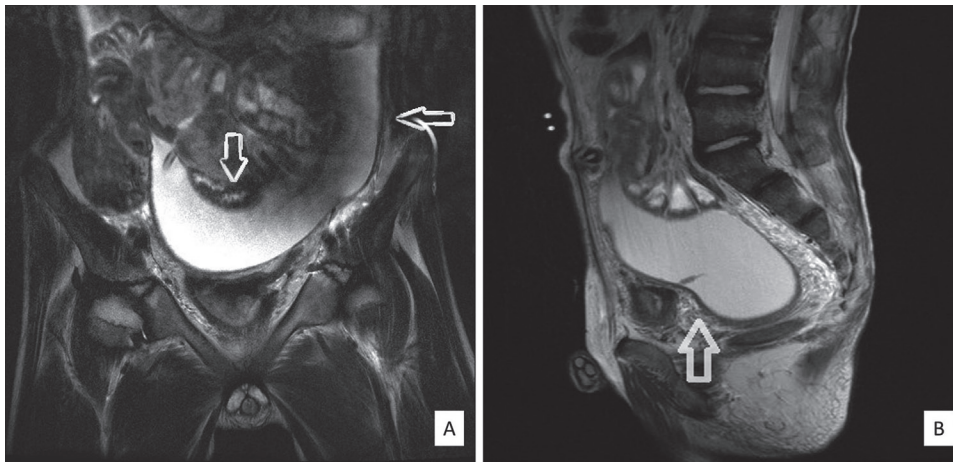

Figure 1A and B – Magnetic resonance imaging T2 WI scans in coronal and sagittal positions demonstrated thickened enhancing peritoneum and hyperintense, loculated fluid collection in the loops of the small bowel (white arrows).

underwent diversionary surgery followed by subtotal bladder excision and bladder augmentation cystoplasty with the sigmoid at the age of 7 years. Two years later, peritoneal dialysis was commenced for renal replacement and associated with several episodes of bacterial peritonitis. After seven years, due to ultrafiltration failure, the PD catheter was taken out and hemodialysis (HD) commenced. Three months after the removal of the peritoneal catheter the patient developed abdominal symptoms consisting of distension and diffuse abdominal pain, associated with loss of appetite, nausea, and intermittent vomiting. It was noted that his weight had reduced by 10 kg the past year.

A plain X-ray of the abdomen showed multiple dilated loops of small bowel with air-fluid levels indicating an obstruction. An abdominal ultrasound demonstrated an echogenic thickening of the bowel walls of uncertain etiology while MRI (magnetic resonance imaging) indicated a thickened peritoneum and hyperintense, loculated fluid collections between the loops of the small bowel (Figure 1A and B).

After a short course of the conservative treatment that consisted of close monitoring, nasogastric suction, and intravenous hydration, the patient underwent a laparotomy that was performed through the anterior approach with a long midline incision. A thorough abdominal exploration was carried out. The small bowel was covered with a thick cocoon that could not be separated from the intestinal wall. During the procedure there was a perforation of the mid ileum which was repaired with seromuscular single-layered sutures. The findings were consistent with EPS (Figure 2A).

Biopsy of the thickened peritoneum was done during laparotomy and the specimen was submitted to histopathology. It confirmed a thick fibrous capsule that

was composed of scattered fibroblasts, fibrinous material with dense inflammatory infiltrates of both mononuclear and polymorphonuclear cells.

During the post-operative course there was development of an enteric fistula. Total parenteral nutrition was established and the patient was transferred to the specialized tertiary center for further treatment.

After a two-week period of stabilization with total parenteral nutrition, regular dialysis and antibiotics, the patient was re-explored. Through a long midline laparotomy, the abdominal cavity was carefully entered. The entire small gut was encased in a granulating and fibrotic visceral peritoneal cocoon. There was a cavity anterior to the cocoon extending into the left hypochondrium, containing feculent material. A punched out everted perforation was seen in the cocooned mass. With careful dissection, the encasing cocoon was dissected off the bowel wall, releasing

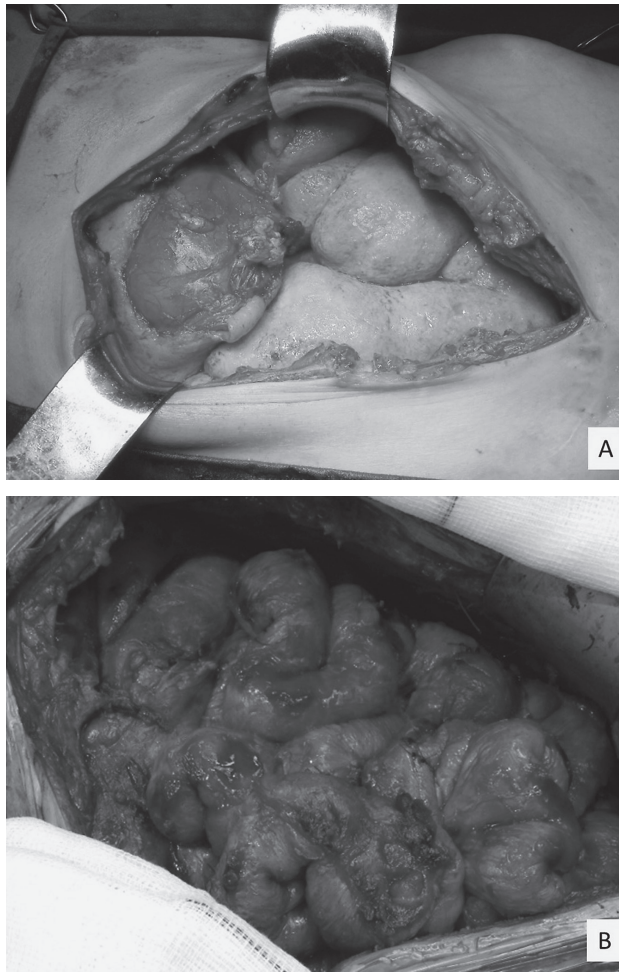

Figure 2 – Gross appearance of encapsulating peritoneal sclerosis before and after enterolysis: peritoneal thickening on the visceral peritoneum of the loops of the small bowel (A) and complete enterolysis (B).

loops of cocooned small bowel. The entire small bowel was released from the ligament of Treitz to the ileocecal junction. The perforation was localized to the mid ileum. An iatrogenic enterotomy was made in the terminal ileum, which was closed in a single layer. Once a complete enterolysis had been carried out (Figure 2B), the perforation was excised and was brought out in the left iliac fossa as a double-barreled ileostomy. The abdomen was thoroughly lavaged with saline and the abdomen packed with betadine packs. The patient was kept ventilated in the pediatric ICU (intensive care unit) and after 48 hours, re-explored. The gut was found to be healthy without any obvious perforations. The abdomen was closed with interpositioned biologic mesh, Strattice™ with skin closure over the mesh after undermining subcutaneous tissue. A vacuum dressing was placed over the closure. The patient was then woken up gradually and waned off the ventilator after a further 48 hours. There was a 6-week period of recuperation, with wound sepsis with *Vancomycin-Resistant Enterococcus* (VRE) and *Candida*, which required micafungin for 3 weeks. A full oral diet was established after 10 days and parenteral nutrition weaned off.

After 6 months, the patient returned to the specialized tertiary center for planned elective closure of the stoma. A midline laparotomy was carried out and the abdomen inspected. The gut was found to be healthy without any evidence of cocooning or adhesions. The double barrel stoma was taken down and closed in a single layer after excising the mucocutaneous edges. The abdomen was closed.

After initially doing well, the patient developed an enterocutaneous fistula by the end of a week, draining about 500 ml of enteric contents towards the bottom of the laparotomy incision. This was treated conservatively by parenteral nutrition for about 8 weeks at the end of which the fistula completely settled and he was established on a full oral diet. He rapidly put on weight after that, with normal nutritional and inflammatory markers.

During a 7-year follow-up, there have been no further episodes of small bowel obstruction documented. He still continues to be on regular hemodialysis and is awaiting a deceased donor kidney transplant.

Discussion

EPS has been primarily described secondary to treatment with peritoneal dialysis (PD) in adults (Plum et al., 2001; Kawanishi and Moriishi, 2005). It is very uncommon in pediatric population and there are only very few reported and well documented cases of EPS in children (Hoshii et al., 2000; Ekim et al., 2005; Tan et al., 2005). However, the reported outcome of pediatric EPS cases is significantly better with a lower mortality and morbidity compared with adult patients (Shroff et al., 2013; Jagirdar et al., 2019).

Regardless the patient's age and the underlying factors that cause EPS, the principles of management remain the same. Our case illustrates the morbidity that could be associated with this difficult condition and the importance of early definitive diagnosis and effective multidisciplinary surgical intervention.

For the proper treatment of EPS, Nakamoto (2005) proposed that the development of EPS should be divided based on abdominal symptoms, inflammation, encapsulation, and intestinal findings into four stages: stage 1 (pre-EPS), stage 2 (inflammatory), stage 3 (encapsulating), and stage 4 (chronic EPS).

There is a strong evidence that the duration of the PD therapy is linked with the development of EPS (Kawanishi et al., 2004; Brown et al., 2009). While the length of time alone may not be the strongest factor, that in combination with recurrent episodes of peritonitis and other predisposing factors in all likelihood causes overt disease. It has also been noted that more than two-thirds of EPS cases are diagnosed after discontinuation of PD therapy (Kawanishi et al., 2004), or a modality shift; i.e. PD to HD or PD to successful transplantation. Yamamoto et al. (2010) have suggested that retaining the PD catheter and regular lavage may be a possible limiting factor for the accumulation of factors that encourage the development of the disease. Our case reflects all these etiologic aspects because the presentation of EPS occurred seven years after the introduction of PD therapy and three months after discontinuation of PD.

No gold standard exists for the diagnosis of EPS. At present, there are no reliable predictive markers for EPS. However, in any patient on long term PD with abdominal symptoms, persistently raised inflammatory markers and a declining albumin, the diagnosis of EPS should be considered. The diagnosis of EPS is based on a constellation of clinical findings and confirmed by imaging techniques (CT – computed tomography, or ultrasound) or by laparotomy (Nakamoto, 2005; Moinuddin et al., 2014). Consequently, there are no consensus guidelines on the management of EPS. The mainstay of management consists of the termination of PD and the use of immunosuppressive, antifibrotic medicines, aggressive nutritional support, and surgical treatment when necessary. There is no definite medical therapy for the disease although some small case studies showed the usefulness of corticosteroids, particularly in the treatment of EPS in its early inflammatory stages, and tamoxifen (Korte et al., 2011; Kawanishi, 2012). However, other studies did not confirm the significant utility of tamoxifen, a selective estrogen receptor modulator with strong anti-fibrotic properties related to inhibition of cytokine TGF-β (transforming growth factor-β) (Balasubramaniam et al., 2009). Surgical treatment in EPS was previously associated with high morbidity and mortality rates (Kittur et al., 1990). However, more recently, surgical enterolysis has been shown to be the definitive therapeutic option in almost all patients with advanced EPS with acute or subacute intestinal obstruction (Kawanishi et al., 2005, 2011). One of the more important reasons for this increased success is the conduct of treatment by experienced surgeons familiar with this pathology. This therapeutic approach appeared to work in our pediatric case, as the patient had no more recurrent episodes of intestinal obstruction. The management of our patient reflects the challenges that can be faced in the surgical treatment of EPS. It also shows that EPS may affect children and that an aggressive surgical management can be effective

and lifesaving for these patients. Additionally, this report could alert pediatric nephrologists to this rare but a life-threatening complication of chronic PD and emphasize the need for prompt diagnosis and timely conversion to hemodialysis (HD) in high-risk patients with ultrafiltration failure.

References

Augustine, T., Brown, P. W., Davies, S. D., Summers, A. M., Wilkie, M. E. (2009) Encapsulating peritoneal sclerosis: clinical significance and implications. *Nephron Clin. Pract*. **111(2)**, c149–154; discussion c154.

Balasubramaniam, G., Brown, E. A., Davenport, A., Cairns, H., Cooper, B., Fan, S. L., Farrington, K., Gallagher, H., Harnett, P., Krausze, S., Steddon, S. (2009) The Pan-Thames EPS study: Treatment and outcomes of encapsulating peritoneal sclerosis. *Nephrol. Dial. Transplant*. **24(10)**, 3209–3215.

Brown, M. C., Simpson, K., Kerssens, J. J., Mactier, R. A.; Scottish Renal Registry (2009) Encapsulating peritoneal sclerosis in the new millennium: a national cohort study. *Clin. J. Am. Soc. Nephrol*. **4(7)**, 1222–1229.

Celicout, B., Levard, H., Hay, J., Msika, S., Fingerhut, A., Pelissier, E. (1998) Sclerosing encapsulating peritonitis: Early and late results of surgical management in 32 cases. French Associations for Surgical Research. *Dig. Surg*. **15(6)**, 697–702.

Cornelis, T., Oreopoulos, D. G. (2011) Update on potential medical treatments for encapsulating peritoneal sclerosis; human and experimental data. *Int. Urol. Nephrol*. **43(1)**, 147–156.

Ekim, M., Fitoz, S., Yagmurlu, A., Ensari, A., Yuksel, S., Acar, B., Ozcakar, Z. B., Kendirli, T., Bingoler, B., Yalcinkaya, F. (2005) Encapsulating peritoneal sclerosis in paediatric peritoneal dialysis patients. *Nephrology (Carlton)* **10(4)**, 341–343.

Fieren, M. W., Betjes, M. G., Korte, M. R., Boer, W. H. (2007) Posttransplant encapsulating peritoneal sclerosis: a worrying new trend? *Perit. Dial. Int*. **27(6)**, 619–624.

Gandhi, V. C., Humayun, H. M., Ing, T. S., Daugirdas, J. T., Jablokow, V. R., Iwatsuki, S., Geis, W. P., Hano, J. E. (1980) Sclerotic thickening of the peritoneal membrane in maintenance peritoneal dialysis patients. *Arch. Intern. Med*. **140(9)**, 1201–1203.

Hoshii, S., Honda, M., Itami, N., Oh, S., Matsumura, C., Moriya, S., Mori, M., Hatae, K., Ito, Y., Karashima, S. (2000) Sclerosing encapsulating peritonitis in pediatric peritoneal dialysis patients. *Pediatr. Nephrol*. **14(4)**, 275–279.

Jagirdar, R. M., Bozikas, A., Zarogiannis, S. G., Bartosova, M., Schmitt, C. P., Liakopoulos, V. (2019) Encapsulating peritoneal sclerosis: Pathophysiology and current treatment options. *Int. J. Mol. Sci*. **20(22)**, 5765.

Jorres, A., Topley, N., Gahl, G. M. (1992) Biocompatibility of peritoneal dialysis fluids. *Int. J. Artif. Organs* **15(2)**, 79–83.

Kawaguchi, Y., Kawanishi, H., Mujais, S., Topley, N., Oreopoulos, D. G. (2000) Encapsulating peritoneal sclerosis: Definition, etiology, diagnosis, and treatment. International Society for Peritoneal Dialysis Ad Hoc Committee on Ultrafiltration Management in Peritoneal Dialysis. *Perit. Dial. Int*. **20**, S43–S55 (Suppl. 4).

Kawanishi, H. (2012) Surgical and medical treatments of encapsulation peritoneal sclerosis. *Contrib. Nephrol*. **177**, 38–47.

Kawanishi, H., Moriishi, M. (2005) Epidemiology of encapsulating peritoneal sclerosis in Japan. *Perit. Dial. Int*. **25**, S14–S18 (Suppl. 4).

Kawanishi, H., Kawaguchi, Y., Fukui, H., Hara, S., Imada, A., Kubo, H., Kin, M., Nakamoto, M., Ohira, S., Shoji, T. (2004) Encapsulating peritoneal sclerosis in Japan: a prospective, controlled, multicenter study. *Am. J. Kidney Dis*. **44(4)**, 729–737.

Kawanishi, H., Watanabe, H., Moriishi, M., Tsuchiya, S. (2005) Successful surgical management of encapsulating peritoneal sclerosis. *Perit. Dial. Int*. **25**, S39–S47 (Suppl. 4).

Kawanishi, H., Shintaku, S., Moriishi, M., Dohi, K., Tsuchiya, S. (2011) Seventeen years' experience of surgical options for encapsulating peritoneal sclerosis. *Adv. Perit. Dial*. **27**, 53–58.

Kittur, D. S., Korpe, S. W., Raytch, R. E., Smith, G. W. (1990) Surgical aspects of sclerosing encapsulating peritonitis. *Arch. Surg*. **125(12)**, 1626–1628.

Korte, M. R., Fieren, M. W., Sampimon, D. E., Lingsma, H. F., Weimar, W., Betjes, M. G.; investigators of the Dutch Multicentre EPS Study (2011) Tamoxifen is associated with lower mortality of encapsulating peritoneal sclerosis: results of the Dutch Multicentre EPS Study. *Nephrol. Dial. Transplant*. **26(2)**, 691–697.

Liu, H. Y., Wang, Y. S., Yang, W. G., Yin, S. L., Pei, H., Sun, T. W., Wang, L. (2009) Diagnosis and surgical management of abdominal cocoon: results from 12 cases. *Acta Gastroenterol. Belg*. **72(4)**, 447–449.

Moinuddin, Z., Summers, A., Van Dellen, D., Augustine, T., Herrick, S. E. (2014) Encapsulating peritoneal sclerosis – A rare but devastating peritoneal disease. *Front. Physiol*. **5**, 470.

Nakamoto, H. (2005) Encapsulating peritoneal sclerosis – A clinician's approach to diagnosis and medical treatment. *Perit. Dial. Int*. **25**, S30–S38 (Suppl. 4).

Plum, J., Hermann, S., Fusshöller, A., Schoenicke, G., Donner, A., Röhrborn, A., Grabensee, B. (2001) Peritoneal sclerosis in peritoneal dialysis patients related to dialysis settings and peritoneal transport properties. *Kidney Int. Suppl*. **78**, S42–S47.

Samarasam, I., Mathew, G., Sitaram, V., Perakath, B., Rao, A., Nair, A. (2005) The abdominal cocoon and an effective technique of surgical management. *Trop. Gastroenterol*. **26(1)**, 51–53.

Schmitt, C. P., von Heyl, D., Rieger, S., Arbeiter, K., Bonzel, K. E., Fischbach, M., Misselwitz, J., Pieper, A. K., Schaefer, F.; Mid European Pediatric Peritoneal Dialysis Study Group (MEPPS) (2007) Reduced systemic advanced glycation end products in children receiving peritoneal dialysis with low glucose degradation product content. *Nephrol. Dial. Transplant*. **22(7)**, 2038–2044.

Shroff, R., Stefanidis, C. J., Askiti, V., Edefonti, A., Testa, S., Ekim, M., Kavaz, A., Ariceta, G., Bakkaloglu, S., Fischbach, M., Klaus, G., Zurowska, A., Holtta, T., Jankauskiene, A., Vondrak, K., Vande Walle, J., Schmitt, C. P., Watson, A. R.; European Paediatric Dialysis Working Group (2013) Encapsulating peritoneal sclerosis in children on chronic PD: A survey from the European Paediatric Dialysis Working Group. *Nephrol. Dial. Transplant*. **28(7)**, 1908–1914.

Tan, F. L., Loh, D., Prabhakaran, K. (2005) Sclerosing encapsulating peritonitis in a child secondary to peritoneal dialysis. *J. Pediatr. Surg*. **40(5)**, e21–e23.

Yamamoto, T., Nagasue, K., Okuno, S., Yamakawa, T. (2010) The role of peritoneal lavage and the prognostic significance of mesothelial cell area in preventing encapsulating peritoneal sclerosis. *Perit. Dial. Int*. **30(3)**, 343–352.

 Prague Medical Report / Vol. 121 (2020) No. 4, p. 262–266

A Severe Case of Anaplastic Large Cell Lymphoma in a Previously Healthy Woman: Diagnostic and Therapeutic Challenges

Petya Angelova[1], Robert Brock[1], Alexandra-Teodora Negoescu[1], Lara-Marie Schmitt[2], Julia Meißner[2], Sascha Dietrich[2], Carsten Müller-Tidow[2], Jan Philipp Novotny[2]

[1]Heidelberg Medical Faculty, Heidelberg University, Heidelberg, Germany; [2]Department of Internal Medicine V, University Hospital Heidelberg, Heidelberg, Germany

Received May 9, 2020; Accepted November 2, 2020.

Key words: Lymphoma – Anaplastic – Anaplastic large cell lymphoma – Hemophagocytic lymphohistiocytosis

Abstract: Anaplastic large cell lymphomas are an aggressive subtype of peripheral T-cell lymphomas that can manifest with a variety of symptoms. Our case highlights the importance of prompt tissue sampling, especially if an associated hemophagocytic lymphohistiocytosis is detected and no clinical improvement is observed upon glucocorticoid treatment.

Mailing Address: Jan Philipp Novotny, MD., PhD., Department of Internal Medicine V, University Hospital Heidelberg, Im Neuenheimer Feld 410, 69120 Heidelberg, Germany; Phone: 062 215 60; e-mail: JanPhilipp.Novotny@med.uni-heidelberg.de

https://doi.org/10.14712/23362936.2020.23

Introduction

Anaplastic large cell lymphomas (ALCL) are pathologically distinct lymphoid neoplasms with clinically aggressive behaviour. ALCL show an incidence of approximately 0.25 per 100,000 person-years and account for approximately 14% of all diagnosed NK/T-cell lymphomas (Morton et al., 2006). The anaplastic lymphoma kinase (*ALK*) is aberrantly expressed in approximately 50 to 80% of all patients with ALCL and correlates with chromosomal rearrangement, e.g. t(2;5)(p23;q35) – resulting in an *ALK-NPM1* fusion. It allows the subdivision into ALK-positive and ALK-negative ALCL, which are listed as distinct entities in the current World Health Organization classification (Swerdlow et al., 2008). In a retrospective analysis, the median age of ALK-positive ALCL was 34 years, whereas the median age of ALK-negative ALCL was 58 (Savage et al., 2008). For both subsets, patients are predominantly male and present with stage III to IV disease, which often involves multiple extranodal sites including skin, soft tissue, bone, lung, intestinal tract, liver, spleen and bone marrow (Falini et al., 1999; Savage et al., 2008; Sibon et al., 2012). B-symptoms and other paraneoplastic phenomena like migratory rash, pruritus, arthralgias, lymph node, and skeletal pain are commonly observed (Shustov and Soma, 2019). Initial laboratory analyses sometimes reveal nonspecific abnormalities, such as lactate dehydrogenase (LDH) elevation, anemia and thrombocytopenia (Savage et al., 2008). Usually the diagnosis of ALCL is suggested by the morphology and confirmed by positive immunohistochemistry for CD30 and eventually ALK (Shustov and Soma, 2019). Early recognition and diagnosis followed by appropriate therapy are critical cornerstones of care. Treatment with Brentuximab vedotin, Cyclophosphamide, Doxorubicin, and Prednisone (A+CHP) can entail a similar rate of adverse effects like febrile neutropenia or peripheral neuropathy, but was shown to be associated with a significantly improved progression free survival when compared to standard CHOP (Vincristine, Doxorubicin, Cyclophosphamide, Prednisone) therapy (Horwitz et al., 2019).

A rare and severe complication of ALCL is hemophagocytic lymphohistiocytosis (HLH). This cytokine-driven hyperinflammatory syndrome can either manifest primarily due to a genetic defect or as a secondary concomitant phenomenon of hematological malignancies, infections, autoimmune processes or drug intake (Vick et al., 2017). HLH is diagnosed in about 23% of all patients with peripheral T-cell lymphomas and is associated with a significantly worse prognosis (Xie et al., 2013). The median overall survival in these cases is less than 1 year and HLH can present with various symptoms. Thus, the clinical diagnosis requires the fulfilment of 5 out of 8 criteria (Vick et al., 2017). Laboratory findings showing cytopenia, hypertriglyceridemia, hyperferritinemia, and elevated soluble IL-2 receptor (sCD25) should heighten the suspicion of HLH.

Case report

A previously healthy Caucasian female in her early fifties was referred by her general practitioner and presented with a one-week history of fever, headache, myalgia, as well as a three-week history of a slightly enlarged and tender right inguinal lymph node. The patient declined any travel history, night-sweat or loss of weight, but stated to suffer from fever (up to 40 °C) and shivering during the last week. Upon physical examination, enlarged cervical, supraclavicular and inguinal lymph nodes were observed. Initial laboratory work-up showed slight leukocytopenia (2.89×10^9/l, range 4–10×10^9/l) with left shift (banded neutrophils 14%, segmented neutrophils 40%, lymphocytes 38%, monocytes 1%, metamyelocytes 1%, myelocytes 2%, atypical lymphocytes 4%), as well as thrombocytopenia (82×10^9/l, range 150–440×10^9/l) and increased lactate dehydrogenase (LDH) of 793 U/l (range < 308 U/l). Furthermore, we observed an increased C-reactive protein (CRP) concentration of 28.9 mg/l (range < 5 mg/l), minimally elevated aspartate-aminotransferase (AST) and elevated lipase and pancreatic amylase, albeit without associated symptoms of pancreatitis. Empirical antibiotic therapy was started with amoxicillin/clavulanic acid and subsequently changed to ceftriaxone and clarithromycin due to persistent fever.

Based on these findings we initially suspected an infectious cause and abdominal sonography revealed hepatosplenomegaly, which was consistent with a possible Epstein-Barr-Virus (EBV) infection. Computed tomography of the neck, chest and abdomen additionally demonstrated several marginally or pathologically enlarged lymph nodes. However, analyses of anti-EBV IgG and IgM demonstrated only positivity for gamma immunoglobulin, indicating a past infection. Further work-up did not reveal any signs of an active or past HIV, cytomegalovirus (CMV) or hepatitis B/C infection and blood cultures remained without microbial growth. We therefore performed a bone marrow aspiration, which showed maturation of all cell-lines. However, toxic granulations were observed within the granulopoietic system and slight dysplastic changes of erythropoiesis, but without the presence of ring sideroblasts or cytologically apparent neoplastic infiltration. In the course of the disease, the patient rapidly developed progressive hyponatremia, as well as markedly elevated liver enzymes (AST up to 2,486 U/l, range < 37 U/l, ALT 1,551 U/l, range < 35 U/l, and GGT 1,136 U/l, range < 40 U/l). Concomitantly, we observed worsening of the international normalized ratio (INR), rise in LDH (up to 3,041 U/l), soluble IL-2 (up to 34,864 U/ml) and ferritin (up to 20,066 µg/l) – indicating an underlying hemophagocytic lymphohistiocytosis (HLH) with hepatic involvement. The most common secondary infectious causes of HLH were ruled out by extensive serological and microbiological testing. We started the patient on 100 mg/day intravenous prednisone, after which liver transaminases decreased. However, the patients' overall condition did not improve and she suffered from constant fever, even with continuous application of novaminsulfon.

Concomitant pathological analyses of an inguinal lymph node, as well as bone marrow biopsy and liver biopsy then revealed a highly proliferating (Ki67: 90–95%)

neoplasm with medium-sized cytomorphology. Immunohistochemistry showed positivity for CD30, ALK-1, Perforin, EMA, CD3 and weak CD4, whilst no signal was observed for CD20, PAX-5, CD68. CD117, CD138, CD5, CD8 and AE1/3. Therefore, the diagnosis of a highly proliferating ALK-positive anaplastic large cell lymphoma (ALCL) was made. Furthermore, marked necroinflammatory and proliferative activity of the liver parenchyma was observed.

We immediately started a treatment with dose-adapted A+CHP (Brentuximab, Cyclophosphamide, Doxorubicin and Prednisone), after which we did not observe a tumour lysis syndrome according to the Cairo-Bishop criteria, but a decrease in renal function with a glomerular filtration rate of minimally 28.5 ml/min/1.73 m^2 according to CKD-EPI and hydropic decompensation that necessitated aggressive diuretic therapy, as well as supportive oxygen. Due to rising CRP and recurrent fever, antibiotic therapy was then escalated to piperacillin/tazobactam and subsequently to meropenem. Computed tomography of the chest revealed bipulmonary infiltrates. We transferred the patient to our intensive care due to progressive respiratory insufficiency and endotracheal intubation was necessary thereafter. The patients' condition worsened with concomitantly rising liver parameters, CRP, LDH and progressive renal insufficiency. Blood cultures showed growth of *Enterococcus faecium*, but no significant growth of pathological microbiota was observed after culture of upper respiratory tract material. Despite maximum catecholaminergic support and anti-infective treatment according to the obtained antibiogram, the patient died of (most likely) pneumogenic neutropenic septic shock with multi-organ failure only 8 days after diagnosis of the underlying ALCL.

Discussion and Conclusion

Hodgkin and non-Hodgkin lymphomas like ALCL can present diagnostic challenges for clinicians. Due to the rarity and broad differential diagnosis these malignancies can remain clinically unrecognized over a long period of time (Mosunjac et al., 2008). Since the clinical symptoms and initial laboratory analyses of patients with ALCL are nonspecific and vary considerably among individuals, immunohistochemical analysis of affected sites is required to confirm the diagnosis (Hapgood and Savage, 2015). Furthermore, a unique feature of our case was that ALCL presented as an inguinal lymph node which was painful, in contrast to lymphomatous nodes, which usually appear to be non-tender (Bilodeau and Fessele, 1998).

The patient's history of prolonged fever and tender inguinal lymph node thus also pointed to an infectious disease as the trigger of her hemophagocytic lymphohistiocytosis. Furthermore, treatment with prednisone did not result in clinical improvement in our patient, which is in contrast to its observed beneficial effects in patients with lymphoid malignancies (Pufall, 2015).

In summary, ALCL should be suspected whenever a patient presents with fever, mild lymphadenopathy, hepatosplenomegaly and laboratory findings consistent with a hyperinflammatory syndrome. Our case report highlights the importance of timely

collection of bioptic material for the early detection and correct identification of an underlying ALCL. Furthermore, maintaining a high degree of suspicion is decisive to identify a hematologic malignancy as the underlying cause for hemophagocytic lymphohistiocytosis because clinical symptoms can overlap.

References

Bilodeau, B. A., Fessele, K. L. (1998) Non-Hodgkin's lymphoma. *Semin. Oncol. Nurs*. **14**, 273–283.

Falini, B., Pileri, S., Zinzani, P. L., Carbone, A., Zagonel, V., Wolf-Peeters, C., Verhoef, G., Menestrina, F., Todeschini, G., Paulli, M., Lazzarino, M., Giardini, R., Aiello, A., Foss, H. D., Araujo, I., Fizzotti, M., Pelicci, P. G., Flenghi, L., Martelli, M. F., Santucci, A. (1999) ALK+ lymphoma: Clinico-pathological findings and outcome. *Blood* **93**, 2697–2706.

Hapgood, G., Savage, K. J. (2015) The biology and management of systemic anaplastic large cell lymphoma. *Blood* **126**, 17–25.

Horwitz, S., O'Connor, O. A., Pro, B., Illidge, T., Fanale, M., Advani, R., Bartlett, N. L., Christensen, J. H., Morschhauser, F., Domingo-Domenech, E., Rossi, G., Kim, W. S., Feldman, T., Lennard, A., Belada, D., Illes, A., Tobinai, K., Tsukasaki, K., Yeh, S. P., Shustov, A., Huttmann, A., Savage, K. J., Yuen, S., Iyer, S., Zinzani, P. L., Hua, Z., Little, M., Rao, S., Woolery, J., Manley, T., Trumper, L., Group, E.-S. (2019) Brentuximab vedotin with chemotherapy for CD30-positive peripheral T-cell lymphoma (ECHELON-2): A global, double-blind, randomised, phase 3 trial. *Lancet* **393**, 229–240.

Morton, L. M., Wang, S. S., Devesa, S. S., Hartge, P., Weisenburger, D. D., Linet, M. S. (2006) Lymphoma incidence patterns by WHO subtype in the United States, 1992–2001. *Blood* **107**, 265–276.

Mosunjac, M. B., Sundstrom, J. B., Mosunjac, M. I. (2008) Unusual presentation of anaplastic large cell lymphoma with clinical course mimicking fever of unknown origin and sepsis: autopsy study of five cases. *Croat. Med. J*. **49**, 660–668.

Pufall, M. A. (2015) Glucocorticoids and cancer. *Adv. Exp. Med. Biol*. **872**, 315–333.

Savage, K. J., Harris, N. L., Vose, J. M., Ullrich, F., Jaffe, E. S., Connors, J. M., Rimsza, L., Pileri, S. A., Chhanabhai, M., Gascoyne, R. D., Armitage, J. O., Weisenburger, D. D.; International Peripheral T-Cell Lymphoma Project (2008) ALK– anaplastic large-cell lymphoma is clinically and immunophenotypically different from both ALK+ ALCL and peripheral T-cell lymphoma, not otherwise specified: Report from the International Peripheral T-Cell Lymphoma Project. *Blood* **111**, 5496–5504.

Shustov, A., Soma, L. (2019) Anaplastic large cell lymphoma: Contemporary concepts and optimal management. *Cancer Treat. Res*. **176**, 127–144.

Sibon, D., Fournier, M., Briere, J., Lamant, L., Haioun, C., Coiffier, B., Bologna, S., Morel, P., Gabarre, J., Hermine, O., Sonet, A., Gisselbrecht, C., Delsol, G., Gaulard, P., Tilly, H. (2012) Long-term outcome of adults with systemic anaplastic large-cell lymphoma treated within the Groupe d'Etude des Lymphomes de l'Adulte trials. *J. Clin. Oncol*. **30**, 3939–3946.

Swerdlow, S. H., Campo, E., Harris, N. L., Jaffe, E. S., Pileri, S. A., Stein, H. (2008) *WHO Classification of Tumours of Haematopoietic and Lymphoid Tissues*. IARC Press, Lyon.

Vick, E. J., Patel, K., Prouet, P., Martin, M. G. (2017) Proliferation through activation: Hemophagocytic lymphohistiocytosis in hematologic malignancy. *Blood Adv*. **1**, 779–791.

Xie, W., Hu, K., Xu, F., Zhou, D., He, J., Shi, J., Luo, Y., Zhu, J., Zhang, J., Lin, M., Ye, X., Huang, H., Cai, Z. (2013) Clinical analysis and prognostic significance of lymphoma-associated hemophagocytosis in peripheral T cell lymphoma. *Ann. Hematol*. **92**, 481–486.

Tubercular Mastitis Mimicking as Malignancy: A Case Report

Wasim Feroz[1], Arwah Mohammad Ali Sheikh[2], Vinodkumar Mugada[1]
[1]Department of Pharmacy Practice, Faculty of Pharmacy, Vignan Institute of Pharmaceutical Technology, Visakhapatnam, India;
[2]Patient Experience Management, Research Specialist, Forum Business Research, Visakhapatnam, India

Received August 12, 2020; Accepted November 2, 2020.

Key words: Breast carcinoma – Tubercular mastitis – Fine-needle – Granuloma – Tuberculosis

Abstract: Tubercular mastitis is a rare form of extrapulmonary tuberculosis commonly seen in multiparous and lactating women in developing countries. It is a diagnostic challenge and commonly misdiagnosed as breast carcinoma. Tubercular mastitis is paucibacillary, and fine-needle aspiration cytology provides an accurate diagnosis – the presence of granulomas with Langerhans giant cells on histopathological examination warrants empirical treatment with anti-tubercular drugs. We report a case of a 31-year-old Indian female who consulted a local physician with chief complaints of a palpable, tender mass in her left breast, with pain, swelling, and purulent discharge past 15 days. The patient's past medical, surgical, medication history, and family history (concerning tuberculosis) were not significant. Initially, the patient suspected of breast malignancy based upon physical examination, mammography, and fine-needle aspiration cytology but an accurate diagnosis of tubercular mastitis made with repeated histopathological examination. Histopathologic examination of excised material showed granulomas composed of histocytes, Langerhans giant cells, and inflammatory cells. The patient underwent surgical drainage on the left breast and put on the anti-tubercular regimen for 6 months with her child also prescribed isoniazid for 6 months. The patient advised for regular follow-ups.

Mailing Address: Dr. Wasim Feroz, Department of Pharmacy Practice, Faculty of Pharmacy, Vignan Institute of Pharmaceutical Technology, Visakhapatnam, India; Phone: +91 701 342 43 68; e-mail: wasimferoz5@gmail.com

https://doi.org/10.14712/23362936.2020.24

Introduction

Breast tuberculosis (TB), also known as tubercular mastitis (TM), is a rare form of extrapulmonary tuberculosis that was first described in 1829 by English surgeon Sir Astley Cooper (Cooper, 1829). The incidence of tubercular mastitis is 0.1% of all breast lesions in developed countries, but in developing countries where endemic is high, it reaches 3–4% (De Sousa and Patil, 2011; Gon et al., 2013). It is common in multiparous, lactating women (Dubey and Agarwal, 1968). It presents a diagnostic challenge as it closely mimics breast carcinoma, idiopathic granulomatous mastitis, and bacterial abscesses that may result in misdiagnosis. TM is paucibacillary, and thus routine diagnostic tests used for pulmonary tuberculosis like culture, microscopy, and polymerase chain reaction (PCR) techniques are not much useful (Pai et al., 2004). Primary tuberculous mastitis particularly refers to the rare cases in which the breast tissue is infected first by tubercle bacilli (Schaefer, 1955), whereas "secondary tuberculous mastitis" refers to the presence of tuberculous co-infection elsewhere in the body (Schaefer, 1955).

Tubercular mastitis generally presents as a single breast lump in the central or upper outer quadrant due to many extensions from axillary lymph nodes to the breast. The lump is usually irregular and hard, painful, mobile, or fixed to the skin or chest wall. In some cases, the lump presented with ulceration of the overlying skin, breast abscess, nipple retraction, and breast oedema (Strazzanti et al., 2018). Fine-needle aspiration cytology (FNAC) is a beneficial technique for detecting granulomas in tuberculosis endemic countries and presence of granulomas with Langerhans giant cells in FNAC warrants empirical treatment for tuberculosis even in the absence of positive acid-fast bacilli (AFB) and culture results (Tauro et al., 2011). Mammography and breast ultrasound imaging techniques do not provide aid in the diagnosis. Anti-tubercular regimen for at least six months in combination with surgical drainage are usually associated with excellent outcome (Kakkar et al., 2000; Tewari and Shukla, 2005).

Following CARE guidelines, we report a rare case of tubercular mastitis in a 31-year-old female, initially suspected as a breast malignancy. However, later on, the patient was correctly diagnosed after histopathological examination of excisional biopsy material.

Case report

On 11th May 2020, a 31-year-old Indian female, house-wife by occupation and mother of three children, consulted a local physician with chief complaints of a palpable, tender mass in her left breast, with pain, swelling and purulent discharge since past 15 days. The right breast was normal. The patient is illiterate and resides in a village. She was afebrile, and her vitals were outlined in Table 1. The patient was a non-smoker, non-alcoholic, consumes a mixed Indian diet, and has a regular sleep pattern. There was no history of loss of weight, loss of appetite, night sweats, and fever. The patient's past medical, surgical, medication history, and family history

Table 1 – Vital parameters of the patient at different periods

Date	Vital parameters
11th May 2020	– Temperature – 36.5 °C – Pulse rate – 96 beats per minute – Respiratory rate – 18 breaths per minute – Blood pressure – 110/70 mm Hg
21st May 2020	– Temperature – 36.5 °C – Pulse rate – 110 beats per minute – Respiratory rate – 16 breaths per minute – Blood pressure – 110/70 mm Hg
26th May 2020	– Eastern Cooperative Oncology Group performance status – 0 – Temperature – 36.4 °C – Pulse rate – 112 beats per minute – Blood pressure – 100/60 mm Hg – SpO_2 – 97%
2nd June 2020	– Temperature – 36.2 °C – Pulse rate – 120 beats per minute – Respiratory rate – 18 breaths per minute – Blood pressure – 110/70 mm Hg – SpO_2 – 98%
3rd June 2020	– Pulse rate – 80 beats per minute – Blood pressure – 120/80 mm Hg

(w.r.t. TB) were not significant. Upon physical examination, the left breast showed a painful lump with abnormal discharge.

The pharmacotherapy is outlined in Table 2. Despite the pharmacotherapy, her symptoms were not relieved. On 21st May 2020, the patient again complained of severe pain and redness in the left breast. Upon physical examination, a painful lump with redness around the nipple area was observed. The lump was observed in the upper, anterior, and central quadrant. Her laboratory investigations and imaging technique results are outlined in Table 3. Ultrasound-guided FNAC of the left breast showed abundant inflammatory infiltrates of polymorphonuclear leucocytes, as well as several loose clusters of ductal cells seen with mild nuclear atypia along with multinucleated giant cells. Clinical differential diagnosis of ductal malignancy with abscess made. The patient referred to the National Cancer Institute (NCI).

On 26th May 2020, the patient visited NCI with severe pain and redness in the left breast, coupled with anorexia. Upon left breast examination, a lump of size measuring 6×5 cm with nipple-areolar complex enhancement was observed. There were no signs of icterus, pallor, bleeding, pedal oedema, clubbing, and cyanosis. Her gynaecologic history was reported as G3P3A0. Her last menstrual period recorded was on 18th May 2020, with the regular flow. The doctor advised for tru-cut biopsy, bilateral digital mammography, complete blood count (CBC),

Table 2 – Details of the pharmacotherapy at different periods

Date	Prescribed drugs	R.O.A.	Notes
11th May 2020	– Tab Amoxicillin (500 mg) + Clavulanic acid (125 mg) – twice daily for 5 days – Diethylcarbamazine citrate – 100 mg – Piroxicam – 10 mg	oral	The treatment was prescribed for a one-week duration.
2nd June 2020	– Tab Amoxicillin (500 mg) + Clavulanic acid (125 mg) – twice daily for 5 days – Tab Pantoprazole (40 mg) – twice daily for 5 days – Tab Diclofenac (50 mg) + Serratiopeptidase (10 mg) – twice daily for 5 days	oral	The patient took medicines for one day. On 3rd June the patient was operated and was prescribed with other medications.
3rd June 2020	– Tab Amoxicillin (500 mg) + Clavulanic acid (125 mg) – twice daily for 5 days – Tab Paracetamol (650 mg) – twice daily for 5 days	oral	none
11th June 2020	Anti-tubercular regimen: – Rifampicin (R) – 150 mg – Isoniazid (H) – 75 mg – Pyrazinamide (Z) – 400 mg – Ethambutol hydrochloride (E) – 275 mg	oral	The course of treatment was 6 months. The child of the mother also prescribed isoniazid – 100 mg.

R.O.A. – route of administration

liver function test (LFT), kidney function test (KFT), CT (computed tomography) scan of chest and abdomen, and bone scan (results mentioned in Table 3). Histopathological examination of left breast mass showed breast parenchyma with epithelioid cell granulomas composed of epithelioid cells, Langerhans giant cells, central necrosis, diffuse lympho-plasmacytic chronic inflammatory infiltrates with the collection of polymorphonuclear leucocytes. Intervening areas show benign breast ducts and lobules with chronic inflammatory infiltrate. Histomorphological findings are suggestive of granulomatous mastitis. ZN (Ziehl-Neelsen) stain for AFB negative. Her bilateral digital mammography of left breast shows heterogeneously dense. It shows a large irregular lesion with serrated margins involving the upper outer and central quadrant extending to the retro-areolar region. Correlative sonomammography reported a lobulated heterogeneously hypoechoeic lesion at 2–3 o'clock position, approximately measuring 4.8×2.8×2.1 cm with retro-areolar extension. There are associated with mixed echoic collections on the lateral aspect of the nipple and medially at 9 o'clock position with mobile internal echoes, appears inflammatory/infective.

Furthermore, few prominent and enlarged left axillary lymph nodes were observed with the largest measuring 2.1×1.1 cm. Bilateral digital mammography of the left breast suggests a large irregular lesion with serrated margins involving upper,

Table 3 – Abnormal laboratory investigation and imaging technique reports of the patient

Date	Laboratory investigation	Imaging technique reports
21st May 2020	Fine-needle aspiration cytology: The reported concluded that the features are suggestive of ductal malignancy with abscess.	none
26th May 2020	Haematology report: – Haemoglobin (Hb) – 10.7 g/dl – PCV – 30.5% – MCV – 69.1 fl – MCH – 24.3 pg Histopathology report: Impression: histomorphological findings are suggestive of granulomatous mastitis. ZN stain for AFB negative	Bilateral digital mammography: Right breast: Impression: bilateral digital mammography reveals: – No evidence of malignancy in the right breast. ACR-BIRADS category 1. – Large irregular lesion with serrated margins involving upper, outer and central quadrant extending to the retro-areolar region as described (ACR-BIRADS category 6).
3rd June 2020	– Random blood sugar – 96 mg/dl – Hb – 10.5 gm/dl – HIV screening – negative – HBsAG screening – negative	none
8th June 2020	Histopathology report: Left breast lump: inflammatory breast pathology – granulomatous mastitis. There was no evidence of carcinoma in the excised breast tissue.	none

Hb – haemoglobin; PCV – packed cell volume; MCV – mean corpuscular volume; MCH – mean corpuscular haemoglobin; HBsAG – hepatitis B virus antigen; ZN – Ziehl-Neelsen; AFB – acid fast bacillus

outer, and central quadrant extending to the retro-areolar region as described – ACR-BIRADS category 6 (ACR-BIRADS category – Table 4; Figure 1). There was no evidence of malignancy in the right breast, and it was normal – ACR-BIRADS category 1. The oncopathologist suggested for a repeat biopsy from the suspicious area/axillary lymph nodes for confirmation/to rule out malignancy.

On 2nd June 2020, the results of bone scan (skeletal scintigraphy) reports came, and there was no visible evidence of osteoblastic skeletal metastasis. The CT scan of the chest and abdomen were also normal. The patient was prescribed medication, as shown in Table 2, on 2 June. She took medications for one day, and later on the other day, she was operated and advised to undergo drainage and excision of the lump in the left breast. On 3rd June, her random blood sugar was 96 mg/dl; she was tested negative for HIV screening and HBsAg screening. At 2 p.m., the patient operated on left breast under general anaesthesia, and excision

Table 4 – Concordance between BI-RADS assessment categories and likelihood of cancer

Assessment	Likelihood of cancer
Category 0: Incomplete – need additional imaging evaluation and prior mammograms for comparison	N/A
Category 1: Negative	essentially 0% likelihood of malignancy
Category 2: Benign	essentially 0% likelihood of malignancy
Category 3: Probably benign	> 0% but ≤ 2% likelihood of malignancy
Category 4: Suspicious	> 2% but < 95% likelihood of malignancy
Category 4A: Low suspicion for malignancy	> 2% to ≤ 10% likelihood of malignancy
Category 4B: Moderate suspicion for malignancy	> 10% to ≤ 50% likelihood of malignancy
Category 4C: High suspicion for malignancy	> 50% to < 95% likelihood of malignancy
Category 5: Highly suggestive of malignancy	≥ 95% likelihood of malignancy
Category 6: Known biopsy-proven malignancy	N/A

N/A – not available

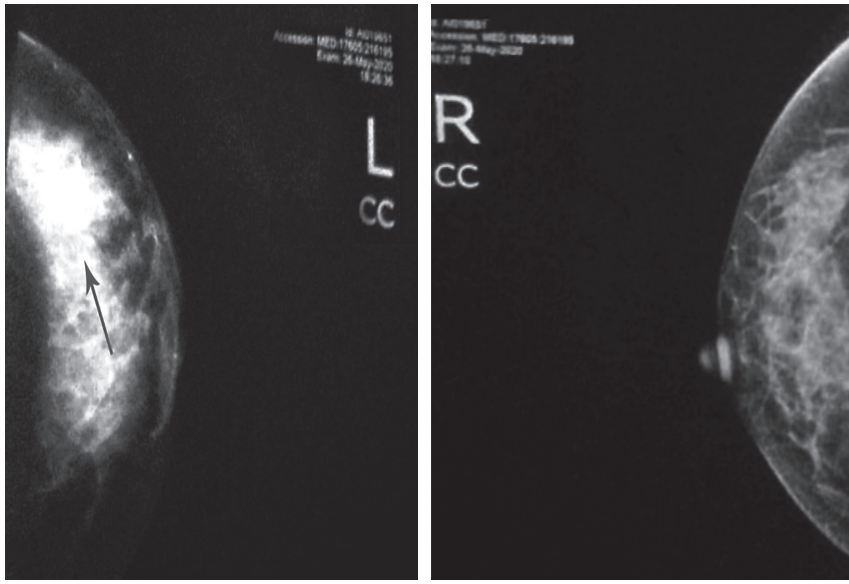

Figure 1 – Mammography of the left breast shows a large irregular lesion involving the upper, outer, and central quadrant.

with drainage performed, and the incisional biopsy material sent for testing. The patient asked to visit again after one week and prescribed medication, as outlined in Table 2. The patient referred to the regional TB hospital for further treatment. On 8th June, the histopathological report revealed a predominantly peri-ductal

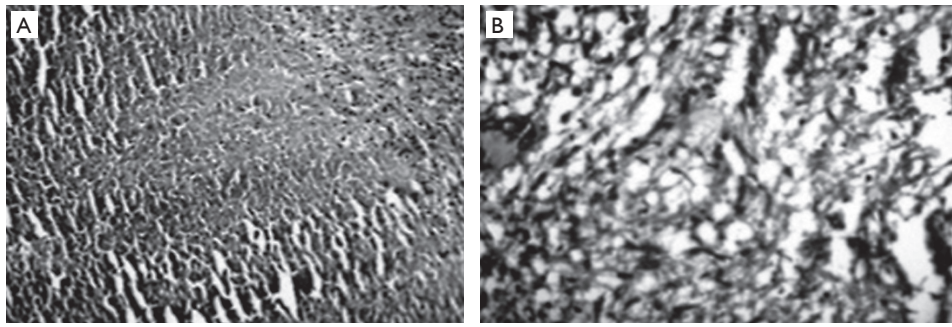

Figure 2 – A) Chronic granulomatous inflammation; B) smear confirms the presence of Langerhan's giant cell and inflammatory cells.

inflammation, peri-ductal fibrosis, and acute and chronic inflammatory infiltrate consisting of polymorphs and lymphocytes (Figure 2a). Granulomas were composed of histocytes, Langerhans giant cells, and inflammatory cells (Figure 2b), and there was no evidence of carcinoma in the excised breast tissue.

On 11th June, the patient visited the regional TB hospital, and her weight was 45 kg. The patient was diagnosed as tubercular mastitis (extrapulmonary TB), and the basis of diagnosis is clinical TB. She has prescribed an anti-tubercular regimen for 6 months and is advised for regular follow-ups.

ACR-BIRADS or BI-RADS stands for American College of Radiology-Breast Imaging Reporting and Data System and is established by the American College of Radiology. "BI-RADS is a scheme for putting the findings from mammogram screening (for breast cancer diagnosis) into a small number of well-defined categories" (American College of Radiology, 2020). "BI-RADS mainly benefits the radiologists who report mammograms (and breast magnetic resonance imaging and ultrasound) findings" (American College of Radiology, 2020).

Discussion

Primary tuberculous mastitis is a rare entity of TB and more commonly seen in developing countries (Madhusudhan and Gamanagatti, 2008). "Tuberculous mastitis contributes between 0.025 and 0.1% of all surgically treated breast diseases" (Kalaç et al., 2002). "Risk factors for breast tuberculosis include multiparity, lactation, trauma, history of suppurative mastitis and immunosuppression" (Tanrikulu et al., 2010). In our case, the patient had no prior history of tuberculosis, and upon physical and radiological examination, there was no evidence of any other tuberculous focus except for left breast. There is a lack of awareness about its presentation among healthcare professionals; thus, it is overlooked in the majority of the patients. The primary form of breast tuberculosis can represent tuberculous mastitis, as supported by the presence of a breast lump, which mimics breast carcinoma (Tewari and Shukla, 2005). Women of reproductive age during the

lactation period carries a higher risk of tuberculous mastitis, and both breasts can be involved with equal frequency (Tewari and Shukla, 2005). Our patient reported to be multiparous, and only left breast was infected as confirmed by mammography and histopathological reports.

"Tuberculous mastitis may present with an irregular, painful lump in the breast (sometimes attached to the overlying skin or the underlying muscle), with or without ulceration of overlying skin and accompanied with purulent nipple discharge" (Tewari and Shukla, 2005; Biswas et al., 2018). Multiple nodules and multiple sinuses may be present, but multiple lumps are uncommon. Tenderness is more frequently seen in breast tuberculosis rather than in breast carcinomas. The upper outer quadrant of the breast is most commonly involved in breast TB. Nipple and areola are not commonly involved (Tewari and Shukla, 2005; Biswas et al., 2018). Our patient also presented with painful irregular lump with purulent nipple discharge in the left breast. The lump was observed in the upper, anterior, and central quadrant with redness around the nipple area. In our case, the patient reported no constitutional symptoms like fever, malaise, night sweats, but the patient was malnourished with a weight of around 45 kg.

"Based on the clinical and radiological features, breast tuberculosis is classified into five different forms: nodular tuberculous mastitis, disseminated tuberculous mastitis, sclerosing tuberculous mastitis, tuberculous mastitis obliterans and acute miliary tuberculous mastitis" (McKeown and Wilkinson, 1952). "The nodulocaseous form presents as a painless, slowly growing and well-circumscribed mass that develops to involve overlying skin and may ulcerate forming discharging sinuses" (McKeown and Wilkinson, 1952). "The disseminated form initiates with numerous foci throughout the breast that caseates later, resulting in sinus formation with or without painful ulceration" (McKeown and Wilkinson, 1952). "The sclerosing form is common in the elderly, with excessive fibrosis dominating than caseation" (McKeown and Wilkinson, 1952). "Tuberculous mastitis obliterans is marked by duct infection-causing proliferation of lining epithelium with noticeable epithelial and periductal fibrosis" (McKeown and Wilkinson, 1952). "Acute miliary tuberculous mastitis is a part of generalized miliary tuberculosis" (McKeown and Wilkinson, 1952). Our case is of the nodular type. The last two forms are uncommon.

Diagnosis of breast tuberculosis is difficult, and the patients have to undertake many investigations before an accurate diagnosis. Mammograms and ultrasonography are of limited value as they do not distinguish breast tuberculosis from breast carcinoma (Tewari and Shukla, 2005). In our case, bilateral digital mammography of the right breast revealed no evidence of malignancy with ACR-BIRADS category 1. In contrast, the left breast results showed large irregular lesions in the upper, outer, and central quadrant extending to the retro-areolar region with ACR-BIRADS category 6. For correct diagnosis, bacteriological and histological examination if of high value (Bailey and Love, 1962). In TM, the bacilli isolated in only 25% of cases, and acid-fast bacilli (AFB) are detected only in 12% of the cases. In our case also,

Ziehl-Neelsen (ZN) stain for AFB reported as negative since the disease is usually paucibacillary in most of the cases (Kakkar et al., 2000). However, for diagnosis of the disease, it is generally enough to identify the presence of caseating granulomas with Langerhans giant cells in the breast tissue, with lymph node involvement. In countries where tuberculosis is epidemic, the presence of granuloma fine-needle aspiration cytology (FNAC) is sufficient to initiate tuberculosis treatment even in the absence of positive AFB and without culture results (Tauro et al., 2011). In our case, based upon first time ultrasound-guided FNAC of the left breast clinical differential diagnosis of ductal malignancy with abscess was made. Histopathological findings for the second time revealed epithelioid cell granulomas, Langerhans giant cells, central necrosis, diffuse lympho-plasmacytic chronic inflammatory infiltrates with the collection of polymorphonuclear leucocytes. These findings suggested granulomatous mastitis. Third-time histopathological report of excisional material revealed a predominantly peri-ductal inflammation, peri-ductal fibrosis, and acute and chronic inflammatory infiltrate consisting of polymorphs and lymphocytes, granulomas composed of histocytes, giant cells, and inflammatory cells. The accurate diagnosis was made as granulomatous mastitis, and there was no evidence of carcinoma in the excised breast tissue.

There are no specific guidelines for the treatment of breast tuberculosis, but many studies have highlighted the role of anti-tubercular therapy for 6 months as the mainstay of treatment (Tewari and Shukla, 2005; Madhusudhan and Gamanagatti, 2008; Gon et al., 2013). "Anti-tuberculous therapy (ATT) includes rifampicin, isoniazid, pyrazinamide, and ethambutol" (Kao et al., 2010). Surgical drainage and resection of the ducts alone is ineffective. In our case, surgical drainage was performed, and the patient was prescribed an anti-tubercular regimen for 6 months. Along with the patient, the child of the patient has also prescribed isoniazid for 6 months. Healing is often slow, and mastectomy is restricted to patients with persistent residual infection (Bailey and Love, 1962). The patient advised for regular follow-ups.

Conclusion

Tuberculous mastitis is a rare form of extrapulmonary tuberculosis. Special care should be taken when diagnosing a breast mass, particularly in endemic areas with tuberculosis, as it may be misdiagnosed as malignancy. Histopathological examination of the excisional biopsy material provides for accurate diagnosis of the disease. Anti-tubercular regimen, surgical drainage, and regular follow-ups are the mainstays of the treatment.

References

American College of Radiology (2020) *Breast Imaging Reporting and Data System*. Available at: https://www.acr.org/Clinical-Resources/Reporting-and-Data-Systems/Bi-Rads

Bailey, H., Love, M. (1962) *A Short Practice of Surgery*. H.K. Lewis, London.

Biswas, S. C., Banerjee, J. L., Sahu, C. R. (2018) Tuberculosis of the female breast: a case report. *Biomed. J. Sci. Tech. Res*. **6(5)**.

Cooper, A. (1829) *Illustrations of the Diseases of the Breast*. Printed by S. McDowall and sold by Longman, Rees, Orme, Brown and Green.

De Sousa, R., Patil, R. (2011) Breast tuberculosis or granulomatous mastitis: a diagnostic dilemma. *Ann. Trop. Med. Public Health* **4(2)**, 122.

Dubey, M. M., Agarwal, S. (1968) Tuberculosis of the breast. *J. Indian Med. Assoc.* **51(7)**, 358–359.

Gon, S., Bhattacharyya, A., Majumdar, B., Kundu, S. (2013) Tubercular mastitis – A great masquerader. *Turk Patoloji Derg.* **29(1)**, 61–63.

Kakkar, S., Kapila, K., Singh, M., Verma, K. (2000) Tuberculosis of the breast. *Acta Cytol.* **44(3)**, 292–296.

Kalaç, N., Özkan, B., Bayiz, H., Dursun, A., Demirağ, F. (2002) Breast tuberculosis. *Breast* **11(4)**, 346–349.

Kao, P. T., Tu, M. Y., Tang, S. H., Ma, H. K. (2010) Tuberculosis of the breast with erythema nodosum: a case report. *J. Med. Case Rep.* **4(1)**, 1–4.

Madhusudhan, K. S., Gamanagatti, S. (2008) Primary breast tuberculosis masquerading as carcinoma. *Singapore Med. J.* **49(1)**, e3–e5.

McKeown, K. C., Wilkinson, K. W. (1952) Tuberculous disease of the breast. *Br. J. Surg.* **39(157)**, 420–429.

Pai, M., Riley, L., Colford, J. (2004) Interferon-γ assays in the immunodiagnosis of tuberculosis: a systematic review. *Lancet Infect. Dis.* **4(12)**, 761–776.

Schaefer, G. (1955) Tuberculosis of the breast; a review with the additional presentation of ten cases. *Am. Rev. Tuberculosis Pulmonary Dis.* **72(6)**, 810–824.

Strazzanti, A., Trovato, C., Gangi, S., Basile, F. (2018) Breast tuberculosis cases rising in Sicily. *Int. J. Surg. Case Rep.* **53**, 9–12.

Tanrikulu, A. C., Abakay, A., Abakay, O., Kapan, M. (2010) Breast tuberculosis in Southeast Turkey: report of 27 cases. *Breast Care (Basel)* **5(3)**, 154–157.

Tauro, L. F., Martis, J. S., George, C., Kamath, A., Lobo, G., Hegde, B. R. (2011) Tuberculous mastitis presenting as breast abscess. *Oman Med. J.* **26(1)**, 53.

Tewari, M., Shukla, H. S. (2005) Breast tuberculosis: Diagnosis, clinical features and management. *Indian J. Med. Res.* **122(2)**, 103.

Massive Dog Bite Injury of the Scalp in One-year Old Boy

Marko Bašković, Anto Pajić, Zoran Barčot
Department of Pediatric Surgery, Children's Hospital Zagreb, Zagreb, Croatia

Received May 5, 2020; Accepted November 2, 2020.

Key words: Dog bite – Scalp avulsion – Child – Plastic surgery

Abstract: A one-year-old boy was referred to our Department of Pediatric Surgery with extensive scalp injury. He was bitten by a neighbour's mixed-breed dog. The wound of the forehead is primary closed while scalp is reimplanted. Due to non-acceptance on the eighth day a necrectomy of devitalized tissue was done. Before applying Integra®, for 2 days, the wound was treated with a V.A.C.® system. After 14 days, Integra® was accepted and split-thickness skin graft (STSG) was transplanted from left upper leg. After 3 months the local status is satisfactory. A hair transplant is planned in the future.

Mailing Address: Marko Bašković, MD., Department of Pediatric Surgery, Children's Hospital Zagreb, Ulica Vjekoslava Klaića 16, 10 000 Zagreb, Croatia; Phone: +385 136 363 79; e-mail: baskovic.marko@gmail.com

https://doi.org/10.14712/23362936.2020.25

Introduction

Of all emergency pediatric conditions, dog bites account for 0.3–1.5% (Daniels et al., 2009; Sabhaney and Goldman, 2012). Particularly at-risk group is children under 10 years of age. Lately, dog bites have been increasingly recognized as a medical and public health issue, as they leave functional, aesthetic and psychosocial consequences (Bernardo et al., 2000).

Case report

We show the case of a one-year-old boy who was referred from a general hospital to our Department of Pediatric Surgery for extensive scalp injury by a neighbour's dog (Figure 1a). In the general hospital, the wound was flushed and the child was administered ceftriaxone. A piece of scalp skin was sent in saline. Upon arrival, the child was vaccinated (tetanus-diphtheria toxoids/tetanus immune globulin). The craniogram showed no signs of fracture. At the operating table, we verified a 22 cm long forehead and scalp injury that extended from the left eyebrow to the middle of the scalp. A swab was taken. Immediately, thinking about the final

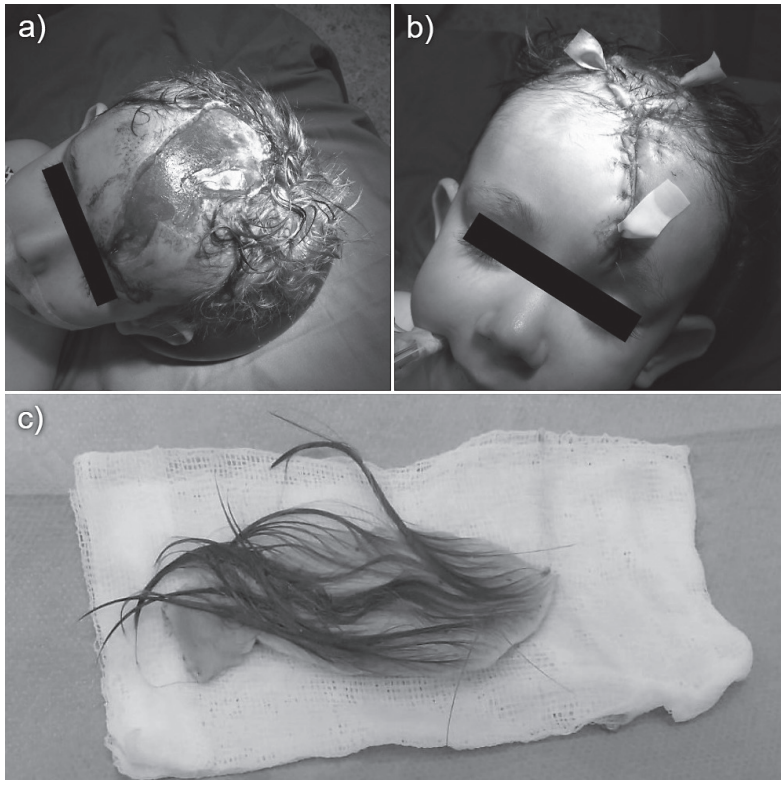

Figure 1 – a) Massive scalp injury; b) appearance after primary forehead closure and scalp reimplantation; c) scalp piece (9 cm × 5 cm).

aesthetic appearance, we decided to primary close the forehead region first. On the part of the scalp that we were unable to primarily close, we reimplanted a piece of boy's scalp measuring 9 cm × 5 cm. The edges of the wound were sutured with Monosyn® 4/0 sutures. 2 drains were placed (Figure 1b and c). Despite regular dressings and monitoring with appropriate antibiotic therapy (the following pathogens were isolated in the swab; *Enterobacter aerogenes*, *Pasteurella multocida*, *Citrobacter freundii* – all resistant to penicillin, ampicillin, amoxicillin-clavulanic acid) the reimplanted part of the scalp was not accepted (Figure 2a). On the eighth day, a necrectomy of the devitalized tissue was performed (Figure 2b). The wound edges were refreshed, treated with Microdacyn®, and a V.A.C.® system (–125 mm Hg) was set up (Figure 2c and d). He worked continuously for 2 days before Integra® was set up. Integra® was fenestrated before placement. After setting Integra® 2 times we changed the V.A.C.® system (Figure 2e). With the acceptance of Integra®, on the 14th day a silicone layer was removed and split-thickness skin graft (STSG)

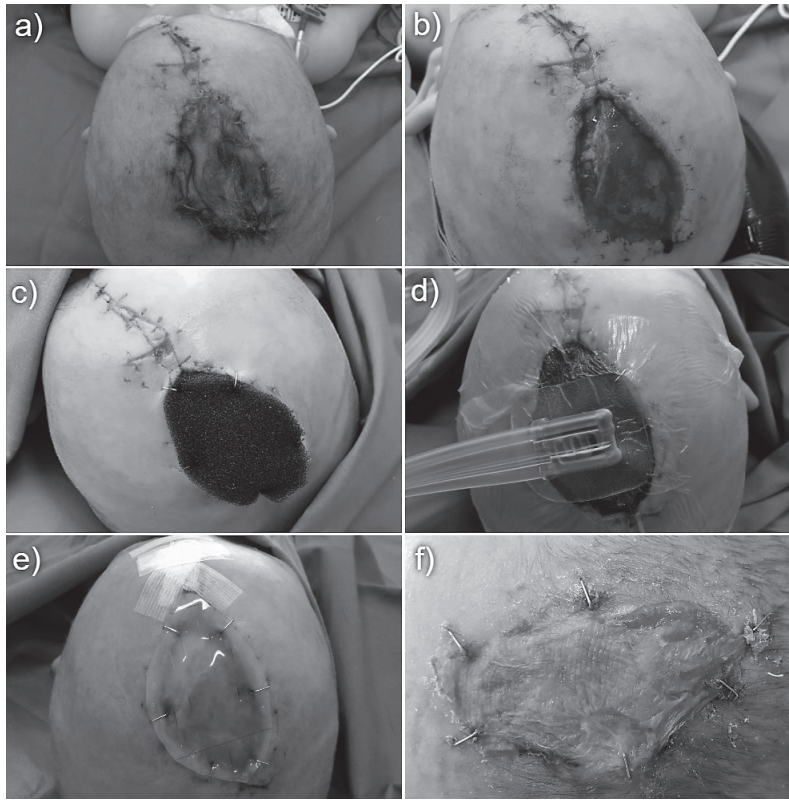

Figure 2 – a) Devitalized scalp tissue; b) refreshed wound edges after necrectomy; c) placement of a sponge; d) activated V.A.C.® system (–125 mm Hg); e) Integra® Dermal Regeneration Template; f) accepted Integra® and split-thickness skin graft (STSG).

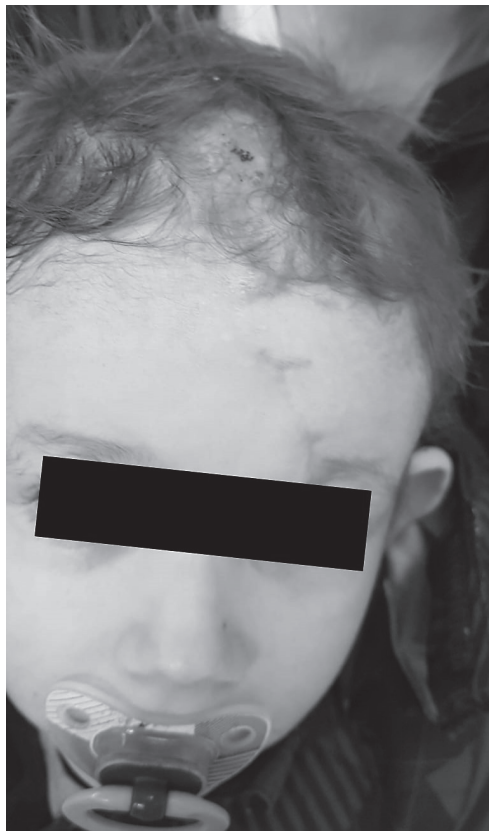

Figure 3 – Appearance of boy's forehead and scalp after 3 months.

was transplanted from the left upper leg. On the STSG Bactrigas® was placed with the V.A.C.® system. By monitoring and replacing the V.A.C.® system, STSG was accepted (Figure 2f). One month after the injury, the boy was released from the hospital. After 3 months the local status is satisfactory (Figure 3). We plan to hair transplantation in the future.

Discussion

Although in our case we continued to use the already started ceftriaxone therapy, amoxicillin-clavulanic acid and first-generation cephalosporins are used as the first-line antibiotics. Complications from dog bites include wound infection, osteomyelitis, cellulitis, septic arthritis, meningitis, sepsis, endocarditis, pneumonia and death. Rates of infection are estimated to range from 1% to 30%. In addition to thorough wound treatment, tetanus vaccination is also required. According to the guidelines of the American Academy of Pediatrics, all children under the age of three must receive tetanus-diphtheria toxoids and tetanus immune globulin. For children older than three years tetanus-diphtheria toxoids is necessary if five or more years have elapsed

since the last dose. Tetanus immune globulin is not required in children older than three years. Depending on the status of the dog, rabies prophylaxis is also important (Sabhaney and Goldman, 2012; Macedo et al., 2016).

As in our case, Bernardo et al. (2000) stated that most of the bites occur exactly from their own (27%) or their neighbour's dog (28%). As for the breed, Chen et al. (2013) report that most bites occur by mixed breed (23.0%), Labrador retriever (13.7%), Rottweiler (4.9%), and German shepherd (4.4%).

Due to the disproportion of the head in relation to the body and their height, younger children are more prone to injuries to the head and face (Chen et al., 2013). Subsequent, inevitable scars have aesthetic and psychological consequences for the children, especially when they found in adolescence (Daniels et al., 2009). Therefore, treatment strategies should include early psychological support for children and their families (Schalamon et al., 2006).

Satteson et al. (2015) support the option that VAC (*vacuum assisted closure*) provides reliable, effective, and durable dressing when traditional surgery is not an option (e.g. primary closure, healing by secondary intention, local tissue transfer, grafts, and flaps). The VAC device works by applying continuous, subatmospheric pressure to a wound through an open-cell polyurethrane sponge secured with an adherent drape. The VAC has been shown to promote wound healing through increasing blood flow and granulation tissue formation, improving oxygenation, decreasing tissue edema, and reducing bacterial load. It has also been demonstrated as a tool for assisting with the preparation of wound beds for subsequent skin grafting and for accelerating the incorporation of Integra®. Satteson et al. (2015) also state, in accordance with our treatment, that standard management included VAC changes 3 times per week on open wounds, whereas the VAC was left in place for 5–7 days over skin grafts and 7–14 days over Integra®.

Integra® is an artificial dermis manufactured as a synthetic bilaminate composed of a bovine collagen lattice covalently linked to chondroitin-6-sulfate and covered with a silastic epidermis. The outer layer is composed of polydimethylsiloxane and serves as an epidermal substitute providing mechanical protection, infection prevention, and moisture modulation. The inner layer promotes cellular ingrowth of fibroblasts, macrophages, and lymphocytes, allowing for the regeneration of a neovascularized tridimensional structure, known as the neo-dermis. Consistent with the study by Watts et al. (2019), we also fenestrated the Integra® matrix because fenestration permits the egress of fluids, reducing the risk of seroma or hematoma formation. Like us, they believe it to be the recommended treatment option in the medically complex patient (Watts et al., 2019).

Konofaos et al. (2014) demonstrated the successful Integra® based scalp reconstruction of a 600 cm^2 defect in a two-year-old male following a dog bite injury where options for skin grafting, local flaps, and free tissue transfer were not available. Although we successfully removed the protective silicone layer after 2 weeks, Konofaos et al. (2014) did it after 3 weeks.

Conclusion

The use of Integra®, followed by an ultrathin skin graft, reduces the morbidity by eliminating the need for large regional or free tissue transfer creating a further defect at the donor site. In addition, the surgical procedure is much faster than with flaps, reducing the risk of anesthesia and the treatment-related comorbidity. Like Konofaos et al. (2014), we also believe that this technique offers another viable option for the treatment of complex scalp wounds in pediatric patients and deserves to be added to the list of reconstructive surgical techniques used by the pediatric plastic surgeons.

References

Bernardo, L. M., Gardner, M. J., O'Connor, J., Amon, N. (2000) Dog bites in children treated in a pediatric emergency department. *J. Soc. Pediatr. Nurs.* **5(2)**, 87–95.

Chen, H. H., Neumeier, A. T., Davies, B. W., Durairaj, V. D. (2013) Analysis of pediatric facial dog bites. *Craniomaxillofac. Trauma Reconstr.* **6(4)**, 225–232.

Daniels, D. M., Ritzi, R. B., O'Neil, J., Scherer, L. R. (2009) Analysis of nonfatal dog bites in children. *J. Trauma* **66**, S17–S22 (Suppl. 3).

Konofaos, P., Kashyap, A., Wallace, R. D. (2014) Total scalp reconstruction following a dog bite in a pediatric patient. *J. Craniofac. Surg*. **25(4)**, 1362–1364.

Macedo, J. L., Rosa, S. C., Queiroz, M. N., Gomes, T. G. (2016) Reconstruction of face and scalp after dog bites in children. *Rev. Col. Bras. Cir.* **43(6)**, 452–457.

Sabhaney, V., Goldman, R. D. (2012) Child health update. Management of dog bites in children. *Can. Fam. Physician* **58(10)**, 1094–1096.

Satteson, E. S., Crantford, J. C., Wood, J., David, L. R. (2015) Outcomes of vacuum-assisted therapy in the treatment of head and neck wounds. *J. Craniofac. Surg.* **26(7)**, e599–e602.

Schalamon, J., Ainoedhofer, H., Singer, G., Petnehazy, T., Mayr, J., Kiss, K., Höllwarth, M. E. (2006) Analysis of dog bites in children who are younger than 17 years. *Pediatrics* **117(3)**, e374–e379.

Watts, V., Attie, M. D., McClure, S. (2019) Reconstruction of complex full-thickness scalp defects after dog-bite injuries using dermal regeneration template (Integra): Case report and literature review. *J. Oral Maxillofac. Surg.* **77(2)**, 338–351.

Instructions to Authors

Prague Medical Report is an English multidisciplinary biomedical journal published quarterly by the First Faculty of Medicine of the Charles University. Prague Medical Report (Prague Med Rep) is indexed and abstracted by Index-medicus, MEDLINE, PubMed, EuroPub, CNKI, DOAJ, EBSCO, and Scopus.

Articles issued in the journal

a) Primary scientific studies on the medical topics (not exceeding 30 pages in standardized A4 format – i.e. 30 lines and 60–65 characters per line – including tables, graphs or illustrations)
b) Short communications
c) Case reports
d) Reviews
e) Lectures or discourses of great interest
f) Information about activities of the First Faculty of Medicine and other associated medical or biological organizations

Layout of the manuscript

a) Title of the study (brief and concise, without abbreviations)
b) Information about the author(s) in the following form:
   - first name and surname of the author(s) (without scientific titles)
   - institution(s) represented by the author(s)
   - full corresponding (mailing) author's reference address (including first name, surname and scientific titles, postal code, phone/fax number and e-mail)
c) Abstract (maximum 250 words)
d) Key words (4–6 terms)
e) Running title (reduced title of the article that will appear at the footer (page break), not more than 50 typewritten characters including spaces)
f) Introduction
   - The use of abbreviations should be restricted to SI symbols and those recommended by the IUPAC-IUB. Abbreviations should be defined in brackets on first appearance in the text. Standard units of measurements and chemical symbols of elements may be used without definition.
g) Material and Methods
h) Results
i) Discussion

j) Conclusion
k) References
   - All the sources of relevant information for the study should be cited in the text (citations such as "personal communication" or "confidential data" are not accepted).
   - It is not permitted to cite any abstract in the References list.
   - References should be listed alphabetically at the end of the paper and typed double-spaced on separate pages. First and last page numbers must be given. Journal names should be abbreviated according to the Chemical Abstract Service Source Index. All co-authors should be listed in each reference (et al. cannot be used).
   - Examples of the style to be used are:
     Yokoyama, K., Gachelin, G. (1991) An Abnormal signal transduction pathway in CD4–CD8– double-negative lymph node cells of MRL *lpr/lpr* mice. *Eur. J. Immunol.* **21**, 2987–2992.
     Loyd, D., Poole, R. K., Edwards, S. W. (1992) *The Cell Division Cycle. Temporal Organization and Control of Cellular Growth and Reproduction.* Academic Press, London.
     Teich, N. (1984) Taxonomy of retroviruses. In: *RNA Tumor Viruses,* eds. Weiss, R., Teich, N., Varmus, H., Coffin, J., pp. 25–207, Cold Spring Harbor Laboratory, Cold Spring Harbor, New York.
     References in the text should be cited as follows: two authors, Smith and Brown (1984) or (Smith and Brown, 1984); three or more authors, Smith et al. (1984) or (Smith et al., 1984). Reference to papers by the same author(s) in the same year should be distinguished in the text and in the reference list by lower-case letters, e.g. 1980a, or 1980a, b.
l) tables, figures, illustrations, graphs, diagrams, photographs, etc. (incl. legends)

Technical instructions

a) Manuscripts (in UK English only) must be delivered in the electronic form via Online Manuscript Submission and Tracking system (http://www.praguemedicalreport.org/). In case of problems, contact the Prague Medical Report Office (medical.report@lf1.cuni.cz). The online submission has to include the complete version of the article in PDF format, separately the manuscript as a MS Word file and a cover letter. The detailed version of the Instructions to Authors can be found at: http://www.praguemedicalreport.org/download/instructions_to_authors.pdf.
b) Text should be written in MS WORD only. We accept only documents that have been spell-checked with UK English as a default language.
c) Please, write your text in Times New Roman script, size 12, and line spacing 1.5.
d) Text should be justified to the left, with no paragraph indent (use Enter key only); do not centre any headings or subheadings.

e) Document must be paginated-numbered beginning with the title page.
f) Tables and graphs should represent extra files, and must be paginated too.
g) Edit tables in the following way: Make a plain text, indent by Tab (arrow key) all the data belonging to a line and finish the line by Enter key. For all the notes in table, use letter x, not *.
h) Make your graphs only in black-and-white. Deliver them in electronic form in TIFF or JPG format only.
i) Deliver illustrations and pictures (in black-and-white) in TIFF or JPG format only. The coloured print is possible and paid after agreement with the Prague Medical Report Office.
j) Mark all the pictures with numbers; corresponding legend(s) should be delivered in an extra file. Mark the position of every picture (photo) in the manuscript by the corresponding number, keep the order 1, 2, 3...

Authors' Declaration

The corresponding (or first author) of the manuscript must print, fill and sign by his/her own hand the Authors Declaration and fax it (or send by post) to the Prague Medical Report Office. Manuscript without this Declaration cannot be published. The Authors' Declaration can be found by visiting our web pages: http://pmr.lf1.cuni.cz or web pages of Prague Medical Report Online Manuscript Submission and Tracking system: http://www.praguemedicalreport.org/.

Editorial procedure

Each manuscript is evaluated by the editorial board and by a standard referee (at least two expert reviews are required). After the assessment the author is informed about the result. In the case the referee requires major revision of the manuscript, it will be sent back to the author to make the changes. The final version of the manuscript undergoes language revision and together with other manuscripts, it is processed for printing.

Concurrently, proofs are electronically sent (in PDF format) to the corresponding (mailing) author. Author is to make the proofs in PDF paper copy and deliver it back to the editorial office by fax or as a scanned file by e-mail. Everything should be done in the required time. Only corrections of serious errors, grammatical mistakes and misprints can be accepted. More extensive changes of the manuscript, inscriptions or overwriting cannot be accepted and will be disregarded. Proofs that are not delivered back in time cannot be accepted.

Article processing charge

Authors do not pay any article processing charge.

Open Access Statement

This is an open access journal which means that all content is freely available without charge to the user or his/her institution. Users are allowed to read, download, copy,

distribute, print, search, or link to the full texts of the articles, or use them for any other lawful purpose, without asking prior permission from the publisher or the author. This is in accordance with the BOAI definition of open access.

Editorial Office
Prague Medical Report
Kateřinská 32, 121 08 Prague 2, Czech Republic
e-mail: medical.report@lf1.cuni.cz
Phone: +420 224 964 570. Fax: +420 224 964 574

Annual Contents

No. 1

No. 2

Primary Scientific Studies

Case Reports

No. 3

Primary Scientific Studies

No. 4

Annual Nominal Index

ISSN 1214–6994

Annual Referee Index

Prague Medical Report thanks to Reviewers, consulted in 2020:

Assoc. Prof. Ondřej Beran, MD., PhD., Department of Infectious Diseases, First Faculty of Medicine, Charles University and Military University Hospital Prague, Czech Republic;

Martin Čepelík, MD., Department of Child Surgery and Traumatology, Third Faculty of Medicine, Charles University and Thomayer Hospital, Czech Republic;

Assoc. Prof. Ivan Chytra, MD., PhD., Department of Anaesthesiology and Intensive Care, Faculty of Medicine in Plzeň, Charles University and University Hospital Plzeň, Czech Republic;

Assoc. Prof. Tomáš Fait, MD., PhD., Department of Obstetrics and Gynaecology, Second Faculty of Medicine, Charles University and University Hospital Motol, Czech Republic;

Prof. Dr. Hassan Farghali, DSc., Institute of Pharmacology, First Faculty of Medicine, Charles University and General University Hospital in Prague, Czech Republic;

Zdeněk Fojtík, MD., PhD., Department of Rheumatology, University Hospital Brno, Czech Republic;

Tomáš Grega, MD., Department of Medicine, First Faculty of Medicine, Charles University and Military University Hospital Prague, Czech Republic;

Assoc. Prof. Tomáš Grus, MD., PhD., 2nd Department of Surgery – Department of Cardiovascular Surgery, First Faculty of Medicine, Charles University and General University Hospital in Prague, Czech Republic;

Petra Havránková, MD., PhD., Department of Neurology, First Faculty of Medicine, Charles University and General University Hospital in Prague, Czech Republic;

Prof. Jiří Homolka, MD., DSc., 1st Department of Tuberculosis and Respiratory Diseases, First Faculty of Medicine, Charles University and General University Hospital in Prague, Czech Republic;

Daniel Hrušák, MD., PhD., Department of Stomatology, Faculty of Medicine in Plzeň, Charles University and University Hospital Plzeň, Czech Republic;

David Kemlink, MD., PhD., Department of Neurology, First Faculty of Medicine, Charles University and General University Hospital in Prague, Czech Republic;

Assoc. Prof. Petr Kozler, MD., PhD., Institute of Physiology, First Faculty of Medicine, Charles University, Czech Republic;

Assoc. Prof. František Liška, MD., PhD., Institute of Biology and Medical Genetics, First Faculty of Medicine, Charles University and General University Hospital in Prague, Czech Republic;

Vladimíra Lošťáková, MD., PhD., Department of Respiratory Medicine, Faculty of Medicine and Dentistry, Palacký University in Olomouc and University Hospital Olomouc, Czech Republic;

Vladimír Machoň, MD., Department of Dental Medicine, First Faculty of Medicine, Charles University and General University Hospital in Prague, Czech Republic;

Petr Nesnídal, MD., Clinic of Spinal Surgery, First Faculty of Medicine, Charles University and University Hospital Motol, Czech Republic;

David Neumann, MD., PhD., Department of Pediatrics, Faculty of Medicine in Hradec Králové, Charles University and University Hospital Hradec Králové, Czech Republic;

Petr Pavlíček, MD., Department of Hematology, Third Faculty of Medicine,

Charles University and University Hospital Královské Vinohrady, Czech Republic;

Assoc. Prof. Jaroslav Pejchal, MD., PhD. et PhD., Department of Toxicology and Military Pharmacy, Faculty of Military Health Sciences, University of Defence in Brno, Czech Republic;

Prof. František Perlík, MD., DSc., Institute of Pharmacology, First Faculty of Medicine, Charles University and General University Hospital in Prague, Czech Republic;

Assoc. Prof. Jaroslav Slípka, MD., PhD., Department of Otorhinolaryngology, Faculty of Medicine in Plzeň, Charles University and University Hospital Plzeň, Czech Republic;

Assoc. Prof. Viktor Soukup, MD., PhD., FEBU, Department of Urology, First Faculty of Medicine, Charles University and General University Hospital in Prague, Czech Republic;

Michal Staník, MD., PhD., Masaryk Institute of Oncology, Brno, Czech Republic;

Assoc. Prof. Jan Trna, MD., PhD., Department of Internal Gastroenterology, Faculty of Medicine, Masaryk University in Brno and University Hospital Brno, Czech Republic;

Prof. Samuel Vokurka, MD., PhD., Department of Oncology and Radiotherapy, Faculty of Medicine in Plzeň, Charles University and University Hospital Plzeň, Czech Republic;

Jiří Wallenfels, MD., National TB Surveillance Unit, Na Bulovce Hospital, Prague, Czech Republic;

Assoc. Prof. Jakub Zieg, MD., PhD., Department of Paediatrics, Second Faculty of Medicine, Charles University and University Hospital Motol, Czech Republic

Prague Medical REPORT

(Sborník lékařský)

Published by the First Faculty of Medicine, Charles University, Karolinum Press,
Ovocný trh 560/5, 116 36 Praha 1 – Staré Město, Czech Republic, www.karolinum.cz

Editorial Office: Prague Medical Report, Kateřinská 32, 121 08 Prague 2, Czech Republic,
Phone: +420 224 964 570, Fax: +420 224 964 574,
e-mail: medical.report@lf1.cuni.cz
Editor in Chief: Kateřina Jandová, MD., PhD.
Editor: Assoc. Prof. Jan Šváb, MD., PhD.
Foreign Language Editor: Prof. Jaroslav Pokorný, MD., DSc.
Executive Editors: Mgr. Jiří Frühauf, Mgr. Lucie Šulcová
Editorial Board: Prof. Jan Betka, MD., DSc.; Zdeněk Kostrouch, MD., PhD.;
Prof. Emanuel Nečas, MD., DSc.; Prof. Karel Smetana, MD., DSc.;
Prof. Karel Šonka, MD., DSc.; Assoc. Prof. Jan Tošovský, MD., PhD.;
Prof. Jiří Zeman, MD., DSc.

Published as quarterly journal. Typeset and printed by Karolinum Press.
Annual subscription (4 issues) EUR 60,–. Single copy EUR 20,–.
Distribution: Karolinum Press, Ovocný trh 560/5,
116 36 Praha 1, Czech Republic, e-mail: journals@karolinum.cz

ISSN 1214-6994 (Print)
ISSN 2336-2936 (Online)

Reg. No. MK ČR E 796